PARTICLE-BLOOD DYNAMICS: ADHESION OF VASCULAR-TARGETED PEGYLATED PARTICLES AND BLOOD CELLS IN FLOW

by

Peter John Onyskiw Jr.

A dissertation submitted in partial fulfillment
of the requirements for the degree of
Doctor of Philosophy
(Chemical Engineering)
in the University of Michigan
2015

Doctoral Committee:

Associate Professor Lola Eniola-Adefeso, Chair
Professor Jennifer J Linderman
Assistant Professor Sunitha Nagrath
Associate Professor Andrew James Putnam

To my Wife, Mom, and Dad

ACKNOWLEDGMENTS

I would like to thank my thesis advisor, Dr. Lola Eniola-Adefeso, for accepting me into her lab and guiding me in becoming a better professional and person; and, my dissertation committee; Dr. Jennifer J. Linderman, Dr. Sunitha Nagrath, and Dr. Andrew James Putnam for their time and their thoughtful suggestions throughout my doctoral work.

My family; Mom, Dad, Natalie, Donald, Eli, Lesia, Scotty, and Christina for their love and support.

Current and former lab members for supporting me on a daily basis and creating an enjoyable atmosphere in the lab.

All the blood donors who participated in my study.

And most of all my wife, Andrea. You stuck by my side from application to completion, through the struggles and shortcomings and never gave up on me – I love you.

TABLE OF CONTENTS

LIST OF FIGURES

LIST OF TABLES

LIST OF EQUATIONS

LIST OF ABBREVIATIONS

ECs	Endothelial Cells
VTCs	Vascular Targeted Carriers
PEG	Poly(ethylene glycol)
RBCs	Red Blood Cells
HUVEC	Human Umbilical Vein Endothelial Cell
sLe^a	Sialyl Lewis^a
ICAM-1	Intercellular Adhesion Molecule-1
aICAM-1	anti- Intercellular Adhesion Molecule-1
kDa	kilo-Dalton
R_f	Flory's radius
WSR	Wall Shear Rate
PPFC	Parallel Plate Flow Chamber
PEG	Poly(ethylene glycol)
PLGA	Poly(lactic-co-glycolic acid)
pRBC	Pig Red Blood Cells
vWF	von Willebrand Factor
CBP	Collagen Binding Peptide
VBP	von Willebrand Factor Binding Peptide
cRGD	cyclic Arginine-Glycine-Aspartic Acid

ABSTRACT

PARTICLE-BLOOD DYNAMICS: ADHESION OF VASCULAR-TARGETED PEGYLATED PARTICLES AND BLOOD CELLS IN FLOW

by

Peter Onyskiw Jr.

Chair: Lola Eniola-Adefeso,

Vascular targeting is a viable strategy for the therapeutic intervention of inflammatory diseases such as cardiovascular disease. The multiple components of blood (red blood cell, leukocytes, platelets, and plasma) create a complex transport process for optimizing tissue specific targeting. Attaching poly(ethylene glycol) (PEG) spacers to a drug carrier's surface (PEGylation) is often proposed as a strategy for avoiding systemic clearance by minimizing plasma protein adsorption onto the drug carrier. However, it is unclear as to whether PEGylation influences ligand-based tissue targeting in blood flow. Additionally, both platelets and leukocytes localize and interact with the vessel wall during inflammation. Little is known whether the presence of inflammation targeting drug carriers in blood or at the vessel wall influences the homeostatic interaction of leukocytes and platelets with the same targeted tissue. Here, I investigate the dynamics between the non-red cell components of blood and vascular

targeted carriers; specifically, how PEGylation influences carrier adhesion in blood and whether inflammation targeting drug carriers affect leukocyte and platelet adhesion to the same targeted tissue. The addition of a 5.5 kDa or 10 kDa PEG spacer to a model drug carrier improved targeting to a model vessel wall in laminar human blood flow, but only for an unfavorable targeting system (aICAM-1/ICAM-1). While PEGylation was unable to neutralize a negative plasma effect on the adhesion of an actual drug delivery system (poly(lactic-co-glycolic) acid spheres) in human blood, a PEG surface density of 35,000 PEG chains/μm^2 maintained the adhesiveness of a model drug carrier in pig blood. Also, high blood concentrations of 500 nm-5 μm targeted spheres ($2.5x10^6$ particles/mL and $1x10^7$ particles/mL) were found to reduce the adhesion of leukocytes to the same targeted tissue under high shear conditions, with nearly a 100% reduction in leukocyte adhesion with 5 μm and 3 μm targeted spheres at $1x10^7$ particles/mL in blood. This work contributes to the design and application of targeted drug carriers by recommending a 5.5 kDa or 10 kDa PEG spacer for targeting high shear areas associated with cardiovascular disease and identifying a new application for inflammation targeting particles through reducing leukocyte accumulation to inflammatory tissue.

CHAPTER 1

INTRODUCTION

1.1. Background

The vasculature of the human body is the network of vessels through which blood is pumped by the heart in order to sustain organ and muscle function. Blood is responsible for transporting vital nutrients to and from organs, immune cells to sites of infection, and is directly involved in repairing damaged vessels after vascular injury. During healthy function, blood is circulated throughout the body with limited interactions with the vasculature tissue itself. However under distress, the vascular wall uses inflammation to signal immune cells and other blood cells to the stimulated site in order to restore the tissue to homeostatic function. Even though the inflammatory signaling process is vital for the body's immune system and sustainability, unregulated or chronic inflammation can significantly enhance the pathogenesis of a several serious injuries. For example, circulating cancer cells localize and interact with inflamed vessels before transmigrating into local tissue and initializing tumor proliferation.[1] The continuous inflammatory recruitment of T-cells, macrophages, and other leukocytes into the pulmonary tissue is responsible for airway obstruction and hyper-responsiveness associated with chronic obstructive pulmonary disorder and asthma.[2] Of the many other inflammatory diseases, cardiovascular disease (CVD) is one of the most common diseases associated with vascular inflammation.

Despite the steady decline in cardiovascular deaths since the 1980s, cardiovascular disease remains the leading cause of death in the United States and the Western World.[3, 4] Atherosclerosis is a chronic inflammatory disease in which the continuous recruitment of leukocytes (white blood cells) to atheroprone areas results in plaque formation between the endothelium, the monolayer of cells lining the lumen of blood vessels, and the underlying smooth muscle tissue (Fig. 1.1).[5, 6] Plaque development is a major concern for CVD due to the potential for rupture and inducing life-threatening cardiac events such as a stroke or heart attack. Current diagnostic techniques for atherosclerosis include contrast imaging or measuring cholesterol levels via blood tests.[7, 8] However, these methods do not provide detailed analysis of atherosclerotic tissue or identify early stages of plaque formation and potential areas of lesion development such as chronically inflamed tissue.

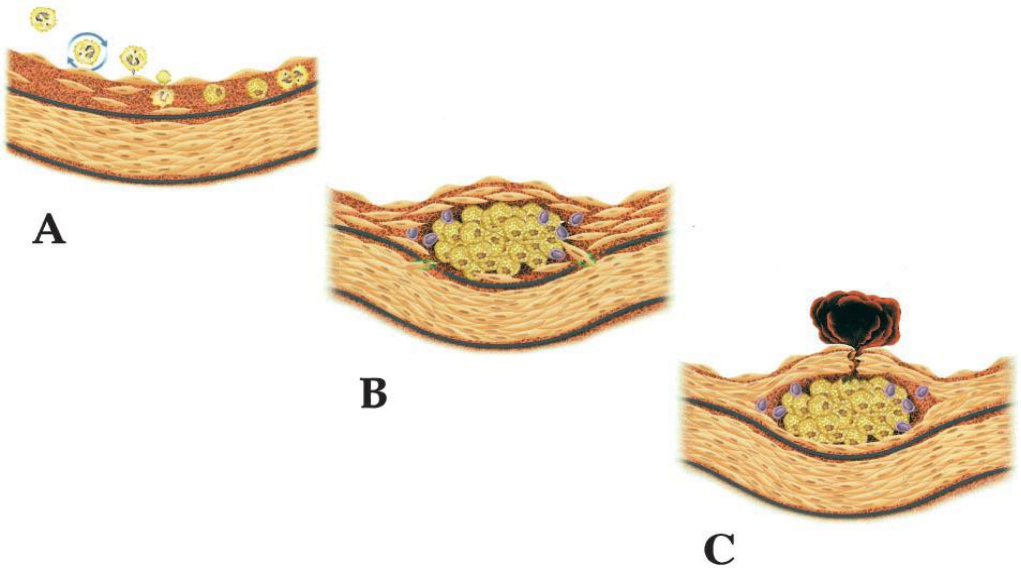

Figure 1.1. Schematic of (A) leukocyte recruitment, (B) plaque development, and (C) plaque rupture as related to atherosclerosis.[6]

Oral administration of therapeutics such as statins is often prescribed as a non-invasive therapy for treating and preventing plaque formation.[9] Though there are many benefits to statin therapy, including stabilizing atherosclerotic plaque to minimize rupture and decreasing overall inflammatory response of the endothelium, there are several serious side-effects associated with the systemic circulation of statins.[10] For example, statins decrease platelet activation and endothelial inflammation which is therapeutically beneficial for atherosclerotic tissue but can negatively impact clotting time and the inflammatory recruitment of immune cells during vessel injury and local infection.[11-13] However, many of these systemic side effects can be minimized by reducing exposure of the therapeutic to healthy tissue. Targeted drug delivery is a tissue-specific therapeutic strategy aimed towards minimizing harmful side-effects through delivering therapeutics directly to diseased tissue. Vascular targeting utilizes blood flow to deliver targeted drug carriers directly to diseased vasculature and is a strong candidate for treating inflammation associated with CVD due to blood directly contacting the diseased tissue, i.e. the inflamed endothelium of blood vessels.

1.1.1. Utilizing Inflammation for Tissue Specific Targeting

Inflammation is a biochemical signaling response of the endothelium to external stimulants such as a local infection, vessel injury, or cholesterol accumulation in the vessel wall. External stimulation induces the production of cytokines such as interleukin-1β (IL-1β) and tumor necrosis factor-α (TNFα) which initiates changes in molecular pathways and alters the receptor expression of the endothelium.[14-16] The primary role of inflammation is to recruit leukocytes to the stimulated tissue in order to return the tissue to homeostatic function. After exposure to cytokines, the endothelium upregulates cell adhesion molecules (CAMs) including

P- and E-selectin, intercellular adhesion molecule-1 (ICAM-1), and vascular cell adhesion molecule-1 (VCAM-1) which initiate the leukocyte adhesion cascade (Fig. 1.2).[17, 18, 19] First, leukocytes are initially captured from blood and roll along the activated endothelium through P- and E-selectin interacting with leukocyte expressed ligands including sialyl lewis^x (sLe^x), sialyl lewis^a (sLe^a), and P-selectin glycoprotein-1 (PSGL-1).[20, 21] Leukocyte rolling is the continuous formation and breaking of bonds with selectins on the endothelium which results in leukocytes translocating across the endothelium in the direction of blood flow. The decreased velocities of rolling leukocytes, relative the velocity of freely circulating leukocytes in blood, allows for firm adhesion to be established via lymphocyte function-antigen-1 (LFA-1) and $\alpha_4\beta_1$ integrin (VLA-4) interacting with ICAM-1 or VCAM-1, respectfully.[22] After firm adhesion is established, leukocytes localize to cell-cell junctions, transmigrate between adjacent cells into tissue, and begin to work towards returning the stimulated tissue to normal function. CAMs make viable targets for inflammation specific drug delivery associated with CVD by marked characteristics such as low basal expression of CAMs by healthy tissue, up-regulation during acute and chronic inflammation, and prevalence near atherosclerotic lesions.[23, 24]

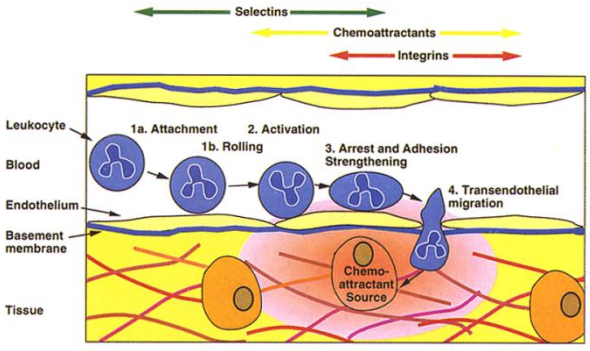

Figure 1.2. Schematic of leukocyte adhesion cascade.[17]

1.1.2. Design of Vascular-Targeted Carriers

Several formulations can be implemented as the drug delivery vehicle used for vascular targeted. Liposomes are attractive for vascular targeting due to their low toxicity and are easy to fabricate. Liposomes are composed of an inner aqueous phase encapsulated by a lipid bilayer. Hydrophilic drugs can be easily loaded into the aqueous phase during fabrication; however, hydrophobic drugs are restricted to the lipid membrane.[25] The fluidity of the lipid membrane significantly impacts hydrophobic drug retention, particularly under high shear.[26] The lipid membrane can be stabilized with the addition of poly(ethylene glycol) (PEG); however, the steric hindrance provided by PEG significantly decreases cellular internalization and reduces the potential for intracellular drug delivery with liposomes.[27, 28] Porous materials such as silicon dioxide (silica) and titanium dioxide have also been explored for vascular targeting; however, therapeutic loading through physio-adsorption makes it difficult to control drug release.[29] Gold and iron oxide nanoparticles have also been implemented in MRI and x-ray imaging of atherosclerotic plaque, although drug loading remains an issue due to the lack of control of the pore size during particle fabrication.[30]

Polymeric spheres are one of the most popular formulations explored for vascular targeting. Biodegradable polymers allows for tailored drug release through control of the polymer's molecular weight, crystallinity, and hydrophobicity.[31] Targeting ligands can be attached to functional groups on the particle's surface provided by the polymer's end- or side chains. Polymeric particles can also be fabricated in a variety of sizes and shapes using scalable oil-in-water emulsion techniques, making polymeric vascular-targeted carriers (VTCs) a strong candidate for treating CVD and optimizing tissue targeting in blood flow.[33-35]

In order for VTCs to effectively target the inflammation, they must first marginate to the vessel wall in flow before establishing firm adhesion through targeted ligands interacting with inflammatory receptors (i.e. CAMs). Margination is the localization to the vessel wall from bulk blood flow. Firm adhesion to the vessel wall is established by decorating the VTC's surface with ligands which interact with CAMs. E-selectin, ICAM-1, and VCAM-1 have all been proposed as inflammatory target molecules; however, their difference in expression during inflammation and reaction kinetics must be considered when optimizing VTCs. For example, E-selectin is often targeted using sialylated tetrasacchrides such as sLe^x or sLe^a found naturally on leukocytes (sLe^a/sLe^x also interact with P-selectin on endothelial cells and platelets, and L-selectin found on leukocytes).[21] Even though E-selectin plays a significant role in rolling adhesion, firm adhesion can be established by decorating the VTC's surface with multivalent sLe^a or by decorating the VTC's surface with ligand densities greater than ~800 sLe^a sites/μm^2.[36, 37] Targeting ICAM-1 or VCAM-1 typically requires higher ligand densities >2,000 ligands/μm^2 for adhesion under high shear conditions (>200 s^{-1} wall shear rate) due to slower reaction kinetics relative to that of selectins with $sLe^{a/x}$.[36, 38] P- and E-selectin are also upregulated during acute inflammation and not during chronic inflammation associated with CVD. For this reason, ICAM-1 and VCAM-1 are often targeted, using peptides or antibodies, in conjugation with E-selectin, due to their upregulation during chronic inflammation and around atherosclerotic lesions.[23, 38-41]

Physical and material characteristics of VTCs including size, shape, and VTC density have all been shown to significantly impact margination and adhesion in hydrodynamic and blood flow.[42-45] For example, in blood, silica particles were shown to marginate more effectively to the vessel wall than neutrally buoyant polystyrene spheres which were

approximately 2.5-fold lower in particle density (Thompson. *In submission.* 2015). Ellipsoidal (rod-shaped) and disk-shaped particles have been shown to marginate more efficiently than spherical particles in hydrodynamic flow, as ellipsoids naturally drift away from the center of flow.[43] Ellipsoidal particles also align in the direction of flow which helps reduce the potential for vessel occlusion and accumulation in organs such as the lungs and liver.[46, 47] Changing particle shape can also influence adhesive dynamics in flow as ellipsoidal particles were shown to have a greater propensity for adhesion due to ellipsoids having less rotational momentum, relative to spheres of the same volume, when interacting with targeted receptors at the vessel wall.[42, 44] In summary, VTC geometry and targeting system are important design parameters probed for optimizing margination and adhesion in flow; however, vascular targeting is also influenced by hemodynamics and blood rheology.

1.1.3. Influence of Blood Rheology on VTC Margination and Adhesion

1.1.3.a. Red Blood Cell Effect on VTC Targeting

When optimizing VTC targeting in flow, it is important to remember that blood is the end-all working fluid and the rheological properties of blood play a significant role in VTC margination and adhesion. Blood is a suspension of red blood cells (RBCs), leukocytes (white blood cells), and platelets in plasma – a concentrated aqueous solution of proteins and other biochemeicals. RBCs constitute 40–45% of the total volume of blood (hematocrit - the volume percent of RBCs in blood) and play a significant role in VTC margination and adhesion.[48] RBCs' deformability and disk shape induce an inertial lift during flow such that RBCs align in the center of flow and generate a RBC-free layer, more commonly the cell-free layer (CFL), several microns thick adjacent to the vessel wall (Fig. 1.3).[49-51] Differences in rigidity, vessel

wall induced lift forces, and heterogeneous collisions with RBCs force more rigid blood cells (leukocytes and platelets) and VTCs to marginate towards to the CFL along the endothelium.[50] RBC induced margination of leukocytes has significant implications in atherosclerotic plaque development such that plaque develops in areas of disturbed flow, such as branching points or recirculation eddies, where marginating leukocytes can accumulate near low shear areas or stagnation points.[52, 53] RBCs also promote firm adhesion to an endothelium by providing a normal force to the marginating VTCs and blood cells which aides in counteracting drag forces experienced at the vessel wall during flow.[36]

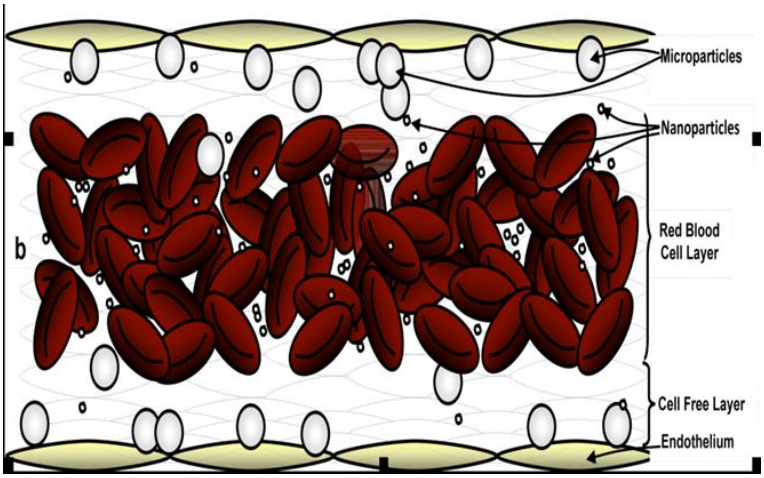

Figure 1.3. Schematic of the RBC-core and cell-free layer and influence on particle margination.[51]

The combined effect of enhanced margination and improved adhesion by the presence of red cells has a drastic effect on the influence of VTC size, geometry, and targeting ability. For example in buffer-only hydrodynamic flow, targeted 5 μm polystyrene microspheres effectively adhere to an activated human umbilical vein endothelial (HUVEC) monolayer at adhesion densities greater than 2 μm targeted spheres.[36] However with the presence of RBCs, the margination of 2 μm spheres is significantly enhanced such that the adhesion of 2 μm spheres is greater than 5 μm targeted spheres with the same ligand density.[36] In fact, 2–3 μm spheres are suggested to be the optimal size of VTC margination and adhesion under RBC flow conditions in laminar and oscillating flow conditions.[54] RBCs also promoted the adhesion of 5 μm sLe^a-targeted spheres at high wall shear rates (WSR >500 s^{-1}) where adhesion was minimal in buffer only systems.[36] The formation of an RBC core in bulk blood flow also significantly impacts the margination and adhesion of spheres < 1 μm such that submicron VTCs do not effectively navigate the RBC core (RBC ~ 6 μm in diameter) and marginate to the vessel wall (Fig. 1.3), resulting in lower adhesion levels relative to microspheres (2-5 μm) *in vivo* and *in vitro*.[36, 37, 51]. This provides a serious challenge for implementing nanospheres for targeted intracellular delivery. Hence, changing VTC shape has been proposed as a means for improving nanosphere adhesion as ellipsoidal particles showed higher levels of margination in buffer-only systems.[42-45] While ellipsoidal VTCs if different aspect ratios (ratio of major length to minor length) showed enhanced margination in buffer-only systems, only ellipsoids with aspect ratios >9 showed enhanced adhesion with the presence of RBCs *in vitro*.[42] Hence, it is clearly evident that optimizing VTC adhesion in buffer-only systems does not translate to VTC targeting in blood flow due to the significant effect on margination and adhesion from the development of the RBC core during blood flow.

1.1.3.b. Plasma Impact on VTC Targeting

Plasma has both physical and biochemical influences on VTC targeting. Plasma provides a physical barrier between the vessel wall and the RBC-core which VTCs must cross before interacting with their targeted molecules. Once bound to the endothelium, VTCs experience viscous drag forces due to the continuous flow of plasma. If the adhesive dynamics are not sufficient to withstand the drag forces from plasma, VTCs will not adhere to or will be removed from the target site. Thus, the shear stresses provided by plasma play a critical role in identifying molecular targeting systems and optimizing the ligand density required for firm adhesion to the vessel wall.

When exposed to blood, plasma proteins rapidly adsorb onto a particle's surface. The adsorption of opsins (G-protein coupled receptors) onto a particle's surface is a key identification marker for the phagocytic cells before they initiate clearance from blood.[57, 58] Protein adsorption also influences biodistribution such that opsonized particles are readily trafficked to the liver and spleen. Plasma protein adsorption is dependent on both physical (size, shape) and chemical (surface charge, functionalization) characteristics of the VTC.[59] For example, NIPAM-BAM (*N*-isopropylacrylamide *N*-*tert*-butylacrylamide) polymeric nanospheres ranging from 70 – 700 nm in diameter were shown to have similar protein adsorption profiles (types of proteins adsorbed onto the particle's surface) but differ in the amount of proteins adsorbed onto the surface.[58] A similar size effect on plasma adsorption has been identified with materials used for optimizing inflammation targeting VTCs including silica and polystyrene spheres.[60] While geometry and surface curvature influence the amount of protein adsorbed onto a particle, VTC chemical characteristics such as hydrophobicity and surface charge affects the types of proteins adsorbed onto a particle's surface. For example, proteins with isoelectric points less

than 5.5 (pH where protein charge is neutralized), such as albumin, were shown to have a greater affinity for adsorbing onto positively charged polymeric spheres, whereas negatively charged spheres showed larger amounts of adsorbed proteins with isoelectric points greater than 5.5.[58] A difference in affinity for protein adsorption was also shown to have a direct influence on VTC adhesion. The presence of particular human plasma proteins adsorbed onto poly(lactic-co-glycolic acid) (PLGA), but not polystyrene, targeted microspheres significantly reduced the adhesion of sLe^a-targeted PLGA spheres in human plasma, relative to their adhesion in plasma-free systems.[33] On the other hand, the adhesion of polystyrene spheres to an activated endothelium in blood was not shown to be dependent on exposure to plasma proteins.[33] Hence, optimizing VTC targeting using model drug carriers (i.e. polystyrene spheres) in plasma systems does not guarantee optimal targeting of VTCs made from other materials, such as PLGA, due to the negative effect on adhesion from adsorbed plasma proteins being dependent on VTC material. However, it may be possible to neutralize this material dependency of decreased VTC adhesion due to plasma adsorption using PEGylation.

PEGylation is a strategy often implemented for minimizing plasma protein adsorption and consists of attaching poly(ethylene glycol) (PEG) chains onto a particle's surface through covalent chemistry, physio-adsorption, or during VTC fabrication itself (such as PEG induced stabilization during liposome formulation). The hydrophilic nature of PEG generates a water-shell around the polymer chain which sterically prevents proteins from adsorbing onto a particle's surface.[61] PEGylation for reducing plasma adsorption has been widely studied and shown to increase *in vivo* circulation time and biodistribution, relative to non-PEGylated spheres.[56, 62] Improving circulatory retention and biodistribution in turn increases the probability of tissue targeting, particularly for passive targeting strategies (targeting due to the

physical relationship between VTC and vessel geometry) such as lung entrapment. However, it is unclear what effect PEGylation has on ligand-based targeting, which would require the targeting ligand to be placed on the end of a PEG chain. Previous work with bimodal PEGylated systems (particles PEGylated with different sized PEG spacers) has shown that adhesive dynamics are reduced when the ligand were attached to a PEG spacer that was shorter than adjacent non-ligated PEG chains, due to the steric hindrance provided by the larger PEG chains.[63, 64] PEG chain flexibility was also shown to improve receptor-ligand dynamics resulting in improved adhesive flux under low shear (RBC-free) conditions.[65] However, it remains unclear if the influence of PEG on receptor-ligand dynamics correlates with differences VTC adhesion, relative to non-PEGylated VTCs, in blood under physiological flow conditions. Also, to my knowledge, PEGylation has not been directly examined as a strategy for restoring the adhesion of plasma-sensitive VTCs (VTCs which exhibited reductions in adhesion in plasma systems, relative to plasma-free systems, due to the adsorption of specific plasma proteins) despite the fact that PEGylation has been widely implemented for reducing plasma protein adsorption.

1.1.3.c. Influence of VTC-Leukocyte Dynamics on VTC Function

Even though RBCs constitute the largest subclass of blood cells, particle dynamics with leukocytes play a significant role in blood compatibility and overall VTC efficacy. The primary function of neutrophils, monocytes, and macrophages (subclasses of leukocytes) is to localize to the inflammatory site and remove the foreign entities which induced the inflammatory response (i.e. pathogens during infection). Hence, VTCs present at inflammatory tissue will encounter recruited leukocytes and VTC recognition by phagocytic cells will result in the removal of VTCs from the targeted tissue. As a result, particle-leukocyte dynamics have been primarily

investigated with the intention of minimizing leukocyte phagocytosis and recognition. Particle geometry (size and shape), surface charge, and VTC chemistry have all be explored for minimizing phagocytosis and macrophage clearance from the targeted tissue.[47, 66, 67] However, the influence of leukocytes on VTC design and function is not limited to phagocytosis and systemic clearance. The propensity of leukocytes to marginate to the RBC-free layer and interact with CAMs upregulated during inflammation has significant implications on VTC targeting such that the presence of leukocytes were shown to significantly reduce the adhesion density of E-selectin targeting 2 and 5 μm spheres.[55] This suggests that VTC targeting is sensitive to leukocyte concentration in blood which may be altered due to disease or pharmacological side effects, an assessment that would not be identified if VTC adhesion was only examined in leukocyte-free systems.

It is also important to identify whether the presence of VTCs has any impact on leukocyte function; specifically, do inflammation targeting VTCs influence leukocyte recruitment and adhesion to the same inflammatory tissue? VTCs are targeted to inflammatory tissue through targeting moieties that interact with CAMs (such as E-selectin, ICAM-1, and VCAM-1) which are directly involved in the leukocyte recruitment cascade. Hence in blood flow, the margination of both VTCs and leukocytes to the vessel wall and propensity to interact with upregulated CAMs may create competition for the targeted receptors which may have significant implications on leukocyte recruitment to the targeted vessel wall. While an increase in leukocyte recruitment may potentially accelerate VTC removal from the targeted tissue through leukocyte phagocytosis, reducing leukocyte adhesion may prolong VTC retention and possibly provide additional therapeutic benefits to diseases such as atherosclerosis and reperfusion injury, where leukocyte recruitment contributes to disease pathogenesis. To my

knowledge, the influence of VTCs in blood on leukocyte recruitment to targeted inflammatory tissue has not been thoroughly investigated and whether an effect, if any, from particle-leukocyte dynamics on leukocyte adhesion is sensitive to VTC design (i.e. targeting system, VTC size, and shape).

1.1.3.d. VTCs and Platelet Function

The primary role of platelets is to reduce blood loss during vessel injury. Because of their geometry and difference in elasticity relative to RBCs, platelets readily marginate and circulate the vasculature on the peripheries of the blood vessels. Upon activation or exposure to extracellular matrix proteins (i.e. collagen, fibrinogen), platelets rapidly adhere and aggregate at the injury site to minimize blood loss during vessel injury. Unactivated platelets do not regularly interact with the vessel wall due to the endothelium releasing mediators such as nitric oxide and prostacyclin, which keep circulating platelets in a quiescent state; however, there are cases in which disease pathogenesis is enhanced due to the adhesion of activated platelets to inflamed endothelium.[68] For example, circulating tumor cells (CTCs) activate and aggregate with platelets such that activated platelets coat the CTC's surface and act as a protective shield from systemic clearance. The activated platelets then facilitate CTC adhesion to inflammatory sites followed by CTC migration into tissue.[69] In venous thrombosis, activated platelets initiate blood coagulation on the vessel wall after which the thrombus (aggregated platelets cross-linked with a fibrin network) may rupture due to shear stress and initiate a cardiac event such as a stroke or myocardial infarction (heart attack).[70] For VTCs to be fully biocompatible with blood, it is crucial that they do hinder platelet function where necessary (i.e. vascular injury) or induce platelet activation and aggregation at the targeted tissue.

Conversely, there are situations in which inducing platelet adhesion and aggregation are beneficial such as aiding in the clotting time of patients with thrombocytopenia (low platelet concentration, $<1x10^8$ platelets/mL) or decreased platelet function.[71] Synthetic platelets are VTCs designed to mimic platelet function by adhering to exposed extracellular matrix proteins (ECM) and aggregating with activated platelets to initiate a platelet plug at the site of vessel injury. While collagen is often targeted by synthetic platelets to establish adhesion to injured blood vessels, platelet adhesion and aggregation to the ECM under high shear stress ($>800\ s^{-1}$) involves the interaction between platelets and vWF which is released by locally inflamed endothelium or deposited from soluble forms in plasma.[72] For this reason, platelet mimicking VTCs are often decorated with multiple ligands in order to enable ECM targeting in a range of blood flow rates.[73] Peptides that bind to collagen or vWF have been explored as targeting motifs due to their small size, relative to recombinant proteins, limiting steric hindrance when implemented on nanoparticles and scalability for commercialization.[74] Adhesion to collagen can be established through collagen binding peptides (CBP), which are small sequences of -[Glycine-Proline-Hydroxyproline]$_{7-10}$- that self-assemble with similar sequences exposed on damaged collagen fibers.[74-76] Von Willebrand binding peptides (VBP) have been identified from coagulation factor VIII which is coupled with soluble vWF prior to the initiation of the coagulation cascade.[76] Linear or cyclic Arginine-Glycine-Aspartic Acid (cRGD) is often added to the target system to mediate VTC-platelet co-localization to the ECM and initiate aggregation and platelet plug formation at an injury site.[77] Nano-sized liposomes (150-200 nm) with a tri-peptide targeting system composed of collagen and vWF binding peptides along with, VBP, and cRGD have been shown to effectively mimic platelet function; however, there has been little work examining whether microspheres (2-3 μm in diameter) are equally or more

effective in promoting platelet function due their ability to readily marginate to the vessel wall in blood flow relative to nanospheres.[73-75]

1.2. Summary of Work

The complexity of blood provides a unique challenge when optimizing VTC design for targeting inflammation in blood flow. While RBCs are the largest volume percent of blood cells and 40–45% (by volume) of blood, VTC optimization in leukocyte- or plasma-free systems do not provide the complete dynamic environment of blood for evaluating VTC efficacy. It is also crucial to understand what influences VTCs have on blood cell function such that VTCs designed for treatment do not accelerate or initiate abnormal blood cell function. Investigating whether inflammation targeting particles alter the recruitment of platelets and leukocytes to the same targeted tissue may also have therapeutic benefits for diseases associated with platelet or leukocyte accumulation. The aim of this work is to investigate the relationship between VTC adhesion and the non-RBC components of blood in order to gain insight into how particle-blood dynamics influence VTC design and application. First, the influence of VTC-plasma dynamics on particle adhesion is explored with the PEGylation. Specifically, I investigate whether the strategy of attaching PEG spacers onto a particle's surface for minimizing plasma adsorption influences ligand-based targeting in blood flow and whether there is a dependency on the PEG corona properties (PEG molecular weight, conformation) on adhesion. Once the influence of PEGylation on VTC adhesion in blood is understood via model polystyrene VTCs, I examine if PEGylation can be implemented to improve the adhesion of an actual drug delivery system in blood whose adhesion is sensitive to plasma protein adsorption. I also examine VTC-leukocyte and VTC-platelet dynamics and whether presence of VTCs in blood significantly impacts blood

cell recruitment to an inflamed endothelium to determine if particle-blood cell dynamics influences blood cell function during inflammation. The results from this dissertation have significant impact on improving VTC adhesion in blood flow through PEGylation and raises awareness to a new relationship between circulating VTCs and blood cell function.

1.3. Thesis Outline

Chapter 1 provides background and scope of the dissertation.

Chapter 2 contains the materials, preparations, and protocols for the experiments conducted for Chapters 3 – 6.

Chapter 3 explores the influence of PEGylation on ligand based adhesion of inflammation targeting VTCs in blood. Briefly, 2 μm and 500 nm polystyrene spheres were conjugated with a 2.3 kDa, 5.5 kDa, or 10 kDa PEG spacer at a range of PEG grafting densities. The particle adhesion in laminar blood flow to an activated human umbilical endothelial vein (HUVEC) monolayer was examined over a range of physiological wall shear rates (200 s^{-1}–1,000 s^{-1}) using a parallel plate flow chamber. The results of this work provide insight into the relationship between VTC adhesion in blood and PEGylation, and identify situations where vascular targeting benefits from PEGylation.

Chapter 4 expands on the relationship between PEGylation and VTC adhesion in blood as PEGylation was implored to determine if the addition of PEG can improve the adhesion of a model and actual drug delivery system, which were previously shown to be sensitive to plasma protein adsorption.

Chapter 5 investigates the influence of inflammation targeting VTCs on leukocyte adhesion in blood flow. VTC parameters such as particle size, shape, blood concentration, and

targeting system along with hemodynamics were altered to explore (1) whether VTCs in blood affect the inflammatory recruitment of leukocytes to and activated endothelium, and (2) the dependency of leukocyte adhesion to VTC design and hemodynamics. This work demonstrates that particle-leukocyte dynamics have significant implications on the inflammatory recruitment of leukocytes in blood flow.

Chapter 6 explores the impact of particle-platelet dynamics on platelet adhesion to an activated endothelium and extracellular matrix proteins (collagen and vWF). Specifically, the adhesion of unactivated and activated platelets was examined with presence of 2 μm sLe^a-targeted spheres and spheres containing collagen and vWF binding peptides. The aims of this work was to (1) determine if the presence of sLe^a-targeted spheres alters the homeostatic interaction between an activated endothelium and platelets and (2) whether 2 μm platelet mimicking VTCs can enhance platelet adhesion to collagen or vWF in order to improve clotting time for patients with low platelet concentration in blood. The results of this chapter offer insight into the blood-compatibility of VTCs and their influence on platelet function.

Chapter 7 provides significant conclusions from the experimental work and potential future directions.

References

[1] Grivennikov, S.I., Greten, F.R., and Karin, M., *Immunity, Inflammation, and Cancer*. Cell, 2010. **140**(6): p. 883-899.

[2] Caramori, G. and Adcock, I., *Pharmacology of Airway Inflammation in Asthma and COPD.* Pulmonary Pharmacology & Therapeutics, 2003. **16**(5): p. 247-277.

[3] Clearfield, M., Pearce, M., Nibbe, Y., et al., *The "New Deadly Quartet" for Cardiovascular Disease in the 21st Century: Obesity, Metabolic Syndrome, Inflammation and Climate Change: How does Statin Therapy Fit into this Equation?* Current Atherosclerosis Reports, 2013.

[4] Young, F., Capewell, S., Ford, E.S., et al., *Coronary Mortality Declines in the U.S. Between 1980 and 2000: Quantifying the Contributions from Primary and Secondary Prevention.* American Journal of Preventive Medicine, 2010. **39**(3): p. 228-234.

[5] Insull, W., *The Pathology of Atherosclerosis: Plaque Development and Plaque Response to Medical Treatment.* The American Journal of Medicine, 2009. **122**(1A): p. S3-S14.

[6] Libby, P., Ridker, P.M., Maseri, A., *Inflammation and Atherosclerosis*. Circulation, 2002. **105**: p. 1135-1143,

[7] Wierzbicki, A.S., *New Directions in Cardiovascular Risk Assessment: the Role of Secondary Risk Stratification Markers.* International Journal of Clinical Practice, 2012. **66**(7): p. 622-630.

[8] Quillard, T. and Libby, P., *Molecular Imaging of Atherosclerosis for Improving Diagnostic and Therapeutic Development.* Circulation Research, 2012. **111**: p. 231-244.

[9] Weber, C. and Noels, H., *Atherosclerosis: Current Pathogenesis and Therapeutic Options.* Nature Medecine, 2011. **17**(11): p. 1410-1422.

[10] Sadowitz, B., Maier, K.G., and Gahtan, V., *Basic Science Review: Statin Therapy-Part-I: The Pleiotropic Effects of Statins in Cardiovascular Disease.* Vascular and Endovascular Surgery, 2010. **44**(4): p. 241-251.

[11] Undas, A., Brummel-Ziedins, K.E., and Mann, K.G., *Statins and Blood Coagulation.* Arteriosclerosis, Thrombosis, and Vascular Biology, 2005. **25**: p. 287-294.

[12] Weber, C., Erl, W., C., W.K.S., et al., *HMG-CoA Reduetase Inhibitors Decrease CD11b Expression and CD11b-Dependent Adhesion of Monocytes to Endothelium and Reduce Increased Adhesiveness of Monocytes Isolated from Patients with Hypercholesterolemia.* JACC, 1997. **30**(5): p. 1212-1217.

[13] Alfon, J., Palazon, C.P., Royo, Y., et al., *Effects of Statins in Thrombosis and Aortic Lesions Development in a Dyslipemic Rabbit Model.* Thrombosis and Haemostasis, 1999. **81**: p. 822-827.

[14] Tedgui, A. and Mallat, Z., *Cytokines in Atherosclerosis: Pathogenic and Regulatory Pathways.* Physiological Reviews, 2006. **86**(2): p. 515-581.

[15] Warner, S.J. and Libby, P., *Human Vascular Smooth Muscle Cells. Target for and Source of Tumor Necrosis Factor.* Journal of Immunology, 1989. **142**: p. 100-109.

[16] Warner, S.J., Auger, K.R., and Libby, P., *Human Interleukin 1 Gene Expression in Human Vascular Smooth Muscle Cells.* Journal of Exploratory Medecine, 1987. **165**: p. 1316-1331.

[17] Springer, T.A, *Traffic Signals for Lymphocyte Recirculation and Leukocyte Emigration: The Multistep Paradign.* Cell, 1994. **76**: p. 301-314.

[18] Wyble, C.W., Desai, T.R., Clark, E.T., et al., *Physiologic Concentrations of TNFα and IL-1β Released from Reperfused Human Intestine Upregulate E-selectin and ICAM-1*. Journal of Surgical Research, 1996. **63**: p. 333-338.

[19] Haraldsen, G., Kvale, D., Lien, B., et al., *Cytokine-Regulated Expression of E-selectin, Intercellular Adhesion Molecule-1 (ICAM-1), and Vascular Cell Adhesion Molecule-1 (VCAM-1) in Human Intestinal Microvascular Endothelial Cells.* Journal of Immunology, 1996. **156**(7): p. 2558-265.

[20] Lowe, J.B., *Selectin Ligands, Leukocyte Trafficking, and Fucosultransferase Genes.* Kidney International, 1997. **51**: p. 1418-1426.

[21] Nelson, R.M., Dolich, S., Aruffo, A., et al., *Higher-affinity Oligosaccharide Ligands for E-selectin.* Journal of Clinical Investigation, 1993. **91**(3): p. 1157-1166.

[22] Sullivan, G.W., Sarembock, I.J., and Linden, J., *The Role of Inflammation in Vascular Diseases.* Journal of Leukocyte Biology, 2000. **67**: p. 591-602.

[23] Davie, M.J., Gordon, J.L., Gearing, A.J.H., et al., *The Expression of the Adhesion Molecules ICAM-1, VCAM-1, PECAM, and E-selectin in Human Atherosclerosis.* Journal of Pathology, 1993. **171**: p. 223-229.

[24] Muller, A.M., Hermanns, M.I., Cronen, C., et al., *Comparative Study of Adhesion Molecule Expression in Cultured Human Macro- and Microvascular Endothelial Cells.* Experimental Molecular Pathology, 2002. **73**: p. 171-180.

[25] Schwendener, R.A., *Liposomes as Vaccine Delivery Systems: A Review of the Recent Advances.* Therapeutic Advances in Vaccines, 2014. **2**(6): p. 159-182.

[26] Allen, T.M. and Cullis, P.R., *Liposomal Drug Delivery Systems: From Concept to Clinical Applications.* Advanced Drug Delivery Reviews, 2013. **65**(1): p. 36-48.

[27] Song, L.Y., Ahking, Q.F., Rong, Q., et al., *Characterization of the Inhibitory effect of PEG-lipid Conjugates on the Intracellular Delivery of Plasmid and Antisense DNA Mediated by Cationic Lipid Liposomes.* Biochemica et Biophysica Acta - Biomembranes, 2002. **1558**(1): p. 1-13.

[28] Shi, F., Wasungu, L., Nomben, A., et al., *Interference of Poly(ethylene glycol)-Lipid Analogues with Cationic-lipid-mediated Delivery of Oligonucleotides; Role of Lipid Exchangeability and Non-Lamellar Transition.* Biochemical Journal, 2002. **366**: p. 333-341.

[29] Slowing, I.I., Trewyn, B.G., Giri, S., et al., *Mesoporous Silica Nanoparticles for Drug Delivery and Biosensing Applications.* Advanced Functional Materials, 2007. **17**(8): p. 1225-1236.

[30] Tassa, C., Shaw, S.Y., and Weissleder, R., *Dextran-Coated Iron Oxide Nanoparticles: A Versatile Platform for Targeted Molecular Imaging, Molecular Diagnostics, and Therapy.* Accounts of Chemical Research, 2011. 44(10): p. 842-852.

[31] Sah, H., Thoma, L.A., Desu, H.R., et al., *Concepts and Practices Used to Develop Functional PLGA-based Nanoparticulate Systems.* International Journal of Nanomedicine, 2013. **8**: p. 747-765.

[32] Mohamed, F., Christopher, F., and Walle, V.D., *Engineering Biodegradable Polyester Particles With Specific Drug Targeting and Drug Release Properties.* Journal of Pharmaceutical Sciences, 2007. **97**(1): p. 71-87.

[33] Sobczynski, D., Charoenphol, P., Heslinga, M., et al., *Plasma Protein Corona Modulates the Vascular Wall Interaction of Drug Carriers in a Material and Donor Specific Manner.* PLoS ONE, 2014. **9**(9): p. e107408.

[34] Freitas, S., Merkle, H.P., and Gander, B., *Microencapsulation by Solvent Extraction/Evaporation: Reviewing the State of the Art of Microsphere Preparation Process Technology.* Journal of Controlled Release, 2005. **102**: p. 313-332.

[35] Heslinga, M., Willis, G.M., Sobczynski, D., et al., *One-step Fabrication of Agent-loaded Biodegradable Microspheroids for Drug Delivery and Imaging Applications.* Colloids and Surfaces B: Biointerfaces, 2014. **116**: p. 55-62.

[36] Charoenphol, P., Huang, R.B., and Eniola-Adefeso, O., *Potential Role of Size and Hemodynamics in the Efficacy of Vascular-Targeted Spherical Drug Carriers.* Biomaterials, 2010. **31**(6): p. 1392-1402.

[37] Namdee, K., Thompson, A.J., Phapanin, C., et al., *Margination Propensity of Vascular-Targeted Spheres from Blood Flow in a Microfluidic Model of Human Microvessels.* Langmuir, 2013. **29**(8): p. 2530-2535.

[38] Eniola-Adefeso, O., Willcox, J., and Hammer, D.A., *Interplay Between Rolling and Firm Adhesion Elucidated with a Cell-free System Engineered with Two Distinct Receptor-Ligand Pairs.* Biophysical Journal, 2003. **85**: p. 2720-2731.

[39] Nakashima, Y., Raines, E.W., Plump, A.S., et al., *Upregulation of VCAM-1 and ICAM-1 at Atherosclerosis-Prone Sites on the Endothelium in ApoE-Deficient Mouse.* Arteriosclerosis, Thrombosis, and Vascular Biology, 1998. **18**: p. 842-851

[40] Namdee, K., Thompson, A.J., Golinski, A., et al., *In Vivo Evaluation of Vascular-Targeted Spheroidal Microparticles for Imaging and Drug Delivery Applications in Atherosclerosis.* Atherosclerosis, 2014. **237**(1): p. 279-286.

[41] O'Brian, K.D., McDonald, T.O., Chait, A., et al., *Neovascular Expression of E-selectin, Intercellular Adhesion Molecule-1, and Vascular Cell Adhesion Molecule-1 in Human Atherosclerosis and Their Relation to Intimal Leukocyte Content.* Circulation, 1996. **93**: p. 672-682.

[42] Thompson, A.J., Mastria, E.M., and Eniola-Adefeso, O., *The Margination Propensity of Ellipsoidal Micro/Nanoparticles to the Endothelium in Human Blood Flow.* Biomaterials, 2013. **34**(23): p. 5863-5871.

[43] Gentile, F., Chiappini, C., Fine, D., et al., *The Effect of Shape on the Margination Dynamics of Non-neutrally Buoyant Particles in Two-Dimensional Shear Flows.* Journal of Biomechanics, 2008. **41**(10): p. 2312-2318.

[44] Toy, R., Hayden, E., Shoup, C., et al., *The Effects of Particle Size, Density and Shape on Margination of Nanoparticles in Microcirculation.* Nanotechnology, 2011. **22**(11).

[45] Lee, S.Y., Ferrari, M., and Decuzzi, P., *Shaping Nano-/Micro-particles for Enhanced Vascular Interaction in Laminar Flows.* Nanotechnology, 2009. **20**(49).

[46] Decuzzi, P., Godin, B., Tanaka, T., et al., *Size and Shape Effects in the Biodistribution of Intravascularly Injected Particles.* Journal of Controlled Release, 2010. **141**(3): p. 320-327.

[47] Champion, J.A. and Mitragotri, S., *Role of Target Geometry in Phagocytosis.* PNAS, 2006. **103**(13): p. 4930-4934.

[48] Cirillo, M., Laurenzi, M., Trevisan, M., et al., *Hematocrit, Blood Pressure, and Hypertention.* Hypertention, 1992. **20**: p. 319-326.

[49] Muller, K., Fedosov, D.A., and Gompper, G., *Margination of Micro- and Nano-particles in Blood Flow and its Effect on Drug Delivery.* Scientific Reports, 2014. **4**.

[50] Kumar, S. and Graham, M.D., *Margination and Segregation in Confined Flows of Blood and Other Multicomponent Suspensions.* Soft Matter, 2012. **8**: p. 10536-10548.

[51] Huang, R.B., Mocherla, S., Heslinga, M.J., Charoenphol, P., Eniola-Adefeso, O., *Dynamic and Cellular Interactions of Nanoparticles in Vascular-Targeted Drug Delivery (Review)*, 2010.**27**(4-6): p. 190-205.

[52] Matharu, N.M., Rainger, G.E., Vohra, R., et al., *Effects of Disturbed Flow on Endothelial Cell Junction: Pathogenic Implications of Modified Leukocyte Recruitment.* Biorheology, 2006. **43**: p. 31-44.

[53] Chiu, J.J. and Chien, S., *Effects of Disturbed Flow on Vascular Endothelium: Pathophysiological Basis and Clinical Perspectives.* Physiological Reviews, 2011. **91**(1): p. 327-387.

[54] Charoenphol, P., Onyskiw, P.J., Carrasco-Teja, M., et al., *Particle-cell Dynamics in Human Blood Flow: Implications for Vascular-Targeted Drug Delivery.* Journal of Biomechanics, 2012. **45**(16): p. 2822-2828.

[55] Charoenphol, P., Mocherla, S., Bouis, D., et al., *Targeting Therapeutics to the Vascular Wall in Atherosclerosis - Carrier Size Matters.* Atherosclerosis, 2011. **217**(2): p. 364-370.

[56] Owens III, D.E. and Peppas, N.A., *Opsinization, Biodistribution, and Pharmacokinetic of Polymeric Nanoparticles*. International Journal of Pharmaceutics, 2006. **307**(1): p. 93-102.

[57] Terakita, *The Opsins.* Genome Biology, 2005. **6**.

[58] Aggarwal, P., Hall, J.B., McLeland, C.B., et al., *Nanoparticle Interaction with Plasma Proteins as it Relates to Particle Biodistribution, Biocompatibility and Therapeutic Efficacy.* Advanced Delivery Reviews, 2009. **61**(6): p. 428-437.

[59] Cedervall, T., Lynch, I., Foy, M., et al., *Detailed Identification of Plasma Proteins Adsorbed on Copolymer Nanoparticles.* Angewandte Chemie, 2007. **46**: p. 5754-5756.

[60] Gessner, A., Paulke, B., and Muller, R., *Influence of Surface Charge Density on Protein Adsorption on Polymeric Nanoparticles: Analysis by Two-Dimensional Electrophoresis.* European Journal of Pharmaceutics and Biopharmaceutics, 2002. **54**(2): p. 165-170.

[61] Wattendorf, U. and Merkle, H.P., *PEGylation as a Tool for the Biomedical Engineering of Surface Modified Microparticles.* Journal of Pharmaceutical Science, 2008. **97**(11): p. 4655-4669.

[62] Moghimi, S.M. and Szebeni, J., *Stealth Liposomes and Long Circulating Nanoparticles: Critical Issues in Pharmacokinetics, opsonization and Protein-binding Properties.* Progress in Lipid Research, 2003. **42**(6): p. 463-478.

[63] Needham, D. and Kim, D.H., *PEG-covered Lipid Surfaces: Bilayers and Monolayers.* Colloids and Surfaces B: Biointerfaces, 2000. **18**: p. 183-195.

[64] Kim, D.H., Klibanov, A.L., and Needham, D., *The Influence of Tiered Layers of Surface-Grafted Poly(ethylene glycol) on Receptor-Ligand-Mediated Adhesion between Phospholipod Monolayer-Stabilized Microbubbles and Coated Glass Beads.* Langmuir, 2000. **16**: p. 2808-2817.

[65] Ham, A.S., Klibanov, A.L., and Lawrence, M.B., *Action at a Distance: Lengthening Adhesion Bonds with Poly(ethylene glycol) Spacers Enhances Mechanically Stressed Affinity for Improved Vascular Targeting of Microparticles.* Langmuir, 2009. **25** (17): p. 10038-10044.

[66] He, C., Hu, Y., Yin, L., et al., *Effects of Particle Size and Surface Charge on Cellular Uptake and Biodistribution of Polymeric Nanoparticles.* Biomaterials, 2010. **31**(13): p. 3657-3666.

[67] Doshi, N. and Mitragotri, S., *Macrophages Recognize Size and Shape of Their Targets.* PLoS ONE, 2010. **5**(4): p. e10051.

[68] Klinger, M.H.F. and Jelkmann, W., *Role of Blood Platelets in Infection and Inflammation.* Journal of Interferon & Cytokine Research, 2002. **22**: p. 913-922.

[69] Gay, L.J. and Felding-Habermann, B., *Contribution of Platelets to Tumor Metastasis.* Nature Reviews Cancer, 2011. **11**(123-134). doi:10.1038/nrc3004.

[70] Turpie, A. and Emson, C., *Venous and Arterial Thrombosis - Pathogenesis and the Rationale for Anticoagulation.* Thrombosis and Haemostasis, 2011. **105**.

[71] Lee, G.M., Arepally, G. M., *Diagnosis and Management of Heparin-Induced Thrombocytopenia.* Hematol. Oncol. Clin. North Am., 2013. **27**(3): p. 541-563.

[72] Ikeda, Y., Handa, M., Kawano, K., et al., *The Role of von Willebrand Factor and Fibrinogen in Platelet Aggregation Under Varying Shear Stress.* Journal of Clinical Investigation, 1991. **87**(4): p. 1234-1240.

[73] Modery-Pawlowski, C.L., Tian, L.L., Pan, V., et al., *Approaches to Synthetic Platelet Analogs.* Biomaterials, 2013. **34**(2): p. 526-541.

[74] Cejas, M.A., Kinney, W.A., Chen, C., et al., *Thrombogenics Collagen-Mimetic Peptides: Self-Assembly of Triple Helix-Based Fibrils Driven by Hydrophobic Interactions.* PNAS, 2008. **105**(25): p. 8513-8518.

[75] Ravikumar, M., Modery, C.L., Wong, T.L., et al., *Peptide-Decorated Liposomes Promote Arrest and Aggregation of Activated Platelets under Flow on Vascular Injury Relevant Protein Surfaces in Vitro.* Biomacromolecules, 2012. **13**: p. 1495-1502.

[76] Nogami, K., Shima, M., Giddings, J.C., et al., *Relationship Between the Binding Sites for von Willebrand Factor, Phospholipid, and Human Factor VIII C2 Inhibitor Alloantibodies within the Factor VIII C2 Domain.* International Journal of Hematology, 2007. **85**: p. 317-322.

[77] Huang, G., Zhou, Z., Srinivasan, R., et al., *Affinity Manipulation of Surface-Conjugated RGD-Peptide to Modulate Binding of Liposomes to Activated Platelets.* Biomaterials, 2009. **29**(11): p. 1676-1685.

CHAPTER 2

MATERIALS AND METHODS

This chapter describes all protocols, in detail, particle and blood preparation, and blood along with adhesion assays. In general, particles were ligated using avidin-biotin coupling and ligand densities determined using flow cytometry. Flow assays were conducted using a parallel plate flow chamber and human blood (Chapters 3-6) or pig blood (Chapter 4) at 37°C. Particle, platelet, and leukocyte adhesion to an activated human umbilical vein endothelial cell monolayer (HUVEC) was assessed via brightfield or fluorescent microscope equipped with a digital camera and the adhesion densities normalized to imaged surface area.

2.1. Materials

Carboxylated polystyrene spheres (5.01 μm, 5.07 μm, and 2.07 μm), streptavidin spheres (200 nm), Quantum PE and FITC MESF calibration beads were purchased from Bangs Laboratories (Fishers, IN); carboxylated polystyrene spheres (2.1 μm, 3.1 μm, 0.5217 μm) were purchased from Polysciences, Inc. (Warrington, PA); NeutrAvidin and Avidin-fluorescein was purchased from Pierce Protein Biology Products-Thermo Fisher Scientific, Inc. (Rockford, IL); Biotinylated-PEG-Amine (2.3 kDa, 5.5 kDa, and 10 kDa) was purchased from Laysan Bio, Inc. (Arab, AL); multivalent biotinylated Sialyl Lewis[a] and parallel plate flow chamber were purchased from GlycoTech (Gaithersburg, MD); biotinylated human ICAM-1 antibody (aICAM) clone BBIG-11, thrombin were purchased from R&D Systems (Pittsburgh, PA); biotinylated-

PEG(3.4 kDa)-collagen binding peptide, biotinylated-PEG(3.4 kDa)-collagen binding peptide-fluorescein, biotinylated-PEG(3.4 kDa)-vWF binding peptide, and cyclic RGD peptide were synthesized by Dr. Anirban Sen Gupta's research group (Case Western Reserve University, Cleveland, OH); biotin-fluorescein was purchased from Molecular Probes (Carlsbad, CA); PE-labeled anti-human cutaneous lymphocyte antigen, PE-labeled anti-biotin were purchased from Miltenyi Biotec (San Diego, CA); goat anti-mouse IgG-fluorescein was purchased from Jackson Immuno Research Labs (West Grove, PA); PE-labeled rat IgM isotype and endothelial cell growth supplement were purchased from BD Biosciences (San Jose, CA); M199, fungizone, penicillin/streptomycin, HEPES buffer were purchased from, calcein AM green were purchased from LifeTechnologies (Grand Island, NY); Hyclone bovine calf serum, Hyclone phosphate buffered saline (minus calcium and magnesium ions), and glutamine, glutaraldehyde, acetic acid, Gibco phosphate buffered saline (with magnesium and calcium ions) were purchased from Thermo-Fisher Scientific (Rockford, IL); fetal bovine calf serum was purchased from Cell Generation (Fort Collins, CO); collagen type I form rat tail was purchased from Olaf Pharmaceuticals (Worcester, MA); vWF was purchased from Haematologic Technologies Inc. (Essex Junction, VT) ; recombinant human interleukin-1β was purchased from Fitzgerald Industries International (Concord, MA); poly(D, L-lactide-co-glycolide) 50:50 acid terminated polymers (2.5 A and 1 A inherent viscosity) were purchased from Evonik Industries (Birmingham, AL); collagenase was purchased from Worthington (Lakewood, NJ).; heparinized pig blood was purchased from Lampire Biological Laboratories (Pipersville, PA); poly(vinyl) alcohol, poly(ethylene-alt-maleic anhydride), adenosine diphosphate, and all other chemicals and reagents were purchased from Sigma Aldrich (St. Louis, MO).

2.2. PLGA Particle Fabrication

PLGA microspheres were prepared using an oil-in-water emulsion evaporation technique.[1] 50:50 PLGA polymer with carboxylic acid terminal group was dissolved in 20 mL of dichloromethane (10 mg/mL) and injected into 90 mL of aqueous buffer mixtures composed of 3 wt.% surfactant (95% poly(vinyl alcohol)/5% poly(ethylene-alt-maleaic acid) (PEMA), Table 4.1), 1% PEMA (Table 4.2), or 2% PEMA (Table 4.3) under mixing at 1,800 RPMs. The emulsion mixed for 2 hours to allow for dichloromethane evaporation. Differential centrifugation was utilized to wash and isolate microspheres with diameters between 2-3 μm. PLGA particles were then resuspended in water (3 mL) and instantaneously frozen in liquid nitrogen before drying using a lyophilized for 24-36 hours. After drying, the particles were immediately used for avidin or PEG conjugation followed by use in flow assays. Particles were imaged by brightfield microscopy using a Nikon TE-2000-S inverted microscope with a digital camera (Photometrics CoolSNAP EZ with a Sony CCD sensor) and the particle size measured by digital analysis using Metamorph® imaging software with a calibrated digital scale. A sample image for PLGA spheres used in Chapter 4 is shown in Fig. 2.1.

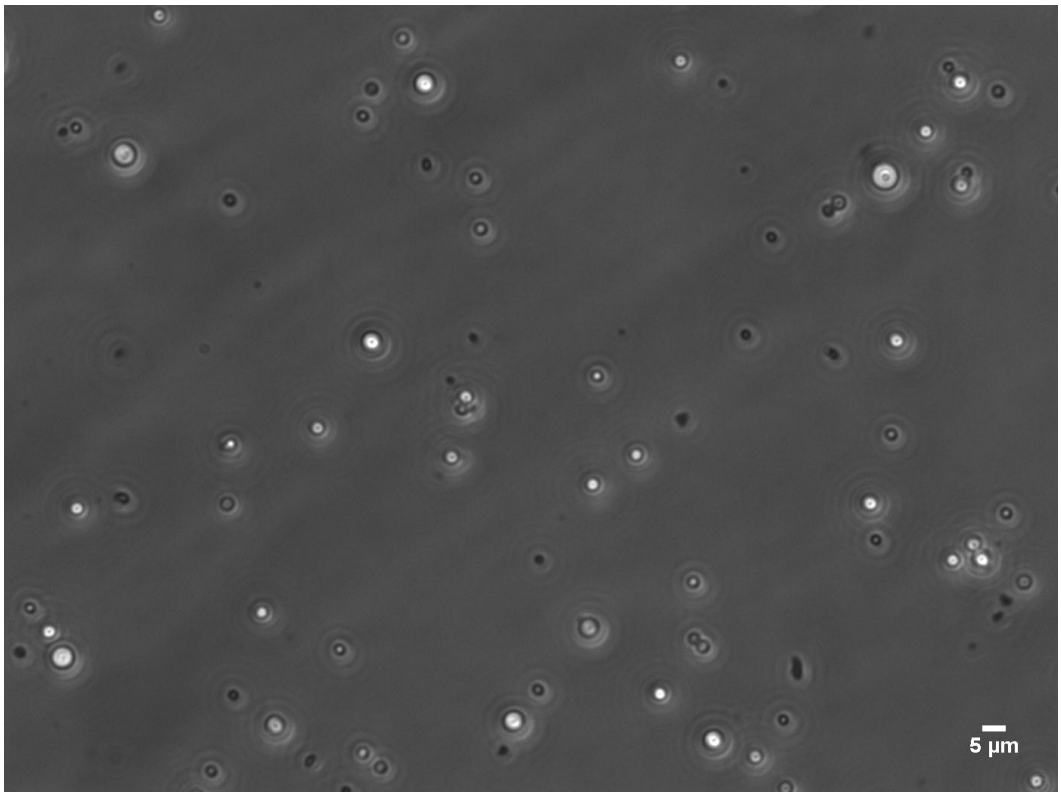

Figure 2.1. Sample image of PLGA spheres used in Chapter 4.

2.3. Fabrication of Polystyrene Rods

Polystyrene rods were fabricated using a polymer film stretching method.[2, 3] 2.1 μm polystyrene spheres were suspended in a 5% poly(vinyl alcohol) solution in a rectangular plastic tray and allowed to dry overnight. The dried films were extracted from the tray and sliced into strips (2 cm x 6 cm or 2 cm x 4.5 cm for aspect ratio 4 or 9, respectfully) before being placed in an 1-dimensional stretching device composed of a parallel clamp system with one clamp movable and the other remaining stationary. The stretching device was contained inside of an oven with a set temperature of 170°C. The films were allowed to reach temperature for 20 minutes before being stretched uniaxially to produce rods. After stretching, the strips were soaked in a 30% isopropanol-water solution overnight to removed residual poly(vinyl alcohol). The rod solution was then washed and centrifuged multiple times with 30% isopropanol-water solution and dried overnight before imaging using a scanning electron microscope (SEM, Phillips XL30 FEG ESEM). The aspect ratio (AR) was calculated by the ratio of the major axis length to the minor axis length measured from the imaged rods. Sample images of 2 μm equivalent volume AR4 and AR9 rods are shown in Fig. 2.2.

(A) AR4 Rods

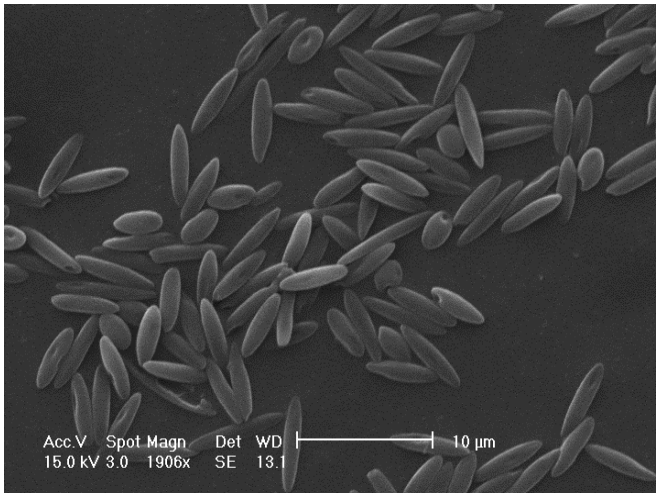

(B) AR9 Rods

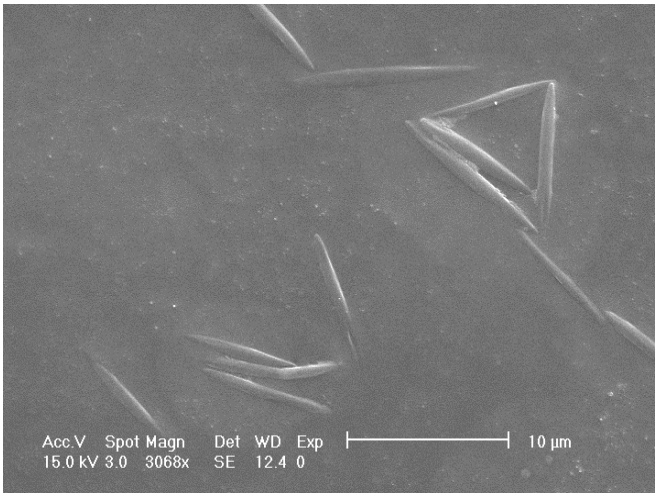

Figure 2.2. SEM images of (A) AR4 and (B) AR9 polystyrene rods used in Chapter 5.

2.4. NeutrAvidin or PEG Attachment to Carboxylated Nano- and Microspheres

NeutrAvidin or Amine-PEG-biotin was covalently coupled to carboxylated polystyrene/PLGA spheres or ellipsoids via carbodiimide chemistry. Carboxylated particles were premixed with 0.2–5 mg/mL of amine-PEG-biotin or 5 mg/mL of NeutrAvidin in MES buffer (97.6 mg/mL) for 15 minutes; after which, equal volume (75 mg/mL) of N-(3-Dimethilaminopropyl)-N'-ethylcarboiimide hydrochloride (EDAC) was added and the pH adjusted to 9. The mixture was then incubated at room temperature for 20 hours at room temperature. For PEGylated microspheres with high PEG density (~35,000 PEG chains/μm^2, Chapter 4), particles were prepared and conjugated in MES buffer (97.6 mg/mL) with 0.6 M Na_2SO_4 for 20 hours at 60ºC. After conjugation, PEGylated or NeutrAvidin spheres were thoroughly washed and stored in 50 mM phosphate buffered saline (PBS).

2.5. Ligand Attachment to NeutrAvidin or PEGylated VTCs

Biotinylated Sialyl Lewis^a (sLe^a) or biotinylated human-anti-ICAM-1-mouse-IgG-1 (aICAM-1) was incubated with the NeutrAvidin conjugated spheres and mixed end-over-end for 45 minutes at room temperature with ligand concentrations corresponding to the desired ligand density (measured by flow cytometry). For ligand attachment to PEGylated spheres, biotinylated ligands were first premixed with 20 µg/mL NeutrAvidin at an equal volume ratio for 20 minutes followed by incubation with PEGylated spheres (100 µL total volume) for 45 minutes at room temperature.[4] For Collagen binding/vWF binding and cRGD peptides, NeutrAvidin coated polystyrene microsphere (2 µm) were incubated with 50-50 mixtures of CBP/VBP and cRGD (5 µg/mL CBP/VBP and 5 µg/mL cRGD working concentrations) for 45 minutes at room temperature. Ligated spheres were washed and stored in PBS buffer containing calcium and

magnesium ions and 1% bovine-serum-albumin (BSA).

2.6. Determination of PEG and Ligand Surface Density

The surface densities of PEG and targeting ligands on spheres were characterized via flow cytometry (BD FACSCalibur, Life Technologies Attune, BD Quanta SC). For measurement of microsphere PEG-biotin surface density, PEGylated spheres were stained with avidin-FITC at 10 µg/mL for 20 minutes at room temperature. For FITC-loaded nanospheres, anti-biotin-PE was used for PEG-biotin surface density measurements. For measurement of ligand surface density, anti-cutaneous lymphocyte antigen-PE or goat-anti-mouse IgG-FITC were used to label sLe^a or aICAM-1, respectfully. Goat-anti-mouse IgG-PE was used to determine the site density of aICAM-1 on nanospheres. Fluorescent intensities were converted to surface densities via a standard calibration curve, fluorescein-to-protein ratio, and microsphere surface area.

2.7. Characterization of PEG Corona

The conformation of the PEG corona was characterized by comparing the distance between adjacent PEG chains (S) to the Flory's radius (R_f) given by the following equations:

$$R_f = aN^{0.64} \quad (2.1) \quad [5]$$

$$S = 2\sqrt{\frac{A}{\pi}} \quad (2.2)$$

where a is the length of one PEG monomer (0.35 nm), N is the number of PEG monomers obtained from the PEG molecular weight divided by the molecular weight of one PEG monomer, and A is the surface area occupied by one PEG chain calculated from the inverse of the PEG surface grafted density (# PEG chains/nm^2). The PEG corona conformation was estimated using

the following criteria (Fig. 2.3): [6]

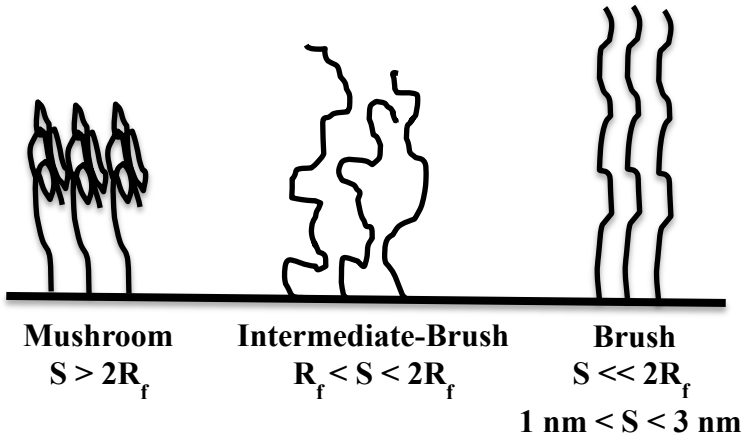

Figure 2.3. Schematic orientation of the PEG corona as estimated by the relationship between the PEG spacer's Flory's Radius (R_f) and distance between adjacent PEG chains (*S*), as calculated by equations 2.1 and 2.2, respectfully.[6]

2.8. Preparation of Endothelial Cell Monolayers

Human umbilical vein endothelial cells (HUVECs) used in all adhesion assays were isolated from fresh umbilical cords (Mott Children's Hospital, Ann Arbor, MI) via collagenase perfusion method pooled from multiple donate umbilical cords.[7] HUVECs were cultured onto 0.2 wt.% gelatin pretreated T-75 culture flasks with M199 medium composed of the following: 10% BCS, 10% FBS, 1% penicillin-streptomycin, 1% fungizone, 1% HEPES buffer, 1 µg/mL heparin 1% glutamine, and 50 µg/mL endothelial cell growth supplement. For flow experiments, HUVECs were cultured onto 30 mm glass coverslips coated with 1% gelatin cross-linked with 0.5% glutaraldehyde and 0.1 M glycine. Coverslips with cultured cells were incubated at 37ºC and 5% CO_2 to allow growth to confluency.[8] Confluent monolayers were activated with 1 ng/mL interleukin-1β (IL-1β) for 4 hours for E-selectin, 4 hours for ICAM-1 (Chapter 5), or 24

hours for ICAM-1 (Chapter 3) prior to use in adhesion assays.

2.9. Preparation of Collagen or vWF Surfaces

Flexiperm gaskets (1 cm x 2 cm) were placed on 30 mm glass coverslips in order to define the coverslip surface area prior to collagen or vWF surface coating. 30 mm glass coverslips were coated with vWF or denatured collagen (500 µg/mL) prepared in PBS buffer or 0.2 M acetic acid, respectfully, and coated onto the defined surface area for 2 hours with gentle shaking at room temperature. The protein solution was then removed and the coated area rinsed twice with PBS buffer (with calcium and magnesium ions). In order to minimize non-specific interaction between blood cells and non-coated glass, the defined coverslip area was then coated with 3% denatured BSA for a minimum of 1 hour and until use in flow assay. Before use in flow assay the BSA solution was removed and coverslip rinsed twice with PBS buffer (with calcium and magnesium ions).

2.10. Blood Preparation

For human whole blood assays (Chapters 3-5), fresh human blood was obtained via venipuncture according to a protocol approved by the University of Michigan Internal Review Board and in line with the standards set by the Helsinki Declaration.[9] Appropriate informed consent was obtained from human subjects. Venous blood was collected from healthy adults into a syringe containing citric acid-sodium citrate-dextrose (ACD) as anticoagulant.

For pig blood preparation (Chapter 4), unspecified Na heparinized pig blood was purchased from Lampire Biological Laboratory (Pipersville, PA). Whole blood was centrifuged at 1,000 g for 30 minutes in order to separate the RBCs from platelet rich plasma. The leukocyte

buffer layer at the RBC-plasma interface was discarded to remove leukocytes. Pig RBCs were washed 3 times with cold PBS buffer (no calcium or magnesium ions) at 1,000 g for 30 minutes. Pig platelets were separated from plasma by centrifuging the platelet-rich-plasma at 2,250 g for 25 minutes. Pig RBCs were reconstituted in flow buffer (PBS buffer with 1% BSA with calcium and magnesium ions) or viscous buffer (flow buffer with 2 wt.% dextran) at the same hematocrits (volume % RBCs) as pig whole blood. Pig whole blood samples were not treated with centrifugation. All blood samples were pre-warmed to 37°C before use in flow assay.

For reconstituted blood used in Chapter 6, human whole blood was centrifuged twice at 300 g for 10 minutes to isolate red blood cells from plasma containing leukocytes and platelets. The platelet and leukocyte plasma was centrifuged at 300 g for 10 minutes to removed leukocytes from platelet-right-plasma which was then centrifuged at 1,000 g for 10 minutes to isolate platelets. Platelets were washed with CGS buffer (120 mM sodium chloride, 13 mM sodium citrate, 30 mM glucose) containing PGE_1 (75 nM). After washing, platelets where resuspended in Tyrodes Buffer (500 mL DI-water, 4.095 g NaCl, 0.1 g KCl, 0.505 g $NaHCO_3$, 0.0275 g NaH_2PO_4, and 0.4955 g Glucose) and stored at room temperature. Platelets were stained with calcein green AM (2.5 µM in DMSO) for 20 minutes and washed three times with CGS buffer with PGE before adding platelets to reconstituted blood and perfused through the flow channel.

2.11. Flow Adhesion Assay Setup

A parallel plate flow chamber (PPFC, Glycotech) was used for all *in vitro* flow adhesion assays. The PPFC was equipped with tygon tubing for the inlet feed, outlet, and vacuum lines. A rectangular silicon gasket (2 cm x 1 cm x 0.0254 cm) was placed on the PPFC to define the

flow channel. Activated HUVEC cultured onto coverslips were placed onto the PPFC (cell side up onto the gasket, i.e. PPFC on top of culture HUVEC monolayer) and held in place via vacuum. The flow channel was gently rinsed with PBS flow buffer (with calcium and magnesium ions and 1% BSA) to removed air bubbles and cell debris prior to the start of the flow assay. Ligand-coated spheres were added to blood at various concentrations ($5x10^5$ particles/mL for Chapters 3, 4, and 6; $5x10^5$ – $1x10^7$ particles/mL for Chapter 5) and perfused over the activated monolayer using a programmable syringe pump (KD Scientific, model no. 780212, Holliston, MA). All flow adhesion assays where conducted at 37°C. After the flow assay, the monolayer was rinsed with flow buffer and the monolayer imaged using a Nikon TE-2000-S inverted microscope with a digital camera (Photometrics CoolSNAP EZ with a Sony CCD sensor). Sample images of HUVEC monolayer with particles are shown in Fig 2.4. For the microchannel flow assays (Chapter 3), a polydimethylsiloxane (PDMS) flow channel was cast from a designed template as previously described.[10] The microchannel used in the flow assays in Chapter 3 was fabricated by Katawut Namdee from the Eniola Lab.

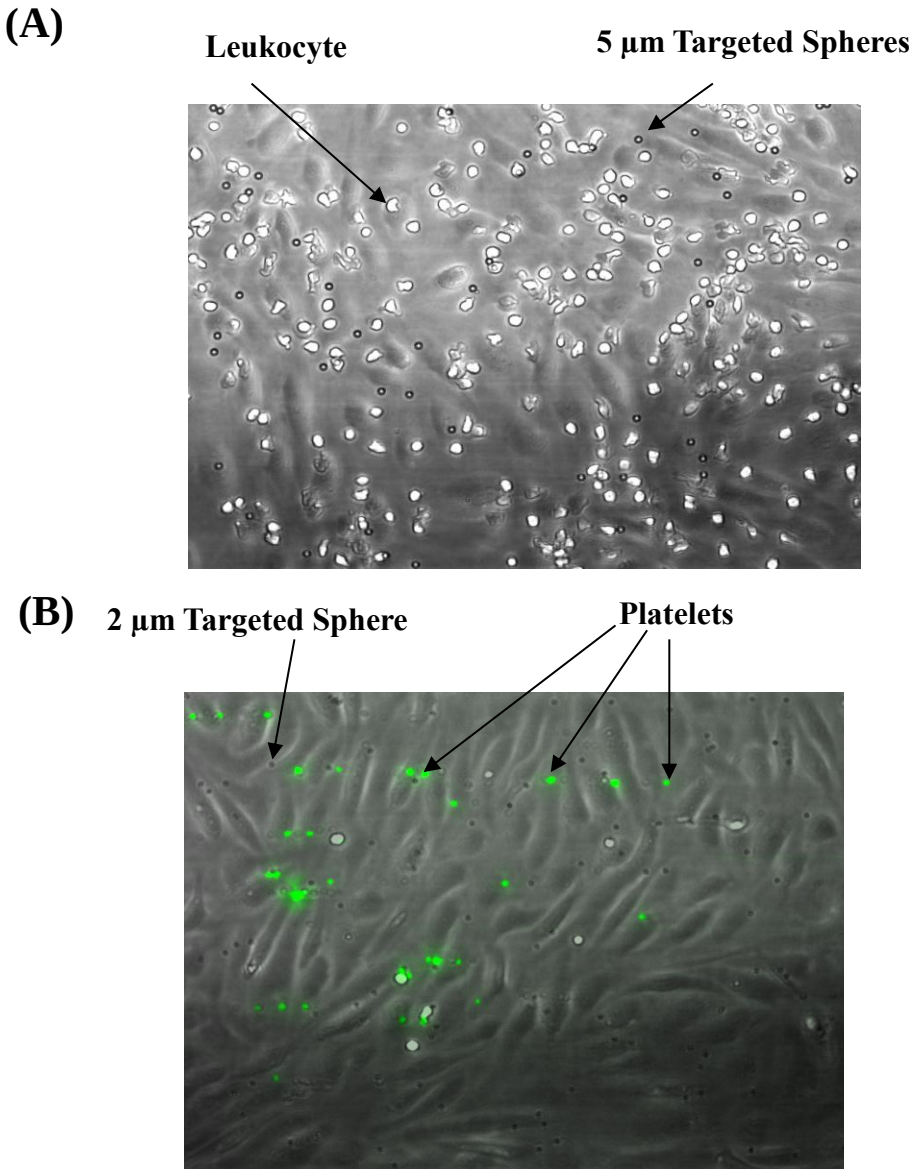

Figure 2.4. Sample images of HUVEC monolayer after flow adhesion assay of (A) whole blood oscillating flow with 5 µm sLe^a-targeted spheres and (B) reconstituted blood flow with platelets (green) and 2 µm sLe^a-targeted spheres (dark gray).

2.11.1. Laminar Flow Assay

The WSR (γ_w) or all laminar flow assays was fixed by controlling the volumetric flow rate (Q) according to the following equation:

$$\gamma_W = \frac{6Q}{h^2 w}; s^{-1} (2.3)$$

where Q is the volumetric flow rate (mL/min), h is the channel height (0.0254 cm for all flow assays), and w is the channel length (1 cm).

2.11.2. Oscillating Flow Assay

Flow oscillating flow assays (Chapter 5), the flow through the channel was controlled by a programmable pump with the following flow conditions: (1) 1.29 mL/min for 8 seconds to fill the chamber with blood, (2) forward flow at 6.45 mL/min (1,000 s^{-1} WSR) for 14 seconds, (3) reverse flow for 6.45 mL/min (1,000 s^{-1} WSR) for 7 seconds, (4) 3.225 mL/min (500 s^{-1} WSR) until the HUVEC surface was imaged. Steps (2) and (3) were looped and allowed to cycle for a total of 15 minutes (5 minutes of forward flow at 1,000 s^{-1} WSR). Oscillating flow profile was previously confirmed by tracking the average velocity of tracking particles as shown in Fig. 2.5. [11]

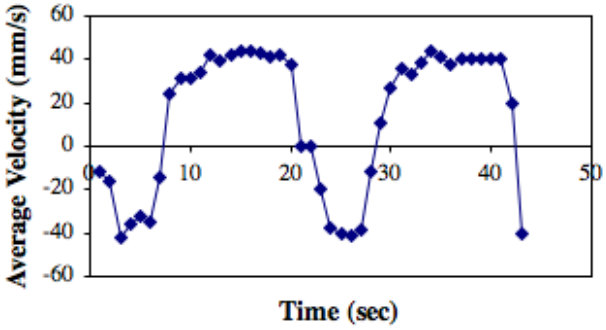

Figure 2.5. Average velocity profile for oscillating blood flow.[11]

2.12. Data Analysis and Statistics

Particle adhesion was normalized to the imaged surface area (0.152 mm^2) in order to obtain the particle adhesion density (#/mm^2). The HUVEC surface was imaged at various widths along the center of the define flow channel in order to account for variation in the adhesion across the monolayer. Particles were considered firmly adherent if the particle was stationary for at least 10 seconds. Each data bar in chapter figures represents a minimum of three trials from different donors which include at least ten fields-of-view per experiment. Binding efficiency in Chapter 3 was calculated by dividing the average particle adhesion density by the total number of particles fed in the flow chamber for a fixed WSR. For leukocyte adhesion in Chapter 5, the leukocyte adhesion density in blood flow containing targeted spheres was normalized to the leukocyte adhesion density in particle-free blood from the same human donor; where a value of 1 indicates no change in leukocyte adhesion density in particle containing blood flow relative to particle free blood. All data is plotted with its corresponding standard error. Statistical significance was determined using a student t-test, one-way ANOVA with turkey post-test, and one-way ANOVA with Bonferroni's multiple comparison test (Chapter 5). Differences were considered statistically significant is $p<0.01$ (i.e. $\alpha=0.01$ for all statistical tests).

References

[1] Sobczynski, D., Charoenphol, P., Heslinga, M., et al., *Plasma Protein Corona Modulates the Vascular Wall Interaction of Drug Carriers in a Material and Donor Specific Manner.* PLoS ONE, 2014. **9**(9): p. e107408.

[2] Champion, J.A., Katare, Y.K., and Mitragotri, S., *Making Polymeric Miro- and Nanoparticles of Complex Shapes.* PNAS, 2007. **104**(29): p. 11901-11904.

[3] Thompson, A.J., Mastria, E.M., and Eniola-Adefeso, O., *The Margination Propensity of Ellipsoidal Micro/Nanoparticles to the Endothelium in Human Blood Flow*. Biomaterials, 2013. **34**(23): p. 5863-5871.

[4] Onyskiw, P.J. and Eniola, O.A., *Effect of PEGylation on Ligand-Based Targeting of Drug Carriers to the Vascular Wall in Blood Flow*. Langmuir, 2013. **29**(35): p. 11127-11134.

[5] Ham, A.S., Klibanov, A.L., and Lawrence, M.B., *Action at a Distance: Lengthening Adhesion Bonds with Poly(Ethylene Glycol) Spacers Enhances Mechanically Stressed Affinity for Improved Vascular Targeting of Microparticles.* Langmuir, 2009. **25** (17): p. 10038-10044.

[6] Wattendorf, U. and Merkle, H.P., *PEGylation as a Tool for the Biomedical Engineering of Surface Modified Microparticles.* Journal of Pharmaceutical Science, 2008. **97**(11): p. 4655-4669.

[7] Burns, A.R., Bowden, R.A., MacDonell, S.D., et al., *Analysis of Tight Junctions During Neutrophil Transendothelial Migration.* Journal of Cell Science, 2000. **113**: p. 45-57.

[8] Charoenphol, P., Huang, R.B., and Eniola-Adefeso, O., *Potential Role of Size and Hemodynamics in the Efficacy of Vascular-Targeted Spherical Drug Carriers.* Biomaterials, 2010. **31**(6): p. 1392-1402.

[9] Charoenphol, P., Onyskiw, P.J., Carrasco-Teja, M., et al., *Particle-cell Dynamics in Human Blood Flow: Implications for Vascular-Targeted Drug Delivery.* Journal of Biomechanics, 2012. **45**(16): p. 2822-2828.

[10] Namdee, K., Thompson, A.J., Charoenphol, C., et al., *Margination Propensity of Vascular-Targeted Spheres from Blood Flow in a Microfluidic Model of Human Microvessels.* Langmuir, 2013. **29**(8): p. 2530-2535.

[11] Charoenphol, P., Mocherla, S., Bouis, D., et al., *Targeting Therapeutics to the Vascular Wall in Atherosclerosis - Carrier Size Matters.* Atherosclerosis, 2011. **217**(2): p. 364-370.

CHAPTER 3

EFFECT OF PEGYLATION ON THE LIGAND-BASED TARGETING OF DRUG CARRIERS TO THE VASCULAR WALL IN BLOOD FLOW

Contents of this chapter have been published as:

Onyskiw, P.J. and Eniola-Adefeso, O. *Langmuir*, 2013. **29**(35): p.11127-11134.

3.1. Introduction

A major challenge for systemic circulating vascular-targeted carriers (VTCs) is the avoidance of the immune response; specifically, the avoidance of plasma protein adsorption onto the VTC's surface which initiates systemic clearance. To date, the most common method used to prevent protein adsorption is PEGylation - the modification of a carriers' surface with poly(ethylene glycol) (PEG). The hydrophilic nature of PEG helps inhibit plasma proteins from adsorbing onto the carrier's surface, resulting in an increase in the carrier's systemic circulation time.[1] Increasing VTC circulation time in turn improves the passive targeting ability of drug carriers to areas such as cancerous tumors, the lungs, liver, and the brain.[2, 3]

Many of the passive targeting (tissue targeting by physical entrapment) benefits from PEGylation, including increased circulation time, are dependent on the orientation of the PEG corona.[4, 5] Improved circulation time is typically achieved when the PEG spacers are oriented in a brush conformation, where the PEG chains protrude away from the carrier's surface rather than the mushroom orientation where the chains are entangled and remain close to the carrier's surface. Achieving the brush versus mushroom conformation is dependent on both the PEG

molecular weight and grafting density, with lower molecular weight chains requiring higher surface grafted densities to achieve the brush orientation than larger molecular weight chains.[6, 7] Surfaces with PEG molecular weights greater than 3.4 kDa with 2-5 mole % surface coverage have been shown to be sufficient conditions for preventing protein adsorption.[4, 8] However, to date, it is not clear what effect PEGylation has on the ligand-based adhesion of VTCs to the vascular wall in human blood flow.

Overall, the effectiveness of VTCs is dependent on the following: the carrier's (1) ability to migrate from the center of bulk blood flow and localize to the blood vessel wall, and (2) capacity to specifically target and adhere to the endothelium in the diseased tissue. VTC localization to the blood vessel wall is dependent on carrier parameters such as size, shape, and hemodynamics.[9-12] Tissue-specificity typically requires modifying the carrier's surface with adhesive ligands whose counter-receptors are upregulated during a diseased state. For PEGylated VTCs this would often entail attaching the adhesive ligand to the free end of the PEG spacer, which has been shown to alter the receptor-ligand dynamics. For example, the binding distance of a biotin-avidin system was previously shown to increase with PEGylated biotin and was a function of the PEG molecular weight.[13, 14] PEG molecular weight and grafted density were also shown to influence ligand induced cellular adhesion and internalization.[15, 16] Similarly, PEGylation improved the binding dynamics of ligands to their counter receptors in shear flow by decreasing bond stress and increasing the frequency of binding in a low shear saline laminar flow system (~100 s^{-1} wall shear rate).[17]. However, it is unclear if improved adhesive dynamics with PEGylation translates to an increase in VTC adhesion to an inflamed endothelium in blood, which is dependent on both the adhesive interactions of the targeting system and VTC margination in blood.[17]

VTC margination in blood has previously been shown to be strongly dependent on the carrier size in the particles <1 μm in diameter do not marginate and adheres to the vascular wall as well as 2 μm and 5 μm targeted spheres.[11, 18] Submicron spheres (0.2–1 μm in diameter) are of particular interest for vascular targeting due to their ability to remain in systemic circulation longer than microspheres.[19] The targeting ability of submicron spheres in small vessels is also of particular interest in treating cancerous tumors, as tumor microvasculature is similar in size to arterioles and venules (20–100 μm in diameter).[20] Inflammation targeting submicron spheres were previously shown to exhibit significantly lower adhesion densities in blood flow compared to microspheres (2 μm and 5 μm) in both large flow channels (>125 μm channel height) and small microchannels (28 μm and 50 μm channel heights). This was attributed to the submicron sphere's poor localization to the endothelial wall in blood flow.[10, 11] With the addition of a PEG spacer, the targeting ligand is moved away from the carrier's surface and is inherently presented closer to the targeted receptors expressed on the endothelium. However, it is unknown if PEGylation will enhance the nanosphere adhesion in blood, particularly in vessels with diameters similar to the microvasculature of cancerous tumors.

In this work, I examine the effect of different size PEG spacers (2.3 kDa, 5.5 kDa, and 10 kDa) on the adhesion of 2 μm and 500 nm polystyrene spheres to activated human umbilical vein endothelial cell (HUVEC) monolayer from human blood at physiological shear rates. The effect of PEG molecular weight and surface density was examined using two receptor-ligand systems commonly explored for targeting endothelial inflammation; E-selectin/Sialyl Lewis^{a} (sLe^{a}) and intercellular adhesion molecule-1 (ICAM-1)/anti-intercellular adhesion molecule-1 (aICAM-1).[21] The results show that PEG spacers improved, diminished, or did not affect the adhesion efficacy of VTCs in blood depending on the PEG size and surface density, and the nature of the

specific receptor-ligand kinetics employed.

3.2. Results

The experimental setup used in this chapter is described in detail in Chapter 2.

3.2.1. Effect of PEG on sLe^a Mediated Adhesion

In order to investigate the effect of PEG molecular weight on particle adhesion to activated endothelial cells (ECs), 2.3 kDa, 5.5 kDa, and 10 kDa PEG spacers were conjugated onto 2 μm spheres at surface densities that correspond to an extended brush conformation for each of the PEG sizes. A PEG brush conformation was estimated using the Flory's radius, R_f. A brush conformation occurs when the distance between adjacent PEG chains (S), estimated based on the PEG surface density, falls between R_f and $2R_f$ ($R_f < S < 2\ R_f$), i.e. chain overlap $R_f/S > ½$, (Fig. 2.3).[1, 17] An R_f of 4.4 nm, 7.7 nm, and 11.3 nm with chain overlaps of 63%, 92%, and 72% were used to achieve an extended brush conformation for the 2.3 kDa, 5.5 kDa, and 10 kDa PEGylated microspheres, respectfully (Table 3.1). It is worth noting that it is possible that the multivalent probes used for determining PEG densities used in the chain overlap calculations may underestimate the PEG surface density, particularly for larger PEG chains that have more mobility on the surface and hence a higher chance of multiple chains reacting with a single multivalent probe. However, there was good agreement in the measured site density for the high molecular weight PEG chains on 2 μm spheres when probed with the avidin-FITC versus the anti-biotin-PE probe (Table 3.2).

Table 3.1. PEG density, R_f, approximate distance between adjacent PEG chains (S), and PEG corona conformation as estimated by $R_f < S < 2R_f$.

PEG Molecular Weight	2.3 kDa PEG	5.5 kDa PEG	10 kDa PEG
PEG Density (chains/μm^2)	25,000 ± 2,300	18,440 ± 50	5,200 ± 300
R_f (nm)	4.4	7.7	11.3
$2R_f$ (nm)	8.8	15.4	22.6
S (nm)	7.1	8.3	15.7
Estimated Conformation	Intermediate Brush	Intermediate Brush	Intermediate Brush

Table 3.2. Comparison of 5.5 kDa and 10 kDa PEG surface density on 2 μm spheres measured with avidin-FITC and anti-biotin-PE

	5.5 kDa PEG (PEG chains/μm^2)	10 kDa PEG (PEG chains/μm^2)
Avidin-FITC	14,800 ± 100	5,520 ± 12
anti-Biotin-PE	12,200 ± 1,100	5,270 ± 90

Fig. 3.1.A shows the adhesion of sLe^a-coated spheres with PEG spacers in the brush conformation as a function of channel WSR for a fixed sLe^a (targeting ligand) density of 1,000 sites/μm^2. There was no significant difference in the adhesion density between the non-PEGylated and PEGylated sLe^a-spheres for all PEG molecular weights at each of the WSRs evaluated. The PEG brush densities used for assays in Fig. 3.1.A were set based on the maximum average density achievable on the 2 μm spheres for each PEG size. To determine whether the lack of a significance difference in adhesion between sLe^a-targeted spheres of different PEG molecular weights was a result of the differences in the actual PEG density on the particle surface, I evaluated the adhesion of 5.5 kDa and 10 kDa PEGylated sLe^a-spheres at a fixed PEG brush density of ~5,200 PEG chains/μm^2 and a fixed sLe^a density of 1,000 sites/μm^2. As shown in Fig. 3.1.B, the adhesion density for the 5.5 kDa PEG sLe^a-spheres was not significantly different from that of 10 kDa PEG sLe^a-spheres at the fixed PEG density ($p=0.1097$ and $p=0.0389$ for 200 and 1,000 s^{-1}, respectfully). Overall, the adhesion of both non-PEGylated and PEGylated sLe^a-spheres increased with increasing WSR. This observation is expected for sLe^a-mediated adhesion of 2 μm spheres in blood flow for the ligand density used based on our previous publication and is due to the normal force impacted by the red blood cells (RBCs) aiding the particles at the wall in overcoming the increase in shear force associated with an increase in WSR, i.e. an increase in the WSR in the absence of a corresponding increase in disruptive force results in higher adhesion.[9] Also, control experiments with non-targeted PEGylated spheres resulted in no adhesion to the EC monolayer, confirming that the actual particle adhesion shown in Fig. 3.1 was mediated by the interaction of targeting ligand (sLe^a) with its EC-expressed receptor(s) (data not shown).

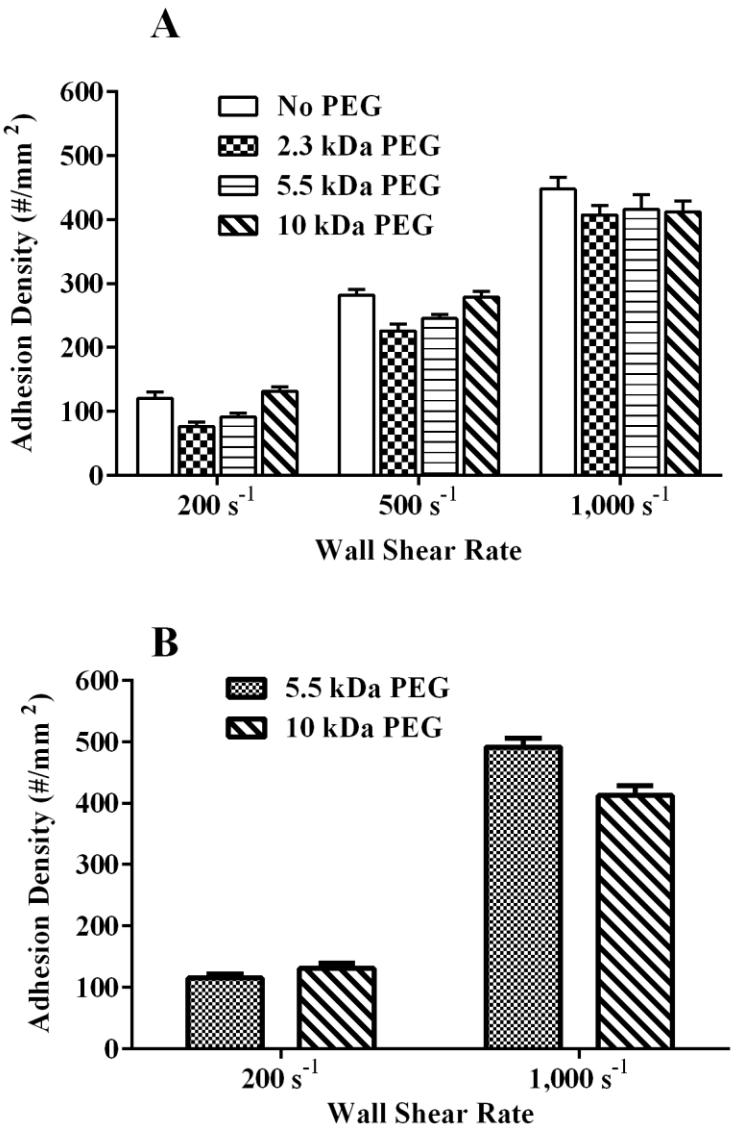

Figure 3.1. (A) Adhesion of sLe^a (1,000 sites/μm^2) PEGylated 2 μm spheres to an activated ECs in laminar whole blood flow as a function of PEG size and channel wall shear rate. (b) Adhesion of 5.5 kDa and 10 kDa-PEGylated 2 μm spheres in laminar whole blood flow for a fixed PEG density of 5,200 PEG chains/μm^2 and sLe^a density of 1,000 sites/μm^2.

To investigate the effect of PEG conformation on the adhesion of sLe^a-targeted spheres in blood, 5.5 kDa PEG was conjugated to the surfaces of 2 μm spheres at either a low or high surface density of approximately 3,500 ± 300 or 11,000 ± 200 chains/μm^2, which were estimated to correspond to a mushroom (chain overlap = 40%) or an intermediate-brush conformation (chain overlap = 72%), respectfully. At 200 s^{-1}, there was no difference in adhesion between non-PEGylated and PEGylated sLe^a-spheres for both PEG conformations at this PEG molecular weight (Fig. 3.2.A). At 500 s^{-1}, the adhesion of the PEG-Mushroom spheres was slightly lower than the adhesion of the non-PEGylated spheres, but there was no significant difference in adhesion between non-PEGylated spheres and the PEG-Brush spheres. For the 1,000 s^{-1} WSR, the adhesion of PEG-Mushroom spheres was approximately 4.5-fold lower than both the non-PEGylated and PEG-Intermediate-Brush spheres. There was no significant difference in adhesion between the non-PEGylated and the PEG-Intermediate Brush spheres. A similar assay with 2.3 kDa PEGylated sLe^a-targeted spheres shows the same trend for particle adhesion at 1,000 s^{-1} where the adhesion of microspheres with a low PEG density of ~12,800 PEG chains/μm^2 (chain overlap = 44%; PEG-Mushroom) was 3-fold lower than the adhesion of particles with a high PEG density of 26,800 PEG chains/μm^2 (chain overlap = 63%; PEG-Intermediate-Brush) and ones that were non-PEGylated (Fig. 3.2.B).

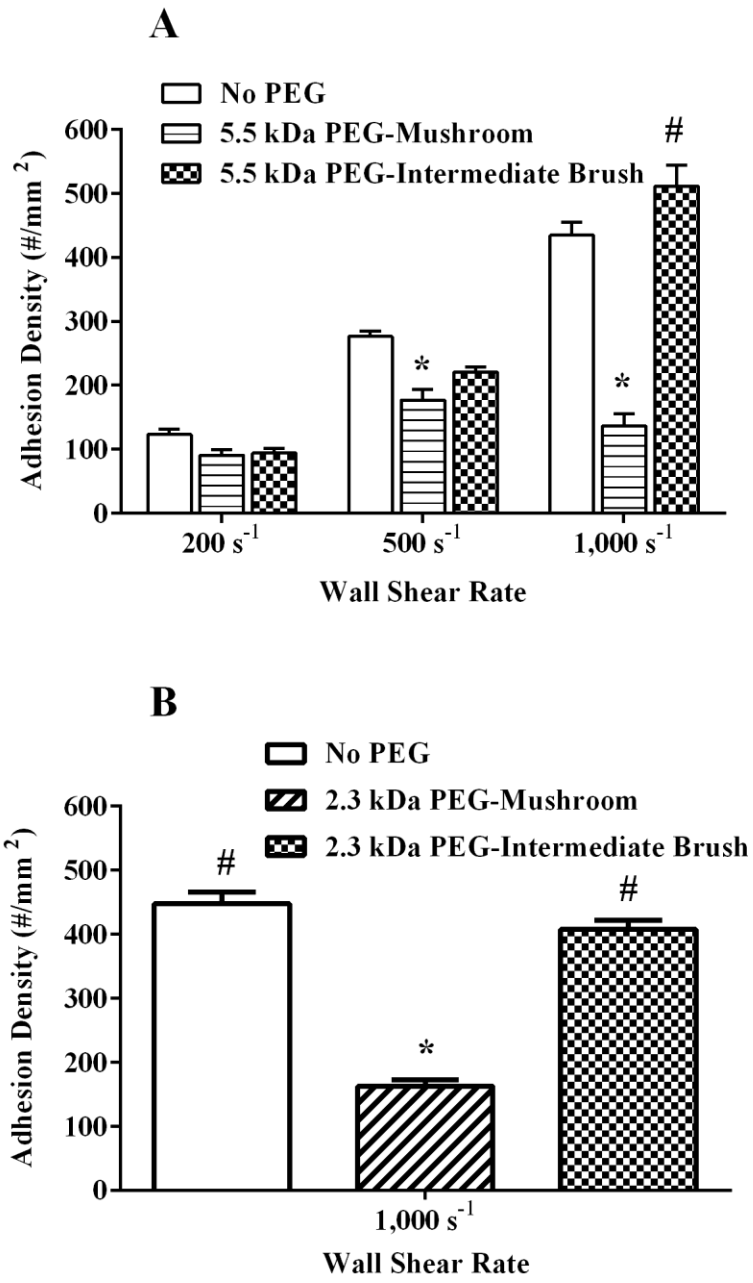

Figure 3.2. Adhesion of (A) 5.5 kDa PEG-Mushroom (3,500 PEG chains/μm^2) and PEG-Intermediate Brush (11,000 PEG chains/μm^2) and (B) 2.3 kDa PEG-Mushroom (12,800 PEG chains/μm^2) and PEG-Brush (26,800 PEG chains/μm^2) 2 μm spheres targeted with 1,000 $sLe^a/\mu m^2$ to activated ECs in laminar whole blood flow as a function of channel wall shear rate (WSR). * indicates $p<0.01$ when compared to the adhesion of non-PEGylated spheres at the same WSR and # indicates $p<0.01$ when compared to the adhesion of PEG-Mushroom spheres (of the same molecular weight) at the same WSR.

3.2.2. Effect of PEG on aICAM-1 Mediated Adhesion

To investigate whether targeting ligand type influences the adhesion of PEGylated spheres, 2 μm PEGylated and non-PEGylated spheres were conjugated with approximately 2,600 sites/μm^2 of anti-ICAM-1 (aICAM-1) antibody to target ICAM-1. Fig. 3.3.A shows the adhesion to activated ECs in blood flow of aICAM-1 spheres containing 2.3 kDa, 5.5 kDa, and 10 kDa PEG spacers in an intermediate-brush conformation, at the respective PEG densities reported in Table 3.1, as a function of channel WSR. At 200 s^{-1}, there was no significant difference in adhesion between the PEGylated and non-PEGylated aICAM-1-spheres. At 500 s^{-1}, the adhesion of non-PEGylated aICAM-1-spheres was approximately 7-fold lower than the adhesion of all PEGylated spheres and no difference in adhesion was observed between the different PEGylated spheres. At 1,000 s^{-1}, no adhesion was observed for non-PEGylated aICAM-1 spheres and the level of adhesion observed for the 2.3 kDa PEG-Brush spheres was 2.8-fold lower than the adhesion of 5.5 kDa and 10 kDa PEG-Brush spheres. There was no significant difference between the adhesion of 5.5 kDa and 10 kDa PEGylated spheres. As with sLe^a-targeting, there was no significant difference in adhesion between the 5.5 and 10 kDa PEG microspheres when a fixed PEG brush density of ~5,200 PEG chains/μm^2 was used at a fixed sLe^a density of 1,000 sites/μm^2 (data not shown).

To determine whether the higher adhesion of PEGylated aICAM-1-spheres with increasing channel WSR was due to improved adhesion kinetics, particle adhesion density was normalized to the total number of particles perfused through the flow channel at a fixed WSR, i.e. fraction of total perfused particle that was bound (adhesion efficiency). Fig. 3.3.B shows the adhesion efficiency of PEGylated and non-PEGylated spheres at different WSRs as a function of PEG molecular weight (Table 3.1). The adhesion efficiency for non-PEGylated spheres

significantly decreased with increasing WSR (compared to the efficiency of the same particles at 200 s^{-1}). The adhesion efficiency of all the PEGylated spheres at 500 s^{-1} was not significantly different from the efficiency at 200 s^{-1}, suggesting that the improved adhesion density, relative to non-PEGylated spheres, was due to improved adhesive dynamics and not particle margination. However, the adhesion efficiency of all PEGylated spheres at 1,000 s^{-1} was significantly lower than the efficiencies of the same spheres at both 200 s^{-1} and 500 s^{-1}.

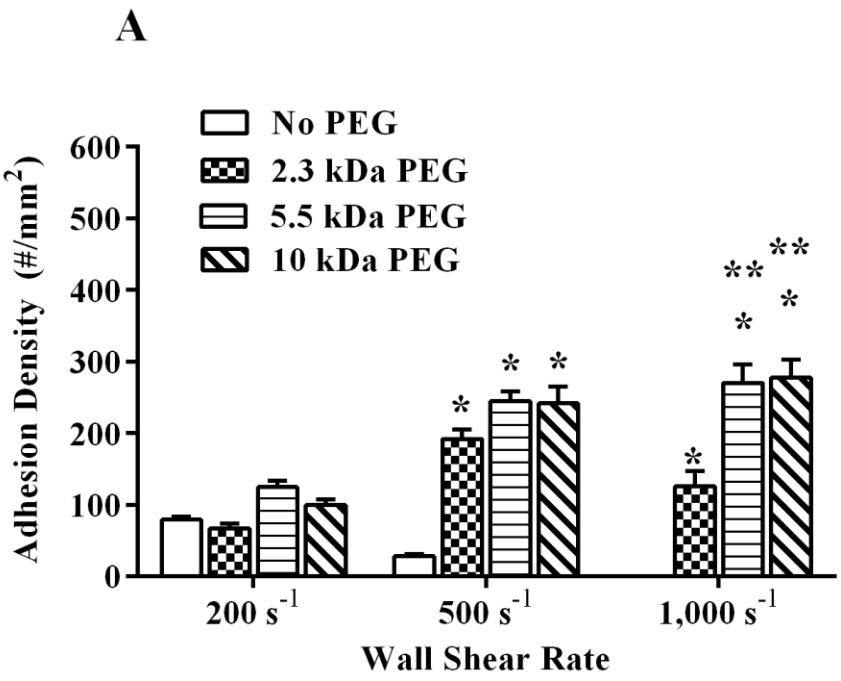

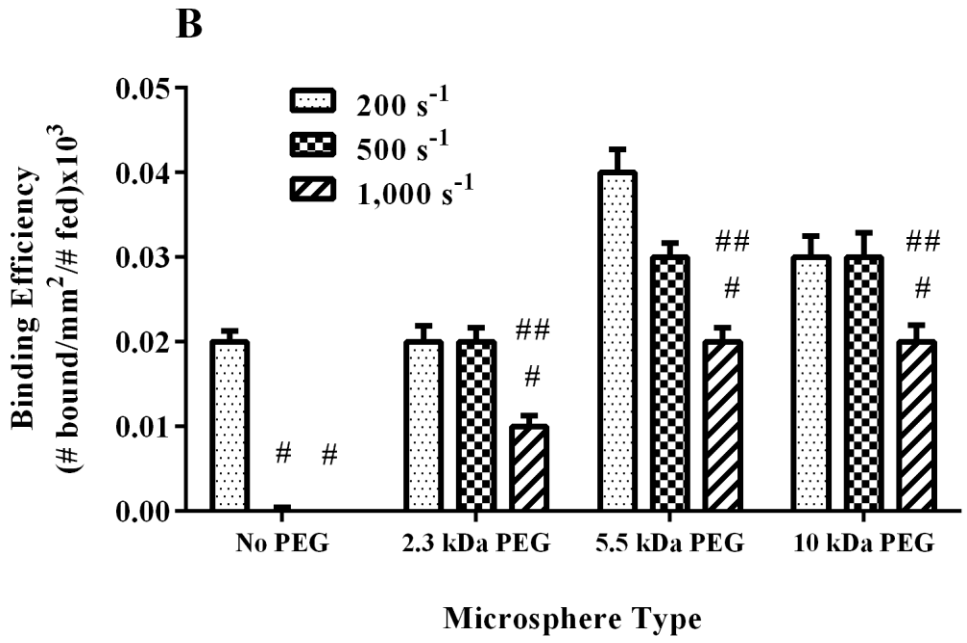

Figure 3.3. (A) Adhesion of aICAM-1 (2,600 sites/μm^2) PEGylated microspheres to activated ECs in laminar whole blood flow as a function of PEG brush length at different wall shear rates (WSR). * indicates $p<0.01$ when compared to the adhesion of non-PEGylated spheres at the same WSR and ** indicates $p<0.01$ when compared to the adhesion of 2.3 kDa PEG spheres at the same WSR. (B) Adhesion density normalized to the number of particles perfused at a given wall shear rate (Binding Efficiency). # indicates $p<0.01$ compared to the adhesion of the same particle at 200 s^{-1} and ## indicates $p<0.01$ compared to the adhesion of the same particle at 500 s^{-1}.

To investigate the effect of PEG conformation on ICAM-1 targeting, 5.5 kDa PEG spacers were conjugated to the surface of 2 μm spheres at a low (3,500 ± 286 PEG chains/ μm^2) or high PEG surface density (11,000 ± 219 PEG chains/μm^2) estimated to be in a mushroom (40% chain overlap) or an intermediate-brush conformation (72% chain overlap), respectfully. There was no significant difference in adhesion between the non-PEGylated and PEGylated aICAM-1-spheres with both conformations at 200 s^{-1} (Fig. 3.4). At 500 s^{-1}, the adhesion of non-PEGylated spheres was 4.5- and 8.6-fold lower than the adhesion of PEG-Mushroom and PEG-Intermediate-Brush spheres, respectfully. At this same WSR, the adhesion of the PEG-Mushroom spheres was 2.0-fold lower than the adhesion of PEG-Intermediate-Brush spheres. At 1,000 s^{-1}, there was no adhesion observed for non-PEGylated spheres and minimal adhesion for the mushroom-oriented PEG spheres. The adhesion of the PEG-Intermediate Brush spheres 1,000 s^{-1} was 9.6-fold higher than that of the PEG-Mushroom spheres at 1,000 s^{-1} WSR.

To determine if improving the adhesion kinetics for non-PEGylated spheres (via increasing aICAM-1 site density) would increase their adhesion density to the level of PEGylated spheres, the adhesion of non-PEGylated spheres with 4,400 sites/μm^2 aICAM-1 density (Fig. 3.4; solid black bars) was compared to the adhesion of non-PEGylated and PEGylated spheres with 2,600 aICAM-1 sites/μm^2. At 200 s^{-1}, the adhesion density of the higher aICAM-1-density non-PEGylated spheres was 1.8-fold higher than all the spheres with 2,600 aICAM-1 sites/μm^2. At 500 s^{-1} WSR, the adhesion of the higher aICAM-1 density spheres was 8.0- and 1.7-fold higher than the adhesion of non-PEGylated and PEG-Mushroom spheres, respectfully; however, there was no significant difference in the adhesion density between the PEG-Intermediate-Brush spheres and the higher aICAM-1 density non-PEGylated spheres. With 1,000 s^{-1} WSR of laminar blood flow, the adhesion of the high aICAM-1 density spheres was

5.0-fold lower than the PEG-Intermediate Brush spheres, and there was no significant difference in adhesion between the higher aICAM-1 density-spheres and the PEG-Mushroom spheres. No adhesion was observed for non-PEGylated spheres with 2,600 aICAM-1 sites/μm^2 at 1,000 s^{-1} WSR.

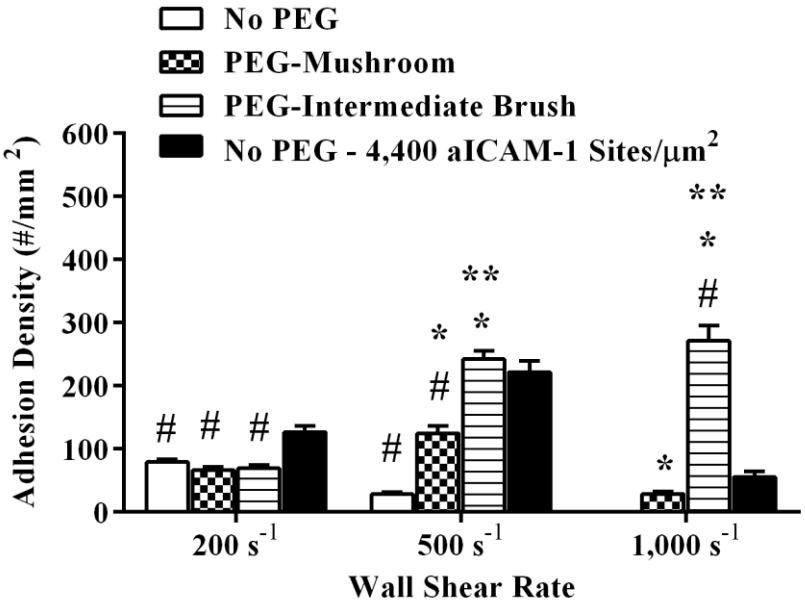

Figure 3.4. Adhesion of 5.5 kDa PEG-Mushroom (3,500 PEG chains/μm^2) and PEG-Intermediate-Brush (11,000 PEG chains/μm^2) 2 μm spheres targeted with 2,600 aICAM-1 sites/μm^2 to activated ECs in laminar whole blood flow as a function of channel wall shear rate (WSR). * indicates $p<0.01$ when compared to the adhesion of non-PEGylated spheres at the same WSR, ** indicates $p<0.01$ when compared to the adhesion of PEG-Mushroom spheres at the same WSR, and # indicates $p<0.01$ when compared to the adhesion of non-PEGylated spheres with 4,400 aICAM-1 sites/μm^2 and the same WSR.

3.2.3. Effect of PEGylation on Targeted Nanosphere Adhesion

To determine whether the effect of PEG spacers on particle adhesion was affected by particle size, I investigated the adhesion of 500 nm spheres conjugated with a 5.5 kDa PEG spacer oriented in the brush conformation (~16,000 PEG chains/μm^2, intermediate-brush conformation) and targeted with either sLe^a or aICAM-1 (1,000 sites/μm^2 and 2,600 sites/μm^2, respectfully). As shown in Fig. 3.5.A, there was no significant difference in adhesion between PEGylated and non-PEGylated sLe^a-spheres at the three WSRs explored, similar to observations with the 2 μm sLe^a-spheres. The adhesion of both PEGylated and non-PEGylated 500 nm sLe^a-spheres increased with increasing WSR between 200 and 500 s^{-1}; however, there was no significant increase in adhesion for both nanosphere types between 500 and 1,000 s^{-1}. Increasing the PEG size to 10 kDa on the sLe^a-targeted spheres did not significantly alter the adhesion compared to both the non-PEGylated and 5.5 kDa PEGylated submicron spheres (data not shown). When targeted with aICAM-1, there was no significant difference between the adhesion of PEGylated and non-PEGylated 500 nm spheres in blood flow at 200 s^{-1} (Fig. 3.5.B), similar to the observation with sLe^a spheres. However, at 500 s^{-1} and 1,000 s^{-1} the adhesion of 5.5 kDa PEGylated spheres was significantly higher than non-PEGylated spheres. There was no significant difference in adhesion between the PEGylated spheres at 500 and 1,000 s^{-1}. Overall, the adhesion of the 500 nm spheres was 4- and 17-fold lower than the adhesion of the 2 μm spheres at the same blood particle concentration for similar PEG conditions and the WSRs evaluated. I also investigated whether PEGylation aided in the capture and adhesion of submicron spheres in blood flow through a microchannel (28 μm channel height). The results were similar to what was observed in the larger (254 μm channel, Fig. 3.5.) in that PEG had no significant effect on the adhesion of sLe^a-targeted submicron spheres (Fig. 3.6.A) and slightly

increased the adhesion of aICAM-1 targeted submicron spheres (Fig. 3.6.B), but only at 500 s^{-1} WSR.

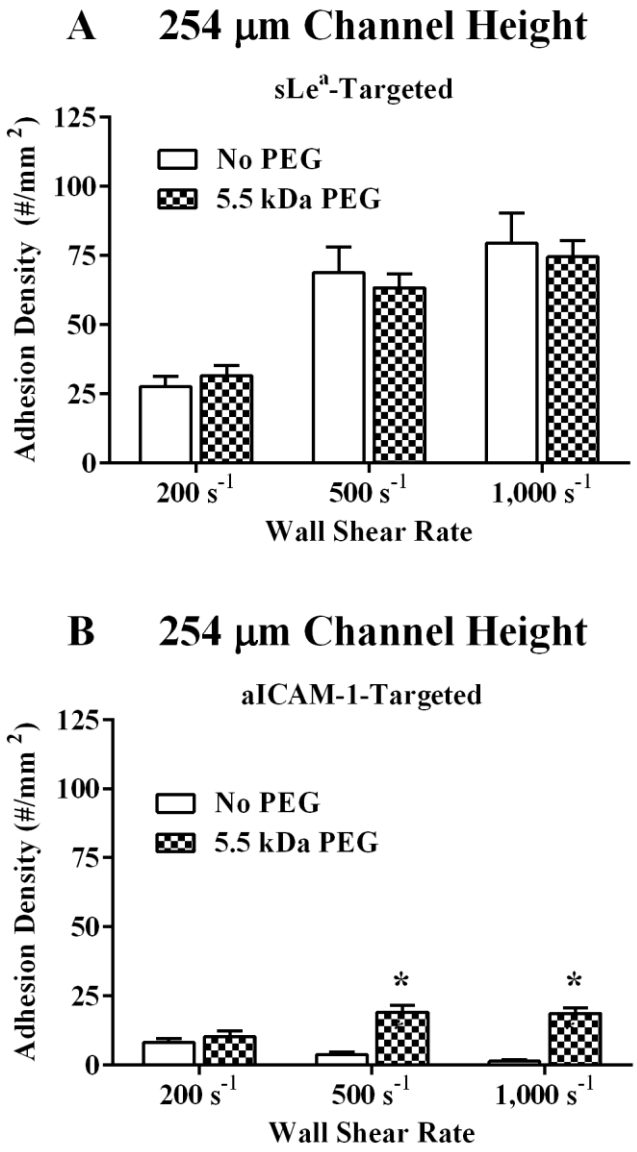

Figure 3.5. Adhesion of (A) sLe^a (1,000 sites/μm^2)-PEGylated and (B) aICAM-1 (2,600 sites/μm^2)-PEGylated 500 nm spheres to activated ECs in laminar whole blood flow at different wall shear rates. * Indicates $p<0.01$ when compared to non-PEGylated spheres at a fixed WSR.

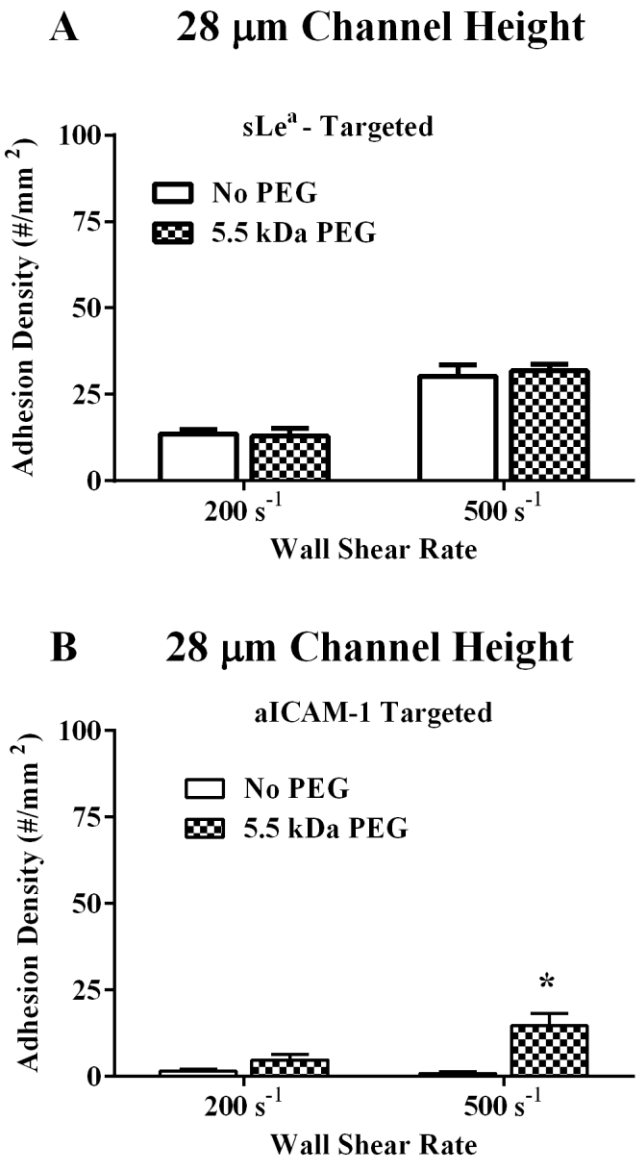

Figure 3.6. Adhesion of (A) sLe^a (1,000 sites/μm^2)-PEGylated and (B) aICAM-1 (2,600 sites/μm^2)-PEGylated 500 nm spheres to activated ECs in laminar whole blood flow through a microchannel. * Indicates $p<0.01$ when compared to non-PEGylated spheres at a fixed WSR.

3.3. Discussion

The addition of PEG onto a carrier's surface is an effective strategy for sterically reducing protein adsorption and increasing systemic circulation time.[2, 4] However, it is unclear if the addition of PEG spacers has an effect on ligand-based adhesion of VTCs to the vascular wall in blood flow at physiological WSRs. In this work I investigated the effects of (1) PEG corona size for the case where PEG chains were in the more extended brush conformation and (2) PEG conformation (i.e. high versus low PEG surface density) on VTC adhesion for both sLe^a and aICAM-1 targeted spheres. Overall, I show that the addition of PEG spacers did not hinder particle adhesion in human blood flow when the VTCs are grafted with a high PEG surface density corresponding to an intermediate brush conformation. However for blood flow at high WSR (1,000 s^{-1}), a low-density PEGylation, where the PEG chains are estimated to be oriented in a more entangled mushroom conformation ($S>R_f$ or chain overlap <50%), resulted in reduced adhesion for VTCs compared to the higher PEG density brush spheres irrespective of the ligand type (Fig. 3.2 and Fig. 3.4).

The addition of a PEG spacer in the intermediate-brush conformation was found to improve the adhesion of 2 μm spheres at intermediate and high WSRs (500 s^{-1} and 1,000 s^{-1}) when the targeting ligand was aICAM-1. This observation is in agreement with a previous report by Ham and coworkers where they showed that the flexibility of the PEG chains improved the ligand adhesion kinetics, and hence adhesive flux, of targeted microspheres for monovalent receptor-ligand systems in low saline flow (~100 s^{-1} WSR) by reducing the bond stress.[17] They also showed that the improved kinetics was dependent on PEG molecular weight.[17] Interestingly, the results showed that increasing the surface density of aICAM-1 on the non-PEGylated spheres can improve the adhesion to levels observed for PEGylated spheres at an

intermediate WSR (500 s^{-1}). It is anticipated that a further increase in aICAM-1 density without PEG would restore adhesion at higher WSRs (e.g. 1,000 s^{-1}) to the level seen for PEGylated spheres at the low ligand density. It may be difficult to achieve such higher ligand density due to steric hindrance that can occur with a high concentration of ligand present in the conjugation medium, resulting in surface saturation. Contrary to Ham and coworkers, there was no significant difference in aICAM-1 microsphere adhesion with the various PEG sizes at the low to intermediate WSRs (200 s^{-1} and 500 s^{-1}) evaluated (Fig. 3.3), which was likely due to the 2 μm spheres used in this work experiencing lower drag forces compared to the 5 μm spheres evaluated by Ham and coworkers. Indeed, when 2 μm spheres were observed at high WSR (1,000 s^{-1}), the PEG size was found to be important where the adhesion of the 2.3 kDa-PEGylated aICAM-1 microspheres was found to be significantly lower than the adhesion of particles with larger PEG size (Fig. 3.3). This suggests that there is a minimum PEG size requirement for PEG spacers to reduce the bond stress in high shear flow, where microsphere adhesion is reaction limited and stronger adhesion kinetics is necessary as is the case for monovalent ICAM-1 targeting.

While Ham and coworkers only focused on monovalent interactions, the addition of PEG to multivalent sLe^a coated spheres used in this work did not improve microsphere adhesion in blood flow. This suggests that an increase in microsphere adhesion from PEGylation is dependent on the baseline adhesion characteristics of the targeting ligand systems. SLe^a has been previously reported to exhibit a fast on-rate (rate of forward reaction) to E-selectin underflow conditions which makes this receptor-ligand system very efficient at mediating the capture of particles to the endothelium from flow in the absence of PEG, unlike the slow reaction kinetics for the aICAM-1-ICAM-1 system evaluated here.[22-24] It is anticipated that the

presence of a PEG spacer would progressively be important for microspheres adhesion with sLe^a ligand at lower ligand densities and/or at very high WSRs where the probability of receptor-ligand interaction is drastically reduced.

The data presented in Fig. 3.2 and Fig. 3.4 shows that PEG surface density significantly influences microsphere adhesion with both targeting ligands evaluated, particularly at 500 s^{-1} (aICAM-1) and 1,000 s^{-1} (aICAM-1 and sLe^a) where microsphere adhesion is reaction limited and highly dependent on ligand density and availability. The decrease in adhesion with the low density PEG spheres (where the PEG corona is estimated to be in a more entangled mushroom conformation based on the $S > 2R_f$) is likely due to poor ligand presentation and steric repulsive forces as a result of the PEG corona length being similar to its equilibrium length, R_f. When the PEG spacers are oriented in a more extended brush conformation ($R_f < S$), the targeting ligand is easily accessible for adhesion with its counter receptor resulting in an adhesion density equivalent or greater than the non-PEGylated spheres (depending on the targeting ligand) (Fig. 3.2 and Fig. 3.4). For both the 2.3 kDa and 5.5 kDa PEG-spheres at low PEG densities, the size of the PEG corona is equivalent to or slightly shorter than its corresponding R_f and hence a higher degree of PEG chain entanglement is anticipated. Higher chain entanglement may then result in poor ligand presentation (i.e. decreased effective valency), which leads to a decrease in particle adhesion as observed for both targeting ligand systems evaluated. Indeed, these findings are in agreement with previous works with bimodal systems (two PEG spacers of different lengths on a carrier's surface) which have shown that when the targeting ligand is attached to a spacer that is significantly shorter than the R_f of the adjacent spacer, adhesion in static conditions is inhibited.[16, 26] However, it may be that improving the ligand valency, via increasing ligand density, on a low-density mushroom-oriented PEG-sphere would be sufficient to increase

particle adhesion to the same level as the non-PEGylated and PEG-Brush spheres. Increasing ligand density, however, may substantially affect tissue selectivity as was recently demonstrated by Zern et al., where nanospheres (~200 nm) with an aICAM-1 ligand density of 200 antibodies/nanoparticle showed lower selectivity towards diseased pulmonary endothelium (*in vivo*) compared to nanospheres with only 50 antibodies/nanoparticle.[26] Incidentally, Cruz et al. previously showed that the cellular internalization of 200 nm spheres targeted to dendritic cells with ligands grafted on a PEG spacer was most efficient (~70% of DC internalizing particles) when PEG sizes between 2-3 kDa were used compared to PEG sizes between 6 - 20 kDa (~40 % of DC internalizing particles), suggesting that the shorter PEG sizes are preferable for situations where cellular internalization is critical.[15] In this case, care must be taken to ensure that the amount of PEG grafted on particles is sufficient (i.e. $S < 2R_f$), to achieve all the targeting ligand in the appropriate orientation for targeting applications that involve blood flow adhesion prior to cellular internalization, since a higher PEG density is required to cross this threshold with smaller PEG sizes (e.g. ~16,000 PEG chains/μm^2 for 2.3 kDa versus ~5,000 PEG chains/μm^2 for 5.5 kDa by my estimation).

To determine if the influence of PEG on VTC adhesion was particle size dependent, the effect of PEG spacers on the adhesion of 500 nm spheres was examined under similar conditions as 2 μm spheres. Submicron spheres, rather than larger microspheres, were explored due to attractiveness for use as VTCs because of their ability to avoid capillary entrapment, thus potentially improving targeting efficiency.[19] The addition of a PEG in an intermediate brush conformation did not significantly improve the adhesion density for sLe^a-targeted 500 nm spheres in either larger flow channel (254 μm channel height) or microchannel (28 μm channel height) (Fig. 3.5. and Fig. 3.6.). While there was a 7-fold increase in adhesion density for

ICAM-1 targeting of these particles at the intermediate to high WSRs in the larger channel (Fig, 3.5.B), this increase in nanosphere adhesion was still minimal compared to the adhesion level observed for 2 μm spheres at the same WSRs (Fig. 3.3.A). This discrepancy is most likely due to spheres < 1 μm not effectively marginating to the vessel wall and remaining entrapped in the RBC core during blood flow.[9-11, 18] The data presented in this work suggests the addition of PEG most likely did not improve the localization of submicron spheres since the adhesion density of both PEGylated and non-PEGylated nanospheres remains substantially lower than that of 2 μm spheres under the same flow assay conditions similar to reports in previous publications.[9, 10, 18]

In summary, the addition of a PEG corona to a VTC's surface was shown to significantly affect VTC adhesion in blood flow. While a low density PEG corona hinders adhesion under high shear condition, PEG with an extended intermediate-brush conformation can improve the adhesion of VTCs for targeting systems with adhesion dynamics similar to the aICAM-1/ICAM-1 systems used in this work. Based on these results, PEG spacers with molecular weights >5.5 kDa with grafting densities corresponding to an intermediate-brush conformation or greater are recommend for maintaining or improving VTC adhesion in blood flow, particularly under high shear conditions such as those present in arteries susceptible to cardiovascular disease.

References

[1] Wattendorf, U. and Merkle, H.P., *PEGylation as a Tool for the Biomedical Engineering of Surface Modified Microparticles.* Journal of Pharmaceutical Science , 2008. **97**(11): p. 4655-4669.

[2] Choi, K.Y., Min, K.H., Yoon, H.Y., et al., *PEGylation of Hyaluronic Acid Nanoparticles Improves Tumor Targetability In Vivo.* Biomaterials, 2011. **32**: p. 1880-1889.

[3] Calvo, P., Gouritin, B., Chacun, H., et al., *Long-Circulating PEGylated Polycyanoacrylate Nanoparticles as New Drug Carrier for Brain Delivery.* Pharmaceutical Research, 2001. **18**(8): p. 1157-1166.

[4] Gref, R., Lück, M., Quellec, P., et al., *'Stealth' Corona-Core Nanoparticles Surface Modified by Polyethylene Glycol (PEG): Influences of the Corona (PEG Chain Length and Surface Density) and of the Core Composition on Phagocytic Uptake and Plasma Protein Adsorption.* Colloids and Surfaces, B, 2000. **18**: p. 301-313.

[5] Unsworth, L.D., Sheardown, H., and Brash, J.L., *Protein-Resistant Poly(ethylene oxide)-Grafted Surfaces: Chain Density-Dependent Multiple Mechanisms of Action.* Langmuir, 2008. **24**: p. 1924-1929.

[6] Kenworthy, A.K., Hristova, K., Needham, D., et al., *Range and Magnitude of the Steric Pressure Between Bilayers Containing Phospholipids with Covalently Attached Poly(ethylene glycol).* Biophysical Journal, 1995. **68**: p. 1921-1936.

[7] Noppl-Simson, D.A. and Needham, D., *Avidin-Biotin Interactions at Vesicle Surfaces: Adsorption and Binding, Cross-Bridge Formation, and Lateral Interactions.* Biophysical Journal, 1996. **70**: p. 1391-1401.

[8] Gombotz, W.R., Guanghui, W., Horbett, T.A., et al., *Protein Adsorption to Poly(ethylene oxide) Surfaces.* Journal of Biomedical Materials Research, 1991. **25**(12): p. 1547-1562.

[9] Charoenphol, P., Huang, R.B., and Eniola-Adefeso, O., *Potential Role of Size and Hemodynamics in the Efficacy of Vascular-Targeted Spherical Drug Carriers.* Biomaterials, 2010. **31**(6): p. 1392-1402.

[10] Charoenphol, P., Mocherla, S., Bouis, D., et al., *Targeting Therapeutics to the Vascular Wall in Atherosclerosis - Carrier Size Matters.* Atherosclerosis, 2011. **217**(2): p. 364-370.

[11] Namdee, K., Thompson, A.J., Phapanin, C., et al., *Margination Propensity of Vascular-Targeted Spheres from Blood Flow in a Microfluidic Model of Human Microvessels.* Langmuir, 2013. **29**(8): p. 2530-2535.

[12] Thompson, A.J., Mastria, E.M., and Eniola-Adefeso, O., *The Margination Propensity of Ellipsoidal Micro/Nanoparticles to the Endothelium in Human Blood Flow.* Biomaterials, 2013. **34**(23): p. 5863-5871.

[13] Wong, J.Y. and Kuhl, T., *Dynamics of Membrane Adhesion: the Role of Polyethylene Glycol Spacers, Ligand-Receptor Bond Strength, and Rupture Pathway.* Langmuir, 2008. **24**(4): p. 1225-1231.

[14] Jeppesen, C., Wong, J.Y., Kuhl, T.L., et al., *Impact of Polymer Tether Length on Multiple Ligand-Receptor Bond Formation.* Science, 2001. **293**(5529): p. 465-468.

[15] Cruz, L.J., Tacken, P.J., Fokkink, R., et al., *The Influence of PEG Chain Length and Targeting Moiety on Antibody-Mediated Delivery of Nanoparticle Vaccines to Human Dendritic cells.* Biomaterials, 2011. **32**(28): p. 6791-6803.

[16] Gabizon, A., Horowitz, A.T., Goren, D., et al., *Targeting Folate Receptor with Folate Linked to Extremities of Poly(ethylene glycol)-Grafted Liposomes: In Vitro Studies.* Bioconjugate Chemistry, 1999. **10**(2): p. 289-298.

[17] Ham, A.S., Klibanov, A.L., and Lawrence, M.B., *Action at a Distance: Lengthening Adhesion Bonds with Poly(ethylene glycol) Spacers Enhances Mechanically Stressed Affinity for Improved Vascular Targeting of Microparticles.* Langmuir, 2009. **25** (17): p. 10038-10044.

[18] Charoenphol, P., Onyskiw, P.J., Carrasco-Teja, M., et al., *Particle-Cell Dynamics in Human Blood Flow: Implications for Vascular-Targeted Drug Delivery.* Journal of Biomechanics, 2012. **45**(16): p. 2822-2828.

[19] Yoo, J.W., Chambers, E., and Mitragotri, S., *Factors that Control the Circulation Time of Nanoparticles in Blood: Challenges, Solutions and Future Prospects.* Current Pharmaceutical Design, 2010. **16**: p. 2298-2307.

[20] Less, J.R., Skalak, T.C., Sevick, E.M., et al., *Microvascular Architecture in a Mammary Carcinoma: Branching Patterns and Vessel Dimensions.* Cancer Research, 1991. **51**: p. 265-273.

[21] Chacko, A.-M., Hood, E.D., Zern, B.J., et al., *Targeted Nanocarriers for Imaging and Therapy of Vascular Inflammation.* Current Opinions in Colloid and Interface Science, 2011. **16**(3): p. 215-227.

[22] Chang, K.-C. and Hammer, D.A., *The Forward Rate of Binding of the Surface-Tethered Reactants: Effect of Relative Motion Between Two Surfaces.* Biophysical Journal, 1999. **76**(3): p. 1280-1292.

[23] Brunk, D.K. and Hammer, D.A., *Quantifying Rolling Adhesion with a Cell-Free Assay: E-selectin and its Carbohydrate Ligands.* Biophysical Journal, 1997. **72**(6): p. 2820-2833.

[24] Eniola, O.A., Willcox, P.J., and Hammer, D.A., *Interplay Between Rolling and Firm Adhesion Elucidated with a Cell-Free System Engineered with Two Distinct Receptor-Ligand Pairs.* Biophysical Journal, 2003. **85**(4): p. 2720-2731.

[25] Needham, D. and Kim, D.H., *PEG-Covered Lipid Surfaces: Bilayers and Monolayers.* Colloids and Surfaces B, 2000. **18**(3-4): p. 183-195.

[26] Zern, B.J., Chacko, A.-M., Liu, J., et al., *Reduction of Nanoparticle Avidity Enhances the Selectivity of Vascular Targeting and PET Detection of Pulmonary Inflammation.* ACS Nano, 2013. **7**(3): p. 2461-2469.

CHAPTER 4

PEGYLATION TO IMPROVE THE ADHESION OF PLASMA-SENSITIVE DRUG DELIVERY SYSTEMS IN BLOOD

Contents of this chapter are being prepared for manuscript submission (Namdee et al. *In preparation. 2015)*. Data from Fig. 4.2 has been published in the following:

Sobczynski, D. J., Charoenphol, P., Heslinga, M. J., Onyskiw, P. J., Namdee, K., Thompson, A. J., and Eniola-Adefeso, O. *Plasma Protein Corona Modulates the Vascular Wall Interaction in a Material in a Donor Specific Manner*, 2014. PLoS ONE **9**(9): e107408. doi: 10. 1371/journal.pone.010408.

4.1. Introduction

Tissue specific drug delivery entails loading a therapeutic agent into a drug delivery system (DDS) which targets diseased tissue through passive (physical entrapment) or active (ligand-based targeting) means. While polystyrene spheres are often the choice as a model DDSs for optimizing the carrier's margination and adhesion in blood, polystyrene itself is not applicable as DDSs due to the toxic nature of its precursor material.[1, 2] Therapeutic release is dependent on the degradation of the DDS and thus, one of the key aspects in designing DDSs is to ensure that the DDS is biocompatible; that is to say, (1) the DDS's core material itself is of low toxicity to the host and (2) the byproducts of degradation are absorbed into biological processes. Poly(lactic-co-glycolic acid) (PLGA) is often proposed as a core material for polymeric DDSs due to its biocompatibility and approval for use as a DDS by the US Food and

Drug Administration; however, little work has been done demonstrating the adhesiveness of PLGA VTCs to the vessel wall in blood flow.[3]

Recently, inflammation targeting PLGA microspheres were shown to have significantly lower adhesion levels in human blood compared to the adhesion in both buffer only and red blood cells-in buffer (RBCs+Buffer) systems.[4] In fact, the adhesion of PLGA spheres in whole blood was reduced to 90-95% of the adhesion in RBCs+Buffer for a wide range of particle sizes (0.3-5 μm).[4] This significant decrease in adhesion of PLGA targeted spheres in human blood, compared to buffer systems, was not observed with model polystyrene spheres in human blood.[4-6] The reduction in PLGA adhesion was attributed to specific plasma proteins, within the 150 kDa molecular weight range, having a greater affinity for absorbing onto PLGA spheres, but not polystyrene spheres, and reducing the adhesiveness of the targeting ligand.[4] Interestingly, the magnitude of the reduction in PLGA adhesion in blood was donor specific, suggesting that VTCs may be less efficient in targeting the vessel wall in patients with greater concentrations of the impacting plasma protein(s).[4] These results identified a material-specific plasma effect on VTC adhesion in blood which suggests that optimizing VTC adhesive trends using model polystyrene targeted spheres would not directly correlate to the adhesion of actual DDSs in blood.

The observed plasma protein interference in vessel wall adhesion of DDSs also appears to extend to animal blood. For instance, a plasma effect similar to that identified in humans has been observed in pig blood where targeted PLGA microspheres exposed to plasma (in RBC+Plasma only or pig whole blood) exhibited minimal adhesion to a model vessel under blood flow (Namdee et al. *In preparation*. 2015). Interestingly, the adsorption of pig plasma proteins not only affected PLGA targeted spheres but also significantly reduced the adhesion of

model polystyrene targeted spheres in blood. Pigs are often proposed as an *in vivo* model to study cardiovascular diseases due to pig blood and vasculature having similar reactivity, blood coagulation and atherosclerotic plaque formation, as humans.[7, 8] Thus, the reduction in targeting ability from the adsorption of plasma proteins onto a DDS's surface provides a limitation in optimizing both model (polystyrene-pig blood) and therapeutic (PLGA-human blood) DDSs *in vitro* and *in vivo* animal systems relevant to cardiovascular disease.

One strategy for restoring or improving the adhesion of plasma sensitive DDSs (PLGA/human blood or polystyrene/pig blood) is to prevent the adsorption of plasma proteins onto the DDS's surface. As previously discussed in Chapters 1 and 3, PEGylation is a common strategy for reducing plasma protein adsorption onto a material's surface. This occurs due to the hydrophilic nature of PEG forming a water-shell around the polymer chain which sterically prevents plasma proteins from adsorbing onto a material.[9] It is generally accepted that in order to achieve the steric hindrance required for preventing plasma protein adsorption, the PEG grafting density on the carrier's surface must be high enough such that the PEG chains are extended away from the carrier's surface (brush conformation).[9, 10] However, there have been some reports of observing reduced plasma adsorption and its corresponding side effects, such as increased circulation time, using low PEG grafting densities or loop conformation in which both ends of the polymer spacer are attached to the particle's surface.[11, 12] Thus, PEG conformation alone is not a sufficiently descriptive criterion for preventing plasma protein adsorption due to the fact that the conformation of the PEG corona is dependent on both PEG molecular weight and grafting density. It is also unclear whether improving the adhesion of plasma sensitive DDSs requires the complete prevention of all plasma proteins or simply reducing the adsorption of negatively impacting proteins (which were previously shown to be

approximately 150 kDa in molecular weight) onto the DDS's surface.[4] In this chapter, I examine if PEGylation can improve the adhesion of (1) sLe^a-targeted PLGA microspheres in human blood, and (2) sLe^a-targeted polystyrene microspheres in pig blood, which were both shown to have reduced adhesion due to the adsorption of plasma proteins, and work towards identifying a PEG density criterion for minimizing plasma effects and restoring adhesion for model and actual DDSs sensitive to plasma adsorption.

4.2. Results

The experimental set up used in this chapter is described in detail in Chapter 2.

4.2.1. Adhesion of PEGylated PLGA Targeted Microspheres in Human Blood

In order to investigate whether PEGylation would restore the adhesion of sLe^a-targeted PLGA microspheres in human plasma systems (RBCs+Plasma or whole blood) to the level of adhesion in buffer systems (Buffer only or RBCs+Buffer), 5.5 kDa and 10 kDa PEG spacers were covalently attached to the surface of PLGA spheres prepared via an oil/water emulsion-evaporation protocol as described in Chapter 2. The 5.5 kDa and 10 kDa PEG spacers were chosen based on the results from Chapter 3, demonstrating that these PEG spacers in an intermediate-brush conformation did not significantly affect the adhesion of sLe^a-targeted spheres (polystyrene) in human blood at the examined WSR (Fig. 3.1). Tables 4.1 – 4.3 show the particle size, PEG surface density (and conformation), and sLe^a density for all PEGylated and non-PEGylated PLGA spheres used in Figs. 4.1. – 4.3. The sLe^a density used in each experiment was based on the maximum sLe^a density achieved on the specific batch of PEGylated PLGA microspheres used in each flow assay.

Table 4.1. PEG surface density (and conformation) and sLe^a density for particles used in Fig. 4.1.

	PLGA-No PEG	PLGA-5.5 kDa PEG
Average Particle Diameter	3.4 μm ± 1.2 μm	
PEG Density (PEG chains/μm^2)	-	3,785 ± 361 (mushroom)
sLe^a Density (sites/μm^2)	453 ± 75	389 ± 122

Table 4.2. PEG surface density (and conformation) and sLe^a density for particles used in Fig. 4.2.

	PLGA-No PEG	PLGA-5.5 kDa PEG
Average Particle Diameter	3.0 μm ± 1.0 μm	
PEG Density (PEG chains/μm^2)	-	16,092 ± 1,247 (intermediate-brush)
sLe^a Density (sites/μm^2)	1,750 ± 186	1,730 ± 144

Table 4.3. PEG surface density (and conformation) and sLe^a density for particles used in Fig. 4.3.

	PLGA-No PEG	PLGA-10 kDa PEG
Average Particle Diameter	2.9 μm ± 0.2 μm	
PEG Density (PEG chains/μm^2)	-	3,222 ± 183 (intermediate-brush)
sLe^a Density (sites/μm^2)	167 ± 53	171 ± 67

Fig. 4.1 shows the adhesion density of PEGylated PLGA spheres with a low PEG density corresponding to a mushroom conformation (3,800 PEG chains/μm^2, Table 4.1) in human RBCs+Buffer, RBCs+Plasma, and whole blood under 200 s^{-1} WSR of laminar flow. There was no significant difference in adhesion density between PEGylated and non-PEGylated PLGA particles in buffer-only flow. The addition of RBCs to buffer increased the adhesion of both non-PEGylated and PEGylated PLGA spheres by 1.4- and 1.9-fold, respectfully. The adhesion of PEGylated PLGA spheres in RBCs+Buffer was 1.4-fold higher than the adhesion of non-PEGylated PLGA spheres in RBCs+Buffer. However, the adhesion of both particles in plasma systems (RBCs+Plasma and whole blood) significantly decreased by approximately 60% relative to their respective adhesions in RBCs+Buffer. The adhesion of PEGylated and non-PEGylated spheres in whole blood was not significantly different than the adhesion level observed for the same particles in RBCs+Plasma. Fig. 4.2 shows the adhesion of PEGylated spheres with a PEG density corresponding to an intermediate-brush conformation (16,000 PEG chains/μm^2, Table 4.2) in buffer and whole blood. There was no significant difference in particle adhesion in buffer or blood flow between the non-PEGylated and PEGylated PLGA spheres. The adhesion of both particles in blood was 85% lower than their respective adhesion densities in buffer flow.

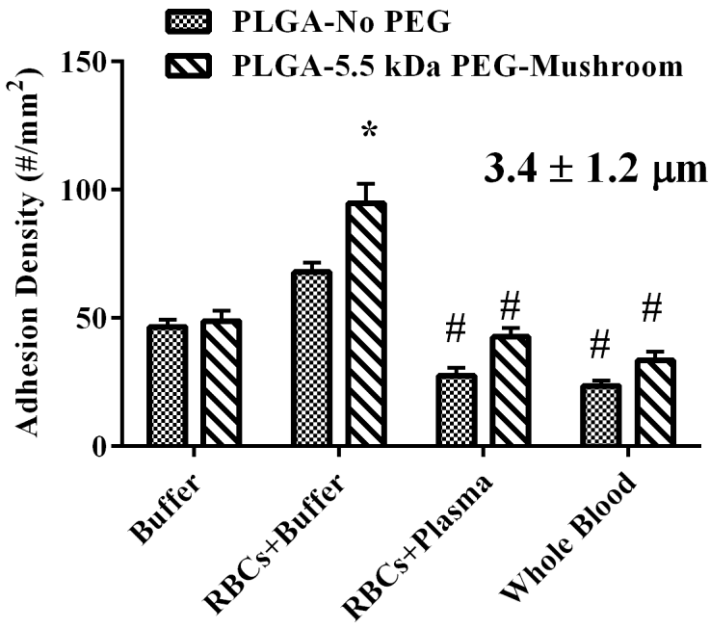

Figure 4.1. Adhesion of non-PEGylated and 5.5 kDa PEGylated (3,785 ± 361 PEG chains/μm^2, mushroom conformation) sLe^a-targeted (~400 sites/μm^2) PLGA spheres (3.4 ± 1.2 μm) in laminar flow at 200 s^{-1} WSR. * indicates significant difference compared to the adhesion of non-PEGylated spheres in the same flow system ($p<0.01$). # indicates significant difference compared to the adhesion of the same particle type in RBCs+Buffer ($p<0.01$).

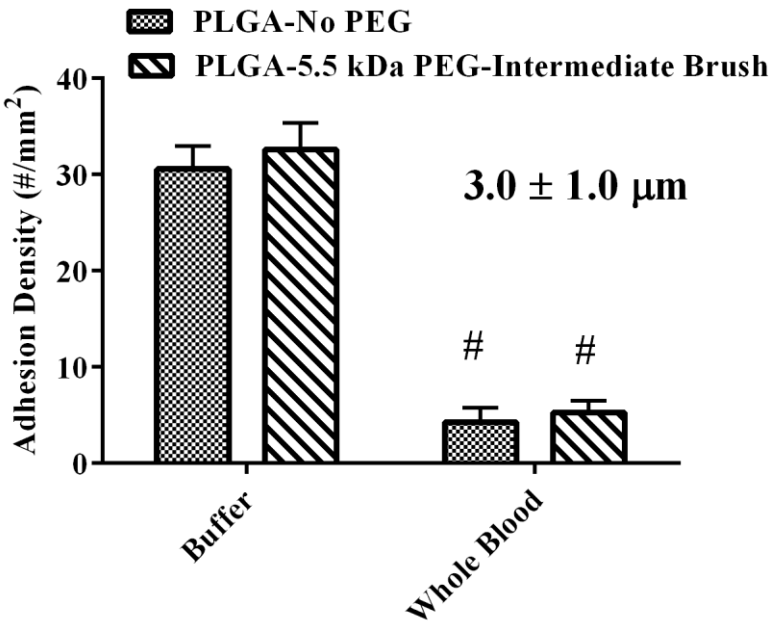

Figure 4.2. Adhesion of non-PEGylated and 5.5 kDa PEGylated (16,092 ± 1,247 PEG chains/μm^2, intermediate-brush conformation) sLe^a-targeted (~1,700 sites/μm^2) PLGA spheres (3.0 ± 1.0 μm) in laminar flow at 200 s^{-1} WSR. # indicates significant difference compared to the adhesion of the same particle in buffer flow ($p<0.01$).

To examine if a higher molecular weight PEG spacer would improve PLGA adhesion in blood, 10 kDa PEG spacers were conjugated to the surface of PLGA sLe^a-targeted spheres with enough density to achieve a similar intermediate brush conformation as the 5.5 kDa PEGylated PLGA spheres used in Fig. 4.2 (Table 4.3) and their adhesion was assessed in buffer and plasma systems at 200 s^{-1} WSR. Similar to what was observed in Figs. 4.1 and 4.2, there was no significant difference in adhesion between non-PEGylated and the 10 kDa PEGylated (3,222 PEG chains/μm^2) PLGA spheres in buffer flow and RBCs+Buffer. In RBCs+Plasma and whole blood, the adhesion of the 10 kDa PEGylated was ~ 3- and 2-fold greater than non-PEGylated PLGA spheres, respectfully. The adhesion level of PEGylated spheres in RBCs+Plasma was not significantly different than that of the same spheres in RBCs+Buffer; however, the adhesion of the PEGylated spheres in whole blood decreased by 60% relative to RBCs+Buffer. The adhesion of non-PEGylated PLGA spheres in RBCs+Plasma and whole blood was ~ 68% lower than that of the same spheres in RBCs+Buffer.

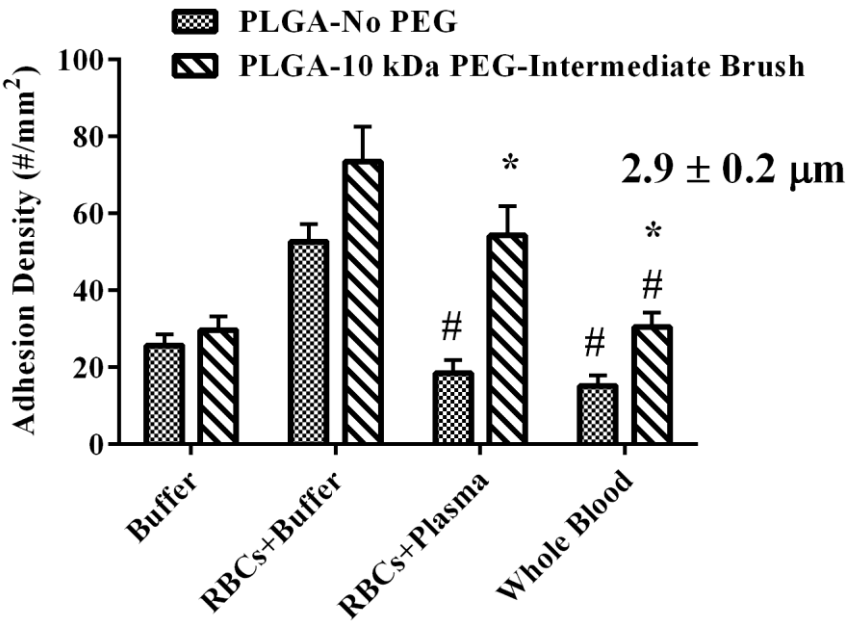

Figure 4.3. Adhesion of non-PEGylated and 10 kDa PEGylated (3,222 ± 183 PEG chains/μm^2, intermediate-brush conformation) sLe^a-targeted (~170 sites/μm^2) PLGA spheres (2.9 ± 0.2 μm) in laminar flow at 200 s^{-1} WSR. * indicates significant difference compared to the adhesion of non-PEGylated spheres in the same flow system ($p<0.01$). # indicates significant difference compared to the adhesion of the same particle type in RBCs+Buffer ($p<0.01$).

4.2.2. Adhesion of PEGylated Polystyrene Microspheres in Pig Blood

To investigate whether PEG can improve the adhesion of model VTC in pig blood, 2 μm polystyrene microspheres were conjugated with 5.5 kDa and 10 kDa PEG with PEG densities corresponding to an intermediate-brush conformation (Table 4.4). Fig. 4.4 shows the adhesion of non-PEGylated and PEGylated polystyrene spheres (sLe^a-targeted, ~1,000 sites/μm^2) in pRBCs+Buffer, pRBCs+Plasma, and whole blood (pRBC – pig red blood cells) under 200 s^{-1} of laminar flow. There was no significant difference in particle adhesion between non-PEGylated and both PEGylated microspheres (5.5 and 10 kDa) in pRBCs+Buffer. The adhesion density for all particles significantly decreased in pRBCs+Plasma and pig whole blood relative to pRBCs+Buffer, resulting in 90%, 86%, and 82% reductions in adhesion for non-PEGylated, 5.5 kDa PEG, and 10 kDa PEG; respectfully. There was no significant difference in adhesion between the PEGylated and non-PEGylated spheres in pRBCs+Plasma and pig whole blood.

Table 4.4. PEG surface densities and conformations of 2 μm polystyrene spheres (PS) used in polystyrene-pig blood flow assays (Fig. 4.4.).

	PS-5.5 kDa PEG	PS-10 kDa PEG
PEG Density	11,960 ± 1,624	4,987 ± 40
PEG Conformation	Intermediate-Brush	Intermediate-Brush

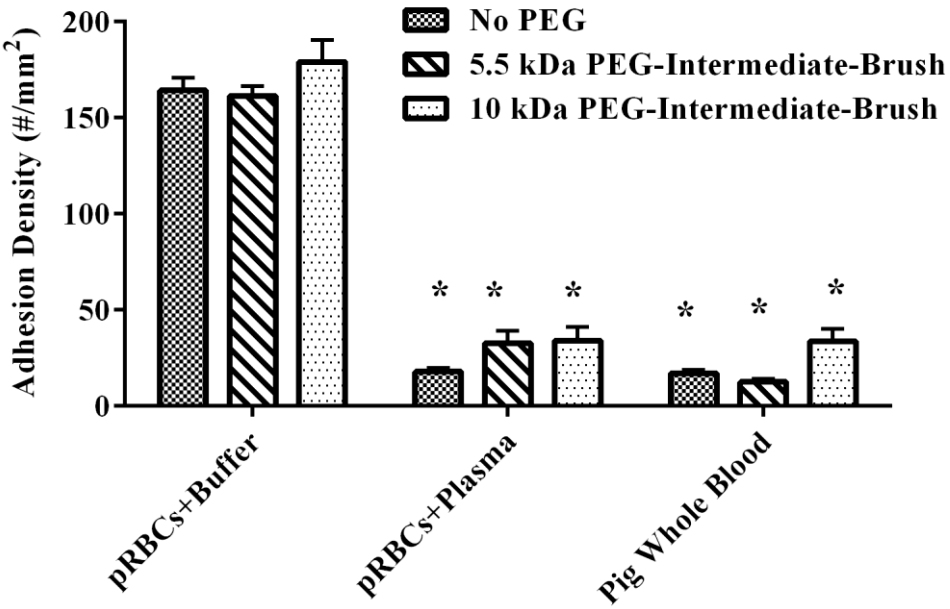

Figure 4.4. Adhesion of non-PEGylated, 5.5 kDa-PEGylated, and 10 kDa –PEGylated polystyrene spheres (2 μm) targeted with sLe^a (~1,000 sLe^a sites/μm^2) in laminar flow at 200 s^{-1} WSR. * indicates significant difference compared to the adhesion of the same spheres in pRBCs+Buffer ($p<0.01$).

To determine if increasing the PEG density would restore the adhesion of polystyrene microspheres in pig blood to the adhesion level observed in pig plasma-free systems, 2 μm polystyrene spheres were conjugated with a 5.5 kDa PEG spacer at 35,367 ± 1,450 PEG chains/μm^2. The increase in PEG density (relative to the PEG density used in Fig. 4.4) was achieved by adjusting the PEG conjugation protocol such that the covalent attachment of PEG occurred under conditions with marginal solvation (higher salt concentration and PEG solution and increase temperature during conjugation).[13] The marginal solvation conditions allowed for reduced chain repulsion resulting in greater PEG packing at the particle surface.[13] Although an increase in PEG density was achieved, the maximum sLe^a density conjugated onto the PEGylated spheres resulted was only 318 ± 51 sites/μm^2. Thus, both the PEGylated and non-PEGylated spheres used in Fig. 4.5 were conjugated with only 318 ± 51 sLe^a sites/μm^2 instead of the 1,000 sLe^a sites/μm^2 used in Fig. 4.4. There was no significant difference in particle adhesion between the non-PEGylated and the high density PEGylated spheres in pRBCs+Buffer or pRBCs+Viscous Buffer in which the viscosity of the reconstituting buffer was matched to that of pig plasma. For the non-PEGylated spheres there was a 95% reduction in the adhesion in plasma systems (pRBCs+Plasma and pig whole blood) relative to their adhesion in pRBCs+Buffer. However, there was no significant difference in adhesion of the high density PEGylated spheres between all pig blood systems examined, and the adhesion of PEGylated spheres was approximately 15- and 10-fold greater than non-PEGylated spheres in pRBCs+Plasma and pig whole blood, respectfully. However, preliminary results suggest that the negatively impacting plasma proteins are present after long-term exposure to pig plasma (~1 hour), which suggests that this high density PEGylation (~35,000 PEG chains/μm^2) may only provide short-term improvements to model VTC adhesion in pig blood (data not shown).

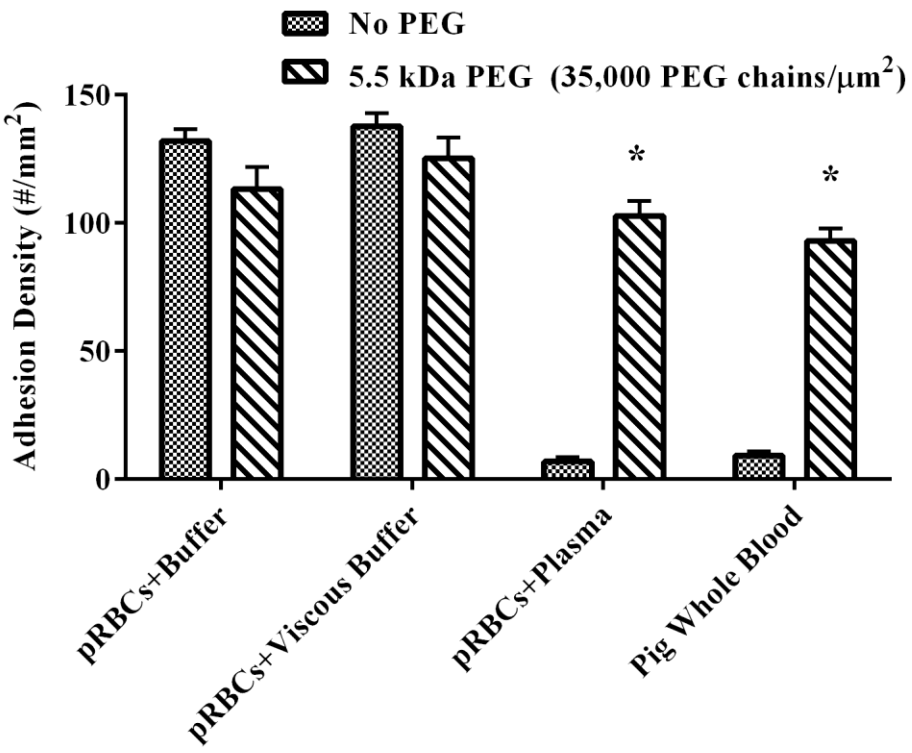

Figure 4.5. Adhesion of non-PEGylated and 5.5 kDa-PEGylated (35,367 ± 1,450 PEG chains/μm^2) polystyrene spheres targeted with sLe^a (318 ± 51 sLe^a sites/μm^2) in laminar flow at 200 s^{-1} WSR. * indicates significant difference compared to the adhesion of non-PEGylated spheres in the same flow system ($p<0.01$).

4.3. Discussion

The recently identified material dependent plasma effect on the adhesion of DDSs in human and animal blood has provided a significant challenge in optimizing vascular targeting. While model DDSs, such as polystyrene spheres, allow for easy manipulation of particle geometry (size and shape) for optimizing margination and adhesion in blood, their adhesive trends cannot be assumed to directly transfer to actual DDSs, such as PLGA spheres, due to human and animal plasma exhibiting minimal or no effect on polystyrene VTC adhesion. Minimizing or reducing plasma adsorption through PEGylation is a viable option for neutralizing the material dependent plasma effect and restoring the adhesion of plasma-sensitive VTCs, such as a PLGA DDSs, in blood. In this chapter, I examine if the addition of PEG onto a PLGA microsphere's surface improves or restores the adhesion of PLGA targeted spheres in blood to the adhesion level of PLGA spheres in plasma-free flow systems (buffer only or RBCs+Buffer systems).

While it is often suggested that a PEG brush orientation is required to prevent sufficient plasma protein adsorption resulting in increases systemic circulation time (*in vivo*), there have been some reports that show improved circulation time and reduced BSA adsorption with a mushroom conformation.[11, 12] For low density PEGylated PLGA spheres corresponding to a mushroom conformation, PEG was unable to improve the adhesion of PEGylated PLGA spheres to the adhesion levels observed in RBCs+Buffer (Fig. 4.1). Interestingly, the adhesion of mushroom oriented PEG was significantly higher than non-PEGylated spheres in RBCs+Buffer. In Chapter 3, I show that polystyrene-PEG particles in a mushroom conformation significantly improved the adhesion of aICAM-1 targeted spheres under unfavorable adhesion conditions (500 s^{-1} WSR, Fig. 3.4). I anticipate a similar effect in that the improved adhesion level of PEGylated

PLGA spheres with a mushroom conformation in RBCs+Buffer is due to PEG improving the adhesive dynamics of the targeting system.[14] This effect was not observed with polystyrene spheres with 1,000 sLe^a sites/μm^2 in Chapter 3, most likely because the higher ligand density already being sufficient for adhesion at the WSRs explored. However, the reduction in adhesion of the mushroom PEGylated PLGA spheres in plasma systems suggests that the improvement in adhesive dynamics with the addition of PEG in the mushroom conformation are negated in the presence of plasma, possibly due to the low PEG density still allowing for sufficient plasma protein adsorption. Thus, I hypothesize that a higher PEG density is required to restore PLGA adhesion in human blood.

The maximum PEG density (5.5 kDa) obtained on PLGA microspheres was ~ 16,000 PEG chains/μm^2 and corresponding to an intermediate-brush conformation (based on the relationship between the distance between adjacent PEG chains and R_f (as described in Fig. 2.3). Surprisingly, this PEG condition did not significantly improve the adhesion of targeted PLGA spheres in plasma systems, relative to non-PEGylated spheres of the same ligand density in whole blood (Fig. 4.2). In fact the adhesion level of PEGylated spheres with 16,000 PEG chains/μm^2 was significantly lower than that observed with the low density PEGylated spheres oriented in a mushroom conformation (~3,800 PEG chains/μm^2), even though the high density PEGylated spheres had 4 times as much sLe^a density. The negative plasma effect on PLGA adhesion in human blood has been shown to be donor specific; that is, the magnitude of the reduction in PLGA adhesion relative to plasma-free systems is dependent on the unique concentration of specific plasma proteins (~ 150 kDa molecular weight) in blood.[4] Thus, it is plausible that the lower adhesion level of the high PEG density PLGA spheres in blood (Fig. 4.2), relative to the mushroom oriented PEG spheres (Fig. 4.1), may be due to the specific donors

used for the assay and not related to the PEG density. The lack of a significant difference in the adhesion density between PEGylated and non-PEGylated PLGA spheres in buffer-only suggests that PEG in the intermediate-brush conformation did not contribute to the reduction in particle adhesion observed with human whole blood (Fig. 4.2). Previous work using a 5.0 kDa PEG reported that a dense brush conformation, where the distance between adjacent PEG chains is < 3 nm, was necessary for reducing plasma protein adsorption onto nanoparticles.[10, 11, 15] The distance between adjacent PEG chains for the 5.5 kDa PEG chain with ~16,000 PEG chains/μm^2 is estimated to be 8.9 nm (estimated using Equation 2.2 from Chapter 2), suggesting that there is still sufficient space between adjacent PEG chains for plasma adsorption onto the PEGylated DDS; and hence, a negative plasma effect on adhesion.

To determine if a larger PEG spacer would improve the adhesion of PLGA spheres in plasma systems, a 10 kDa PEG was conjugated to PLGA spheres such that the PEG corona was oriented in an intermediate-brush conformation (Table 4.3). I anticipated that the larger PEG spacer, relative to the 5.5 kDa PEG, would provide more steric hindrance for blocking plasma protein adsorption and potentially restore PLGA particle adhesion in human blood. The addition of a 10 kDa PEG in an intermediate-brush conformation did improve the adhesion of targeted PLGA spheres compared to non-PEGylated PLGA spheres in plasma systems (RBCs+Plasma and whole blood, Fig. 4.3). However, the adhesion of 10 kDa PEGylated spheres in whole blood was significantly different than the adhesion of the same spheres in RBCs+Buffer and RBCs+Plasma. It remains unclear whether the improved adhesion, relative to non-PEGylated spheres, in plasma systems is due to PEG reducing plasma adsorption or simply improving the adhesion dynamics of the targeting ligand. The distance between adjacent PEG chains for the 10 kDa PEG is estimated to be 19.9 nm which is significantly larger than the estimated distance

between adjacent 5.5 kDa PEG chains with ~16,000 PEG chains/μm^2 (8.9 nm). Similar to the 5.5 kDa PEG with ~16,000 PEG chains/μm^2, it was anticipated that there was still significant plasma protein adsorption with the 10 kDa PEG spacer. Previous work has also shown that the stress on an adhesive bond in shear flow decreases with increase PEG molecular weight.[14] I hypothesize that the improvement in PLGA adhesion in RBCs+Plasma with the 10 kDa PEG in the intermediate-brush conformation, relative to the adhesion of non-PEGylated spheres, is mostly due to improved adhesive dynamics of the targeting ligand and not a reduction in plasma protein adsorption. However in whole blood, the hypothesized improved adhesive dynamics with the addition of a 10 kDa spacers is not sufficient to overcome the combined effects of plasma adsorption and collisions with rolling leukocytes on the endothelium, resulting in a decrease in particle adhesion relative to RBCs+Plasma only (Fig. 4.5).[6]

The results from this work suggest that higher PEG grafted densities than those used in this work (>16,000 and 3,220 PEG chains/μm^2 for 5.5 and 10 kDa PEG, respectfully) are required to reduce the adsorption of negatively impacting plasma proteins on PLGA spheres and improve their adhesion in blood. However, further attempts in increasing the PEG density onto PLGA spheres were not successful. One of the limitations in PEGylating PLGA spheres is the low concentration of carboxyl groups available for PEGylation. This is likely due to low mole fraction of carboxyl groups compared to the number of monomers in the polymer, i.e. the only carboxylic acid group available for conjugation is present at the end chain of the PLGA polymer. I hypothesize that the low density of carboxyl groups available for PEGylation on PLGA spheres is the contributing factor in the unsuccessful attempts in achieving higher PEG densities for the 5.5 and 10 kDa PEG spacers used in this work. A modified protocol applied to polystyrene spheres to increase the PEG density from ~11,000 PEG chains/μm^2 to ~35,000 PEG (Table 4.4)

chains/μm^2 may not be suitable for PLGA spheres due PLGA microsphere experiencing enhanced degradation and plasticization at high temperature, such as that used during high density PEG conjugation (60ºC).[16] As a result, new conjugation or PLGA fabrication techniques may be required in order to conjugate higher PEG densities than those achieved in this work.

Polystyrene spheres are often used as model DDSs when optimizing carrier geometry for margination and adhesion in blood because they are readily available in a variety of uniform sizes and can be easily charged with a high density of carboxyl groups. Recently it was shown that the adsorption of pig plasma onto a targeted polystyrene microsphere significantly reduced the adhesion of sLe^a-targeted spheres in blood flow in a similar manner as the plasma effect of human plasma on PLGA targeted spheres (Namdee et al. *In preparation*. 2015). Pig *in vivo* models are of particular interest in evaluating VTCs for cardiovascular diseases such as atherosclerosis and deep vein thrombosis, because of the similarities in blood coagulation and plaque development as human blood.[7, 8] Similar to what was observed with PEGylated PLGA spheres in human blood, the addition of 5.5 kDa (~16,000 PEG chains/μm^2) or 10 kDa (~5,000 PEG chains/μm^2), both in an intermediate-brush conformation, did not restore the adhesion of sLe^a-targeted spheres in the pig plasma systems (pig whole blood or pig RBCs in pig plasma) compared to pRBCs+Buffer (Fig. 4.4). However, increasing the PEG density of 5.5 kDa PEG to ~35,000 PEG chains/μm^2 did significantly improve the adhesion of sLe^a-targeted spheres in both pig plasma systems (Fig. 4.5). In fact, the adhesion of the high PEG density polystyrene spheres was similar to the adhesion level observed for polystyrene spheres (~1,000 sLe^a sites/μm^2) at the same WSR in human blood (~100 particles/mm^2, Fig. 3.1). Interestingly, the distance between adjacent PEG chains for the 35,000 PEG chains/μm^2 polystyrene spheres (5.5 kDa) is estimated

to be approximately 6 nm, which suggests there is still sufficient room for plasma protein adsorption onto the particle's surface. Previous work has shown the 5 kDa PEG chains with a distance between PEG chains >3 nm did not show the ability to prevent plasma protein adsorption.[11] While it is possible that the high density PEGylated spheres with ~35,000 PEG chains/μm^2 may not be completely prevent plasma adsorption, it may briefly provide enough steric hindrance to reduce the amount of the negatively impacting plasma proteins, which were previously identified to be relatively large in size (150 kDa molecular weight), in order to establish adhesion to the activated endothelium. Thus, the adhesion of polystyrene spheres in pig blood may be restored by limiting, but not completely preventing, plasma protein adsorption. However, it remains unclear if this PEG density (~35,000 PEG chains/μm^2) improves polystyrene adhesion in pig blood beyond the 5 minutes of exposure to plasma as was the case with the flow assays used in this work.

Overall in this chapter, PEGylation was used in an attempt to restore the adhesion of sLe^{a-}targeted spheres which showed reduced adhesion in plasma systems (PLGA/human blood or polystyrene/pig blood). This study shows that for polystyrene spheres in pig blood, a PEG density of ~35,000 PEG chains/μm^2 is sufficient to restore adhesion of sLe^a-targeted spheres in pRBCs+Plasma and pig whole blood to the adhesion level observed in pRBCs+Buffer. However, it is yet to be seen whether improving PLGA adhesion in human blood requires the same PEG density (~35,000 PEG chains/μm^2) that improved polystyrene adhesion in pig blood or if PLGA adhesion in human blood may be improved with lower PEG grafting densities.

References

[1] Bond, J.A. and Bolt, H.M., *Review of the Toxicology of Styrene.* Critical Reviews in Toxicology, 1989. **19**(3): p. 227-249.

[2] Hafeli, U.O. and Pauer, G.J., *In Vitro and In Vivo Toxicity of Magnetic Microspheres.* Journal of Magnetism and Magnetic. Materials, 1999. **194**(1-3): p. 76-82.

[3] Sah, H., Thoma, L.A., Desu, H.R., et al., *Concepts and Practices Used to Develop Functional PLGA-based Nanoparticulate Systems.* International Journal of Nanomedicine, 2013. **8**: p. 747-765.

[4] Sobczynski, D., Charoenphol, P., Heslinga, M., et al., *Plasma Protein Corona Modulates the Vascular Wall Interaction of Drug Carriers in a Material and Donor Specific Manner.* PLoS ONE, 2014. **9**(9): p. e107408.

[5] Charoenphol, P., Mocherla, S., Bouis, D., et al., *Targeting Therapeutics to the Vascular Wall in Atherosclerosis-Carrier Size Matters.* Atherosclerosis, 2011. **217**(2): p. 364-370.

[6] Charoenphol, P., Onyskiw, P.J., Carrasco-Teja, M., et al., *Particle-cell Dynamics in Human Blood Flow: Implications for Vascular-Targeted Drug Delivery.* Journal of Biomechanics, 2012. **45**(16): p. 2822-2828.

[7] Getz, G.S. and Reardon, C.A., *Animal Models of Atherosclerosis.* Atherosclerosis, Thrombosis, and Vascular Biology, 2012. **32**(1104-1115).

[8] Zaragoza, C., Gomez-Guerrero, C., Martin-Ventura, J.L., et al., *Animal Models of Cardiovascular Diseases.* Journal of Biomedicine and Biotechnology, 2011. **2011**: p. 1-13.

[9] Wattendorf, U. and Merkle, H.P., *PEGylation as a Tool for the Biomedical Engineering of Surface Modified Microparticles.* Journal of Pharmaceutical Science, 2008. **97**(11): p. 4655-4669.

[10] Gref, R., Lück, M., Quellec, P., et al., *'Stealth' Corona-Core Nanoparticles Surface Modified by Polyethylene Glycol (PEG): Influences of the Corona (PEG Chain Length and Surface Density) and of the Core Composition on Phagocytic Uptake and Plasma Protein Adsorption.* Colloids and Surfaces B, 2000. **18**: p. 301-313.

[11] Perry, J.L., Reuter, K.G., Kai, M.P., et al., *PEGylated PRINT Nanoparticles: The Impact of PEG Density on Protein Binding, Macrophage Association, Biodistribution, and Pharmacokinetics.* Nano Letters, 2012. **12**: p. 5304-5310.

[12] Peracchia, M.T., Vauthier, C., Passirani, C., et al., *Complement Consumption By Poly(ethylene glycol) in Different Conformations Chemically Coupled to Poly(isobutyl 2-cyanoacrylate) Nanoparticles.* Life Sciences, 1997. **61**(7): p. 749-761.

[13] Kingshott, P., Thissen, H., and Griesser, H.J., *Effects of Cloud-Point Grafting, Chain Length, and Density of PEG Layers on Competitive Adsorption of Ocular Proteins.* Biomaterials, 2002. **23**: p. 2043-2056.

[14] Ham, A.S., Klibanov, A.L., and Lawrence, M.B., *Action at a Distance: Lengthening Adhesion Bonds with Poly(ethylene glycol) Spacers Enhances Mechanically Stressed Affinity for Improved Vascular Targeting of Microparticles.* Langmuir, 2009. **25** (17): p. 10038-10044.

[15] Meng, F., Engbers, G.H.M., and Feijen, J., *Polyethylene Glycol-grafted Polystyrene Particles.* Journal of Biomedical Materials Research A, 2004. **70A**(1): p. 49-58.

[16] Baird, E., Holowka, D., Coates, G., et al., *Highly Effective Poly(ethylene glycol) Architectures for Specific Inhibition of Immune Receptor Activation.* Biochemistry, 2003. **42**: p. 12739-12748.

CHAPTER 5

VASCULAR TARGETED CARRIERS AS A PHYSICAL MECHANISM FOR BLOCKING LEUKOCYTE RECRUITMENT IN INFLAMMATION

Data from this chapter is being prepared for manuscript submission.

5.1. Introduction

During inflammation, activated endothelial cells upregulate cell adhesion molecules such as E-selectin, P-selectin, ICAM-1, and VCAM-1 that facilitate the leukocyte adhesion cascade (LAC) where leukocytes are first captured to the endothelium before firmly adhering and eventually trans-migrating into tissue space.[1, 2] While leukocyte recruitment is crucial for pathogen clearance, non-regulated or over-recruitment can result in or significantly affect the pathogenesis of several serious diseases. For example, atherosclerotic plaque development is enhanced by the continuous recruitment of leukocytes due to chronic inflammation in atheroprone areas, such as in medium to large arteries which experience oscillations or disturbed blood flow.[3, 4] In sepsis, high concentrations of circulating cytokines in blood plasma can induce systemic activation, leading to possible organ failure associated with the accumulation of neutrophils (the largest subclass of leukocytes) the lungs, liver, and kidneys.[5-8] In ischemia/reperfusion injury, hypoxia induced inflammation recruits neutrophils that release reactive oxygen species and proteases, which in turn increase endothelial permeability resulting in severe endothelial dysfunction.[9]

Influencing leukocyte recruitment has been proposed as a therapy for diseases with enhanced pathogenesis due to leukocyte accumulation. For example, in sepsis, reduced leukocyte organ accumulation has been associated with improved survival rates of mice subjected to lethal polymicrobial sepsis.[10, 11] Several strategies using antibodies towards CAMs such as E-selectin have shown limited success in improving recovery from ischemia/reperfusion injury due to short antibody half-life and development of antibody-antigen complexes.[12-14] VTCs are therapeutic systems designed to circulate the vasculature and target the endothelium of diseased tissue via specific molecular recognition. Inflammatory molecules that participate in the LAC, such as E-selectin and ICAM-1, have been proposed as targeted molecules for VTC applications in inflammation-associated diseases including various cancers and cardiovascular disease.[15, 16] The potential benefit of VTCs is in providing site-specific targeting and long term therapeutic delivery, which may alleviate issues with systemic clearance associated with anti-adhesion therapies. However, my knowledge, no systematic study exists on the influence of VTC margination on leukocyte adhesion to the vascular wall in a physiological blood flow environment.

During blood flow, red blood cells (RBCs) align in the center of flow resulting in a RBC-free layer, or cell free layer (CFL), along the endothelium.[17, 18] Margination is the preferential redistribution of cellular/particulate entities towards the endothelial wall and away from the RBC core.[18] Blood leukocytes and platelets are known to actively marginate to the CFL through a combination of low wall-induced lift forces, due to their rigidity, and heterogeneous collisions with RBCs that send them towards the endothelium.[17, 18] For VTCs to be fully effective, they too must efficiently marginate to the cell-free layer before interacting with the endothelium. Design parameters such as carrier size and targeting moieties have

typically been probed for optimizing the functionality of VTCs, including enhancing their margination. However, most VTC optimization has been done with simplified blood such as RBCs only in plasma or buffer which eliminates any opportunity for understanding the effect or impact of marginating leukocytes on VTC functionality and vice versa.[19-21] Previously, leukocytes were shown to significantly decrease the adhesion of microspheres larger than 2 μm, which was attributed to rolling leukocytes colliding with and removing surface-bound particles from the endothelium.[22] However, it currently remains unclear what effect, if any, the VTCs have on the interactions of leukocytes with the same vascular area, particularly when competing for binding to the same endothelial expressed molecules.

In this chapter, I investigate whether inflammation-targeting particles can alter leukocyte adhesion to an activated endothelial monolayer under physiological blood flow conditions. Specifically, targeted polystyrene spheres with diameters ranging from 200 nm - 5 μm were perfused in human blood at various concentrations and the adhesion of leukocytes and particles was assessed in oscillating flow and laminar flow. The results demonstrate that VTCs significantly influence leukocyte adhesion to the same targeted endothelium in blood flow and that the magnitude of the effect is dependent on VTC design parameters such as size and targeting moiety, along with particle endothelial surface coverage and hemodynamics.

5.2. Results

The experimental set up used in this chapter is described in detail in Chapter 2.

5.2.1. Influence of sLe^a-Targeted Spheres and Particle Size on Leukocyte Adhesion

Figure 5.1 (A-E) shows the effect of sLe^a-targeted spheres on leukocyte adhesion to an activated endothelium in oscillating human blood flow as a function of particle size and concentration. Leukocyte adhesion with the presence of particles in blood was normalized to the leukocyte adhesion density observed with particle-free blood of the same blood donor as described is Chapter 2, i.e. a value of 1 indicates the leukocyte adheison density with the presence of VTCs was equivalent to the leukocyte adhesion density in particle-free blood. The presence of the 5 μm targeted spheres at a concentration of $5x10^5$ particles/mL in blood flow resulted in a 22% decrease in leukocyte adhesion relative to particle free blood (Fig. 5.1.A). Increasing the concentraiton of 5 μm targeted spheres to $1x10^6$ and $2.5x10^6$ particles/mL in blood further decreased leukocyte adhesion 54% and 74%, respectfully. A blood concentration of the 5 μm sLe^a-spheres at $1x10^7$ particles/mL decreased leukocyte adhesion by 97% relative to particle-free blood. Unlike the 5 μm targeted spheres, 3 μm targeted spheres at $5x10^5$ particles/mL did not affect leukocyte adhesion in flow (Fig. 5.1.B). When the blood concentration of the 3 μm targeted spheres was increased to $1x10^6$ and $2.5x10^6$ particles/mL, leukocyte adhesion decreased by 40% and 35%, respectively, relative to particle-free blood. There was, however, no significant difference in the normalized leukcotye adhesion level between $1x10^6$ or $2.5x10^6$ particles/mL. Further increasing the concentraiton of 3 μm targeted spheres to $1x10^7$ particles/mL reduced leukocyte adhesion by 98%. For 2 μm spheres (Fig. 5.1.C), there was no significant effect on leukocyte adhesion compared to particle-free blood with blood concentrations of $5x10^5$ and $1x10^6$ particles/mL. At concentrations of $2.5x10^6$ and $1x10^7$ particles/mL, 2 μm spheres significantly decreased leukocyte adhesion by 27% and 69%, respectively.

500 nm spheres (Fig. 5.1.D) in $5x10^5$ and $1x10^6$ particles/mL blood concentrations, did not significantly affect leukocyte adhesion. Increasing the concentration of the 500 nm targeted spheres in blood to $2.5x10^6$ and $1x10^7$ particles/mL significantly decreased leukocyte adhesion by 22% and 39%, respectfully. Fig. 5.1.E shows the effect of 200 nm targeted spheres on leukocyte adhesion. At $1x10^7$ particles/mL there was no significant effect on leukocyte adhesion. Interestingly, when increasing the concentration of 200 nm targeted spheres such that their volume concentration in blood ($1.8x10^8$ particles/mL) was similar to the volume of 500 nm spheres at $1x10^7$ particles/mL, the 200 nm targeted spheres significantly decreased leukocyte adhesion by 40%, a value similar to the reduction observed with 500 nm targeted spheres ($1x10^7$ particles/mL, Fig. 5.1.D).

The particle adhesion densities corresponding to the particles used in Fig. 5.1. (A-E) are shown in Fig. 5.2 (A-E). For 5 μm, 3 μm, 2 μm, and 500 nm targeted spheres, there was no significant difference in particle adhesion between blood with $5x10^5$ anad $1x10^6$ particles/mL (Fig. 5.2.A-D). There was also no signifciant diference between the particle adhesion of 5 μm targeted spheres with $1x10^6$ and $2.5x10^6$ particles/mL. For all particle sizes, the adhesion density increased when increasing the particle blood concentraton from $2.5x10^6$ to $1x10^7$ particles/mL. Overall, the particle adhesion densites for the various sizes followed previously reported trends such that at a fixed blood concentraion the particle adhesion density of 2 and 3 μm > 5 μm > 500 nm > 200 nm spheres.[20, 23]

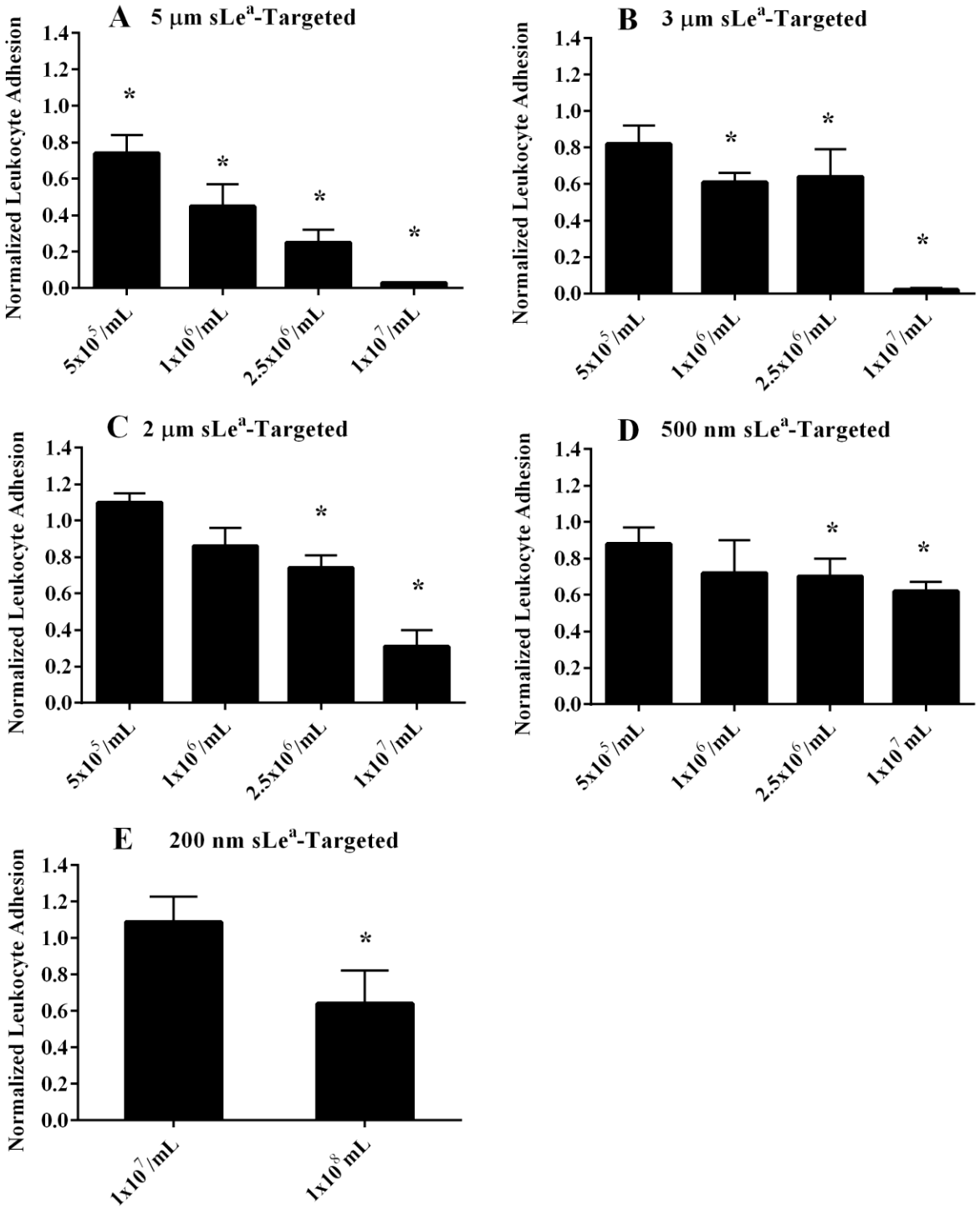

Figure 5.1. Normalized leukocyte adhesion with the presence of (A) 5 μm, (B) 3 μm, (C) 2 μm, and (D) 500 nm, (E) 200 nm sLe^a-targeted spheres (~1,000 sites/μm^2) at various blood concentrations under oscillating flow. * indicates significant difference in leukocyte adhesion relative to particle-free blood ($p<0.01$).

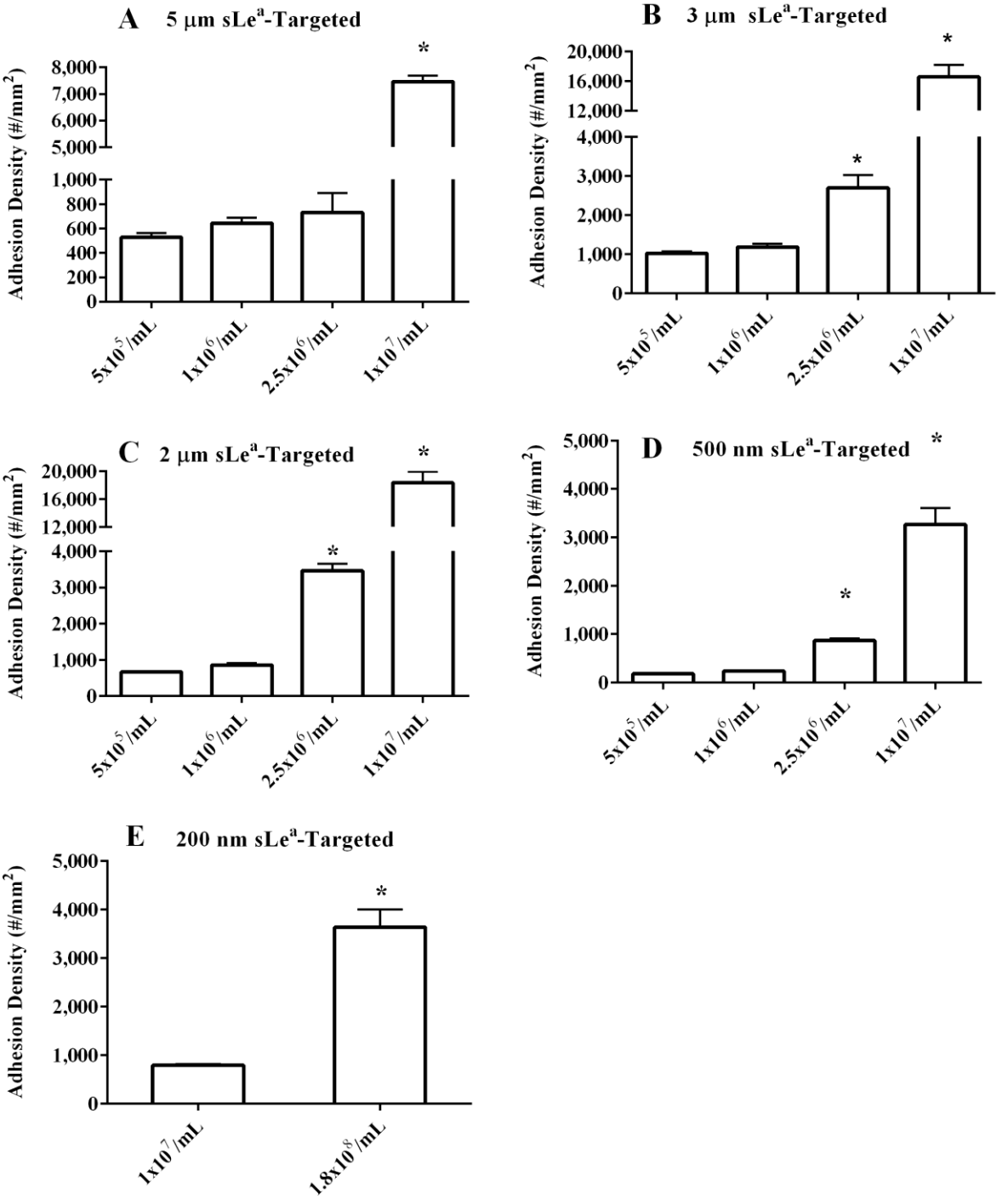

Figure 5.2. Particle adhesion densities for (A) 5 μm, (B) 3 μm, (C) 2 μm, and (D) 500 nm, (E) 200 nm targeted spheres (~1,000 sLe^a sites/μm^2) at various blood concentrations in oscillating flow. * indicates significant difference in particle adhesion relative to adhesion density with $5x10^5$ particles/mL of the same particle size ($p<0.01$).

To determine if the impact of targeted particles on leukocyte adhesion was due to molecular interactions of particles with the targeted molecule or just by their physical presence in flow, I explored the adhesion of leukocytes in blood flow containing non-targeted particles in the various size range explored in Fig. 5.1. Non-targeted 5 μm spheres with blood concentraitons of $1x10^6$, $2.5x10^6$, and $1x10^7$ particles/mL signifcanly reduced leukocyte adhesion by 28%, 53%, and 88%, respectfully, relative to particel free blood (Fig. 5.3.A). There was no significant effect of the 5 μm non-targeted spheres at $5x10^5$ particles/mL. For 3 μm $5x10^5$ particles/mL concentration significantly decreased leukocyte adhesion relative to particle-free blood; however, there was no significant effect on leukocyte adhesion with of any other particle concentrations explored for this particle size (Fig. 5.3.B). No reduction in leukcoyte adhesion was observed with any of the particle concentrations explored for 2 μm, 500 nm, and 200 nm non-targeted spheres (Fig. 5.3 D, C, and E).

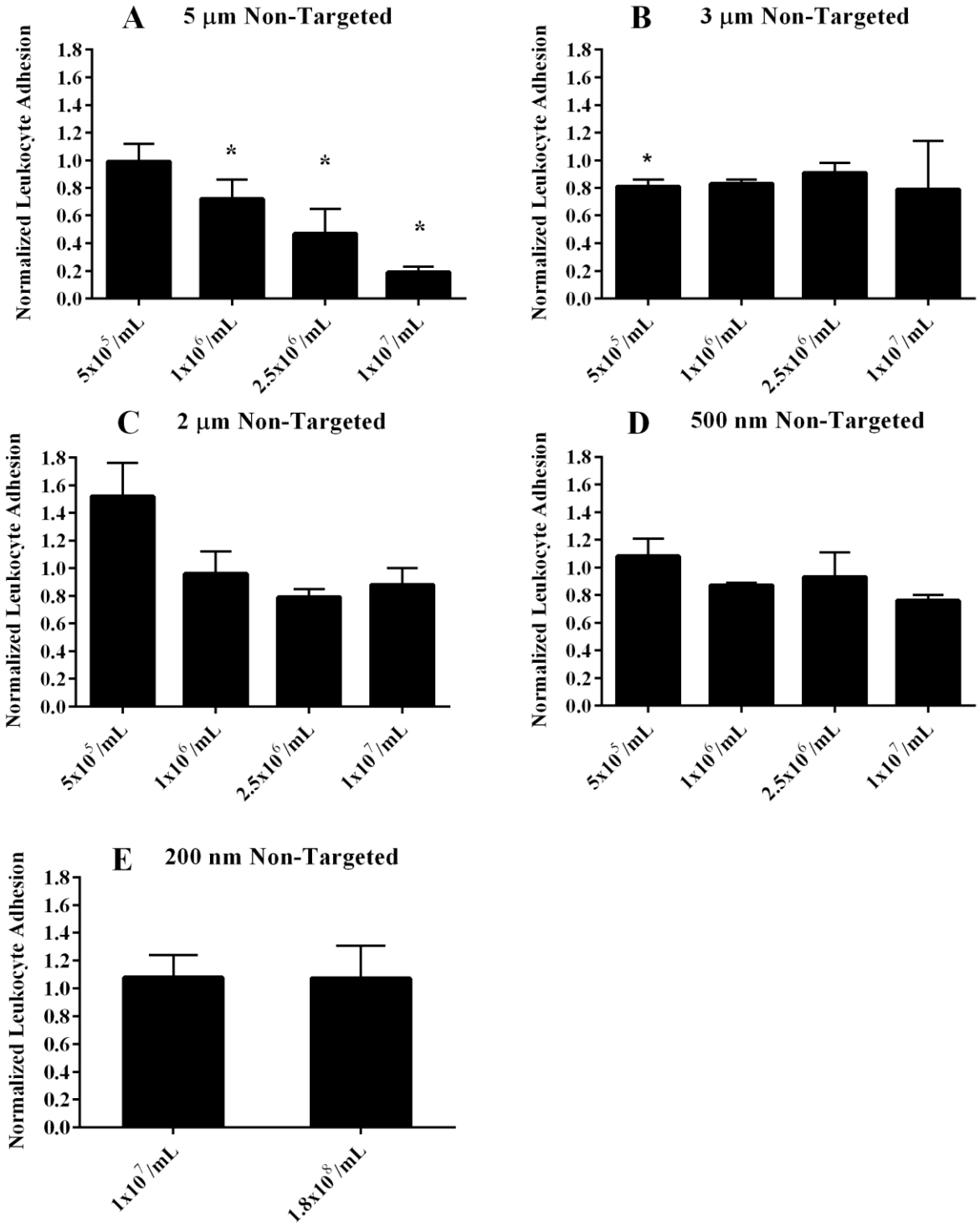

Figure 5.3. Normalized leukocyte adhesion with non-targeted (A) 5 μm, (B) 3 μm, (C) 2 μm, and (D) 500 nm, (E) 200 nm spheres at various blood concentrations. * indicates significant difference in leukocyte adhesion relative to particle-free blood ($p<0.01$).

To elucidate whether competion for adhesion to the endothelium between targeted particles and leukocytes resulted in the reduced leukocyte adhesion shown in Fig. 5.1, I plotted the percent reduction in leukocyte adhesion relative to particle-free blood, along with the corresponding adhesion densities for the sLe^a-targeted particles at $2.5x10^6$ (Fig. 5.4.A) and $1x10^7$ (Fig. 5.4.B) particles/mL concentrations. The maximum reduction in leukocyte adhesion with $2.5x10^6$ particles/mL (75% leuckoyte reduction) was observed when targeted 5 μm spheres were present in blood flow, even though the particle adhesion density for the spheres was aproximately 4-fold less than the particle adhesion of 3 μm and 2 μm spheres (Fig. 5.4.A). There was no significant difference in particle adhesion between 5 μm and 500 nm targeted spheres; however, 500 nm targeted spheres decreased leuckoyte adhesion by only 22%. For the $1x10^7$ particles/mL blood concentration (Fig. 5.4.B), 5 μm and 3 μm spheres decreased leukocyte adhesion by 97% and 98%, respectfully, even though the adhesion of 5 μm spheres was 2-fold lower than 3 μm spheres. The adhesion density of 3 μm spheres was not significantly different than the adhesion of 2 μm spheres; however, 2 μm spheres reduced the leukocyte adhesion by only 69% relative to particle free blood. Interestingly, while the particle adhesion for 2 μm spheres was 4-fold greater than that of 500 nm spheres at the same concentration, the percent reduction in leukocyte adhesion with 2 μm spheres was only 1.8-fold greater than that observed with 500 nm spheres (39% reduction). 200 nm targeted spheres did not affect leukocyte adhesion and its particle adhesion density was significantly lower than all other particle sizes with $1x10^7$ particles/mL concentration in blood.

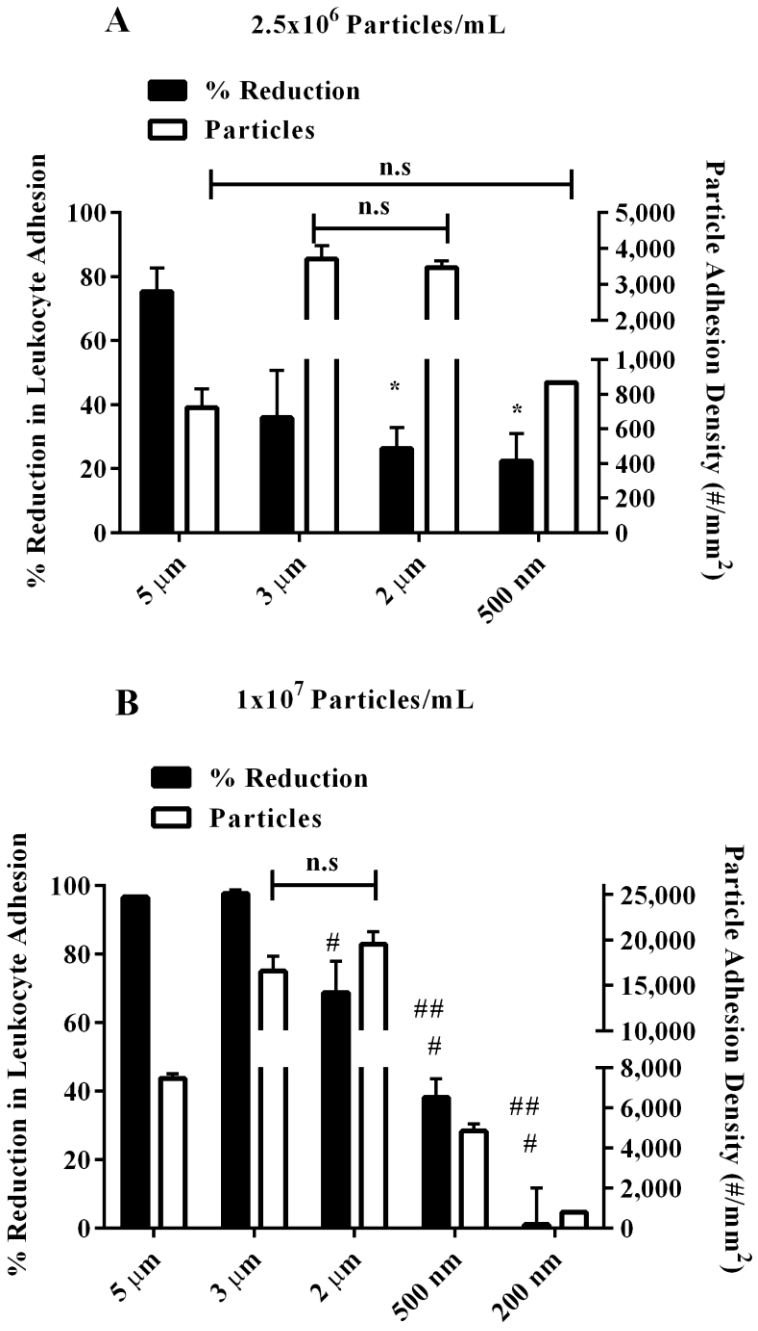

Figure 5.4. Reduction in leukocyte adhesion (black bars. left axis), relative to particle-free blood, with the adhesion densities of sLe^a-targeted spheres (white bars, right axis) at (A) $2.5x10^6$ particles/mL and (B) $1x10^7$ particles/mL in oscillating blood flow. For $2.5x10^6$ particles/mL (A) significance was compared to the reduction in leukocyte adhesion with 5 µm targeted spheres (*). For $1x10^7$ particles/mL (B) significance was compared to the reduction in leukocyte adhesion with 3 µm targeted spheres (#) and 2 µm targeted spheres (##). ($p<0.01$).

The leukocyte adhesion density with the presence of 5 µm or 2 µm non-targeted and targetd spheres in blood with $5x10^5$ particles/mL was also examined over the elapsed experimental time to determine if the reduction in leukocyte adhesion occured instananeously or after particle accumulation at the endothelium. In gerneral, the leukocyte adhesion in particle-free blood linearly increased throughout the experiment (Fig. 5.5.A, B - red circles). The leuckocyte adhesion trend with time was not significantly altered with the presence of non-targeted 5 µm (yellow triangles) or non-targeted 2 µm spheres (yellow diamonds) in blood (Fig. 5.5.A, B). The presence of 2 µm targeted spheres (blue diamonds) had no significant impact on the leukocyte adhesive trend. Interestingly with 5 µm targeted spheres (blue triangles), a separation in the leukocyte adhesive trends between particle-free blood and blood with targeted spheres ocurred aproximately 3-4 minutes into the elapsed experiment. After this, the leukocyte adhesion plateaued while the adhesion in particle-free blood continued to increase with time (Fig. 5.5.A). At this same time range, the particle adhesion for 5 µm spheres also plateaued while adhesion of 2 µm targeted spheres increased linearly with time (Fig. 5.5.C).[22]

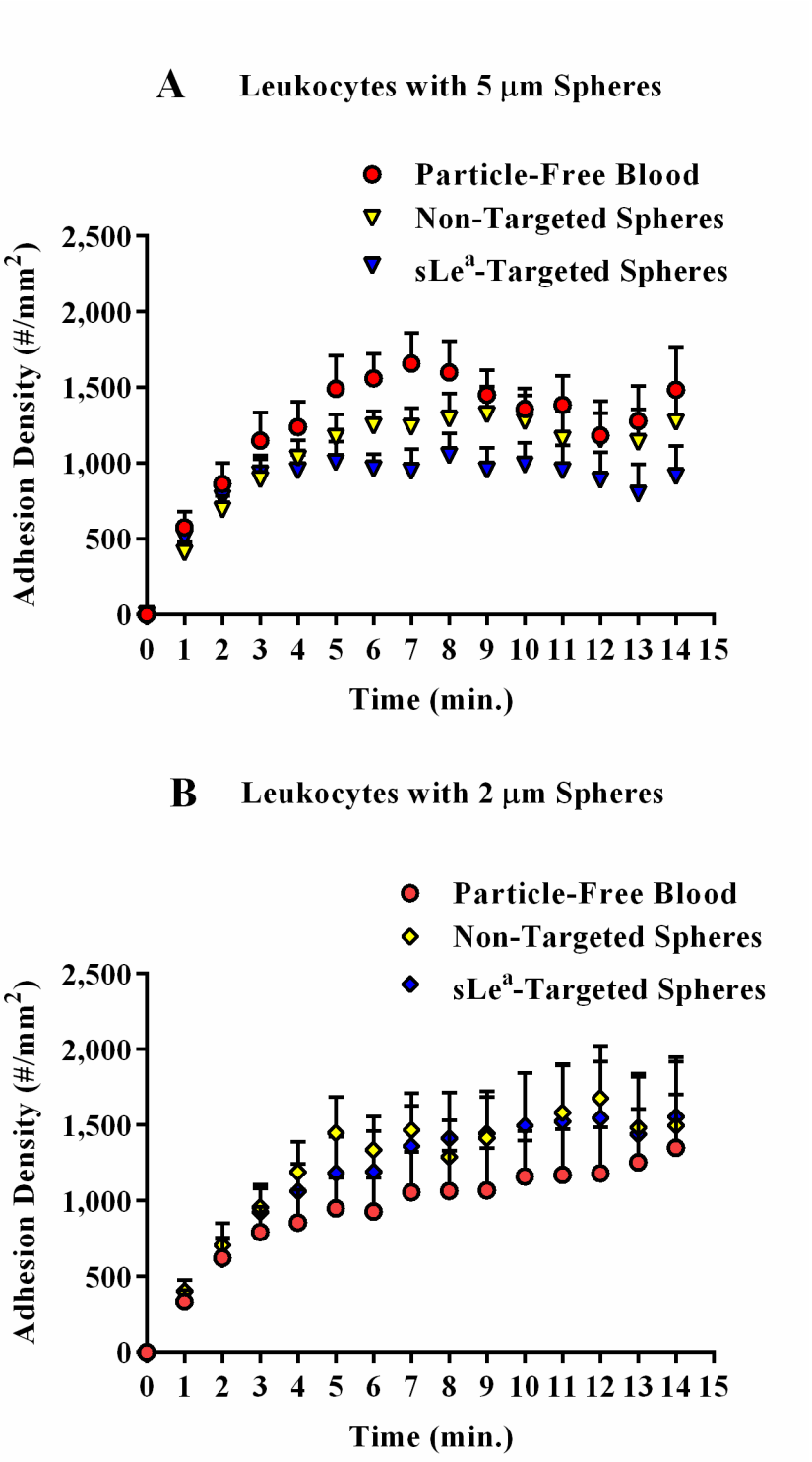
A
Leukocytes with 5 μm Spheres
Particle-Free Blood
Non-Targeted Spheres
sLe^a-Targeted Spheres
Adhesion Density (#/mm^2)
2,500
2,000
1,500
1,000
500
0
0 1 2 3 4 5 6 7 8 9 10 11 12 13 14 15
Time (min.)
B
Leukocytes with 2 μm Spheres
Particle-Free Blood
Non-Targeted Spheres
sLe^a-Targeted Spheres
Adhesion Density (#/mm^2)
2,500
2,000
1,500
1,000
500
0
0 1 2 3 4 5 6 7 8 9 10 11 12 13 14 15
Time (min.)

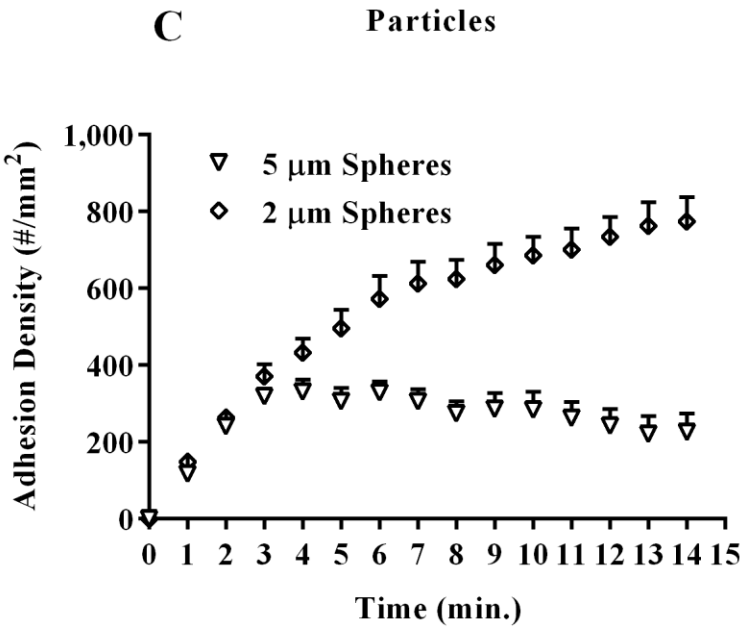

Figure 5.5. Leukocyte adhesion density vs. time with the presence of targeted and non-targeted (A) 5 μm spheres and (B) 2 μm spheres in blood with $5x10^5$ particles/mL in oscillating blood flow, along with (C) the corresponding particle adhesion densities for targeted spheres (1,000 sLe^a sites/μm^2).

5.2.2. Influence of Particle Shape on Leukocyte Adhesion in Oscillating Blood Flow

The influence of VTC shape on leukocyte adhesion was examined in oscillating blood flow using sLe^a-targeted rods of aspect ratio (AR) 4 and 9 (2 μm equivalent spherical volume). Table 5.1 shows the measurements for the major and minor lengths and surface area for AR4 and AR9 rod. There was no significant effect on leukocyte adhesion with the presence of AR4 or AR9 rods with $5x10^5$ particle/mL blood concentrations (Fig. 5.6). The particle adhesion for AR4 rods was not significantly different than the adhesion of 2 μm spheres; however, the adhesion of AR9 rods was 4.6-fold lower than the adhesion of 2 μm spheres and AR4 rods under the same blood flow conditions (Fig. 5.6). The presence of the higher aspect ratio rods in blood did not affect the leukocyte adhesion profile with time, relative to particle-free blood (Fig. 5.7.A). Similar to what was observed with 5 μm sLe^a-targeted spheres (Fig. 5.5.C), the adhesion of AR9 rods linearly increased within the first 5 minutes of blood flow, after which the adhesion decreased throughout the remainder of the flow assay (Fig. 5.7.B).

Table 5.1. Measurements of aspect ratio (AR), major axis length, minor axis length, and surface area of rods used in Fig. 5.6 and 5.7.

	AR 4 Rods	AR 9 Rods
Aspect Ratio	4.26 ± 1.20	8.89 ± 2.68
Major Axis Length	6.32 ± 1.11 μm	11.81 ± 2.03 μm
Minor Axis Length	1.55 ± 0.25 μm	1.31 ± 0.21 μm
Surface Area	24.38 ± 3.13 μm^2	35.76 ± 5.15 μm^2

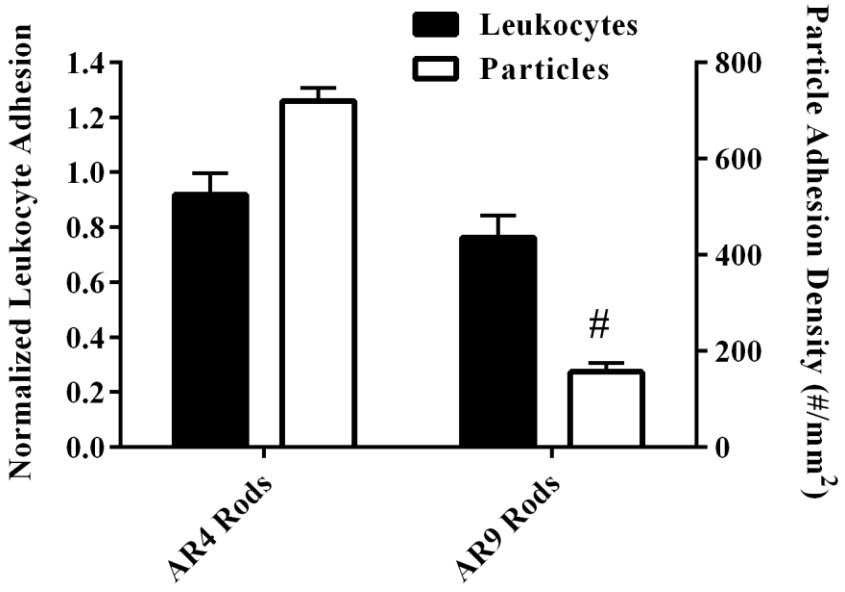

Figure 5.6. Normalized leukocyte adhesion (black bars, left axis) and particle adhesion (white bars, right axis) with the presence of AR4 and AR9 rods in blood with $5x10^5$ particles/mL. # indicates significant difference in particle adhesion relative to AR4 rods ($p<0.01$).

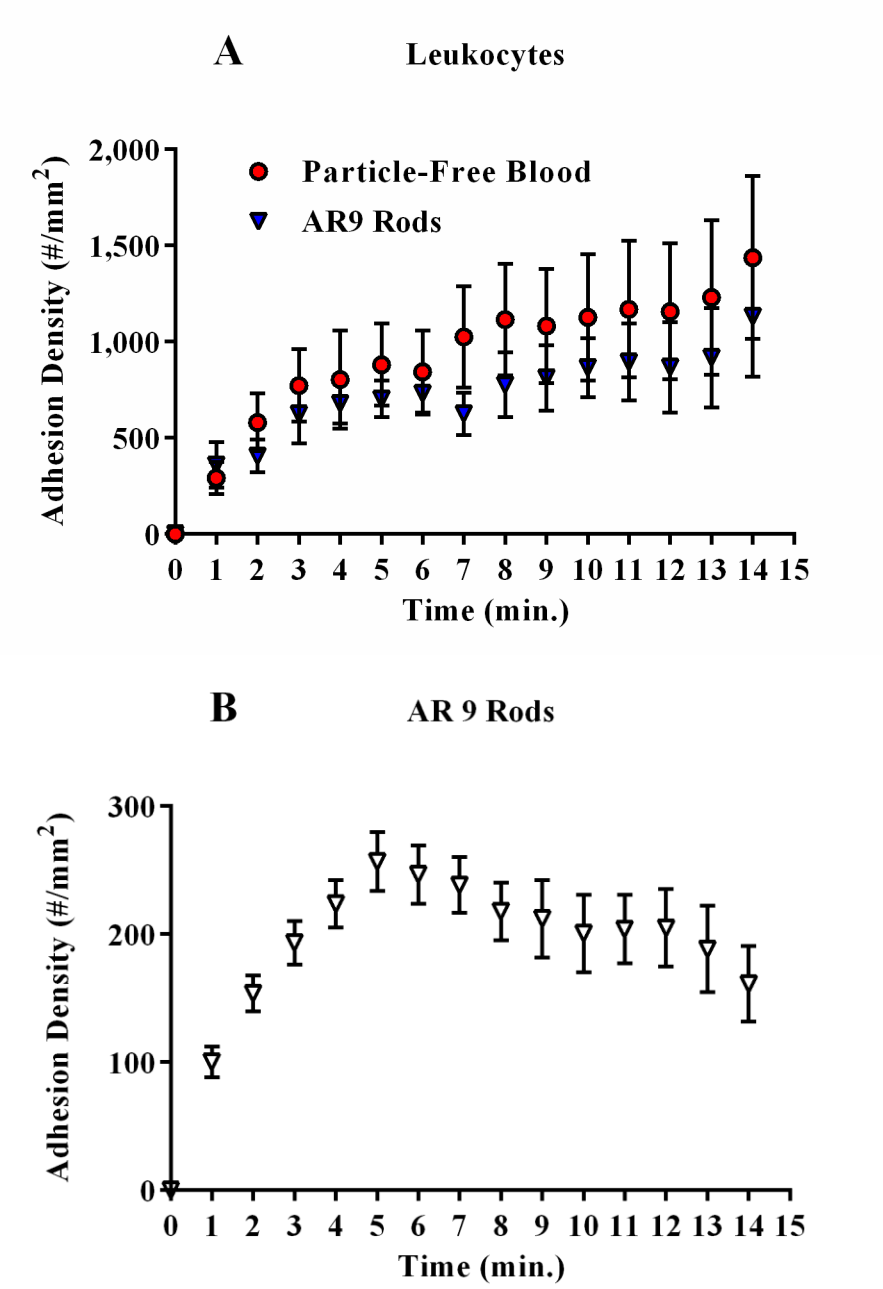

Figure 5.7. (A) Leukocyte and (B) particle adhesion densities vs. time in oscillating blood flow with sLe^a-targeted AR9 rods (open triangles) with 2 μm equivalent spherical volume at $5x10^5$ particles/mL blood concentration.

5.2.3. Influence of sLe^a-Ligand Density on Leukocyte Adhesion

The influence of VTC ligand density was examined to determine if increasing sLe^a density would affect leukocyte adhesion through enhanced molecular interactions between L-selectin present on leukocytes and sLe^a-targeted spheres (as sLe^a interacts with L-selectin expressed on leukocytes). The leukocyte adhesion was examined with 2 μm or 5 μm spheres with either 600 or 2,100 sLe^a sites/μm^2 in oscillating blood flow with a blood concentration of $5x10^5$ particles/mL. There was no significant effect of 2 μm targeted spheres with either 600 or 2,100 sLe^a sites/μm^2 on leukocyte adhesion, relative to particle-free blood (Fig. 5.8.A). The particle adhesion of 2 μm spheres with 600 and 2,100 sLe^a sites/μm^2 was not significantly different than the adhesion of 2 μm spheres with 1,000 sLe^a sites/μm^2 at the same blood concentration ($5x10^5$ particles/mL, Fig. 5.2.C). 5 μm targeted spheres with 2,100 sLe^a sites/μm^2 decreased leukocyte adhesion by 18% (Fig. 5.8.B), relative to particle-free blood, and this decrease was not significantly different compared to the percent reduction in leukocyte adhesion observed with 1,000 sLe^a sites/μm^2 at the same blood concentration ($5x10^5$ particles/mL, Fig. 5.1.A). The particle adhesion for 5 μm spheres with 2,100 sLe^a sites/μm^2 was also not significantly different then the adhesion of 5 μm spheres with 1,000 sLe^a sites.

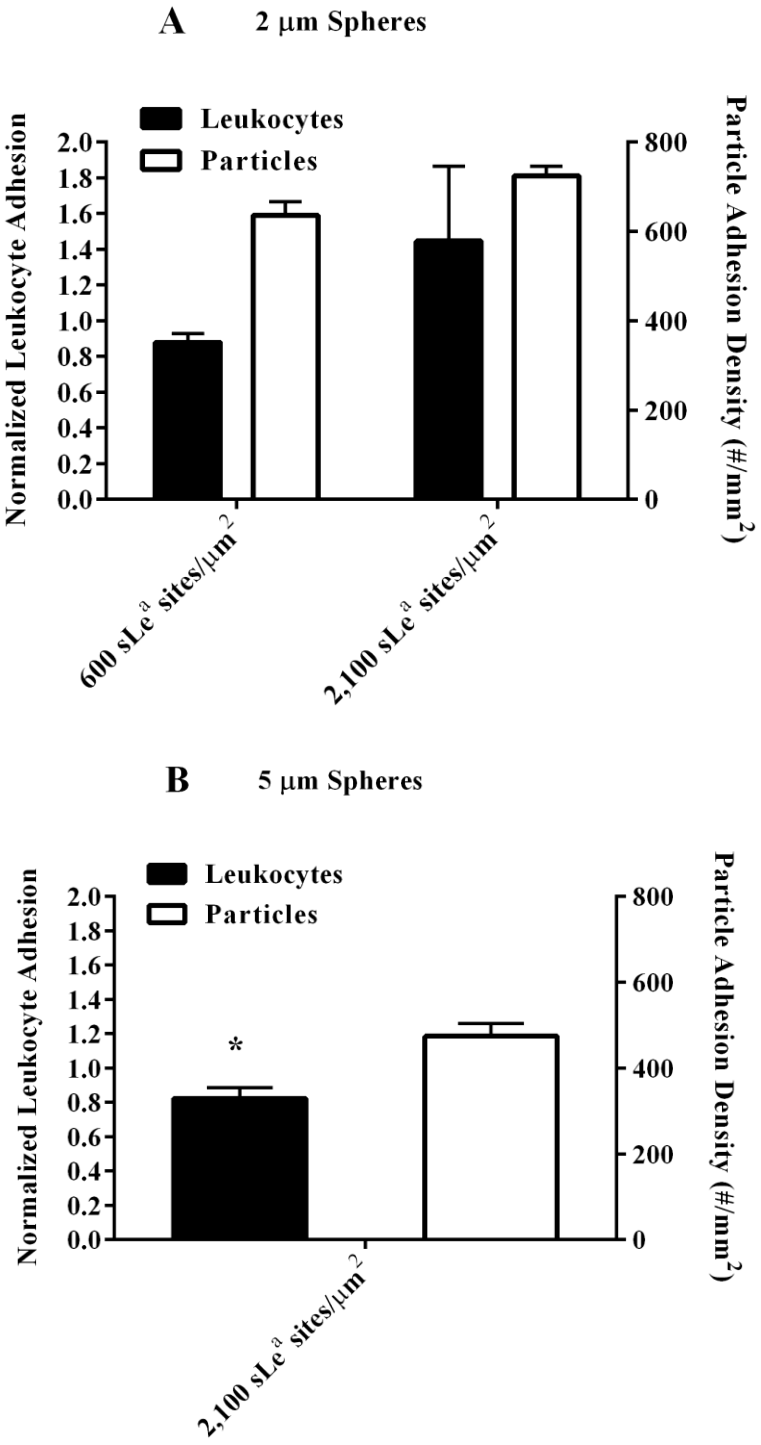

Figure 5.8. Normalized leukocyte (black bars, left axis) and particle adhesion (white bars, right axis) with (A) 2 μm and (B) 5 μm sLe^a targeted spheres with 600 or 2,100 sLe^a sites/μm^2. * indicates significant difference in leukocyte adhesion compared to particle-free blood ($p<0.01$).

5.2.4. Effect of aICAM-1 Targeted Spheres on Leukocyte Adhesion

To determine whether the observed effect of E-selectin-targeted particles on leukocyte adhesion would occur with particles targeted to other inflammatory molecules, I observed the impact of aICAM-1 targeted spheres on leukocyte adhesion for 5 μm, 2 μm and 500 nm spheres in oscillating blood flow (Fig. 5.9). 5 μm aICAM-1-targeted spheres with $5x10^5$ and $2.5x10^6$ particles/mL blood concentrations decreased leukocyte adhesion by 26% and 55%, respectfully, relative to particle-free blood. The reductions in leukocyte adhesion with 5 μm aICAM-1 targeted spheres was not significantly different than what was observed with 5 μm sLe^a-targeted spheres at the same particle concentrations (Fig. 5.1.A). The particle adhesion for 5 μm aICAM-1 targeted spheres with $5x10^5$ particles/mL in blood was 3-fold lower than the adhesion of sLe^a-targeted spheres of the same size and blood concentration (Fig. 5.2.A). There was no difference in the particle adhesion between sLe^a-targeted and aICAM-1 targeted 5 μm spheres with $2.5x10^6$ particles/mL in blood. Contrary to the 5 μm spheres, 2 μm aICAM-1 targeted spheres at $5x10^5$ and $2.5x10^6$ particles/mL did not significantly decrease leukocyte adhesion compared to particle-free blood. There was, however, a 61% reduction in leukocyte adhesion with $1x10^7$ particles/mL concentration for this particle size (Fig. 5.9.B). This percent reduction was not significantly different from that observed with 2 μm sLe^a-targeted spheres at the same particle concentration (Fig. 5.2.C). There was no significant difference in particle adhesion between aICAM-1 and sLe^a-targeted 2 μm spheres with all concentrations explored. For both 2 μm and 5 μm aICAM-1 targeted spheres the particle adhesion density significantly increased with increasing VTC concentration in blood, relative to that observed with same particle size with $5x10^5$ particles/mL. The influence of targeting ligand on leukocyte adhesion was also investigated using 500 nm aICAM-1 targeted spheres in blood with $1x10^7$ particles/mL (Fig. 5.9.C). 500 nm aICAM-1

targeted spheres significantly decreased leukocyte adhesion, relative to particle-free blood, by 37% and this reduction was not significantly different from what was observed with 500 nm sLe^a-targeted spheres at the same particle concentration (Fig. 5.1.D). Interestingly, the particle adhesion of 500 nm aICAM-1 targeted spheres was 2.5-fold greater than the adhesion of 500 nm sLe^a-targeted spheres at the same particle concentration (Fig. 5.2.D)

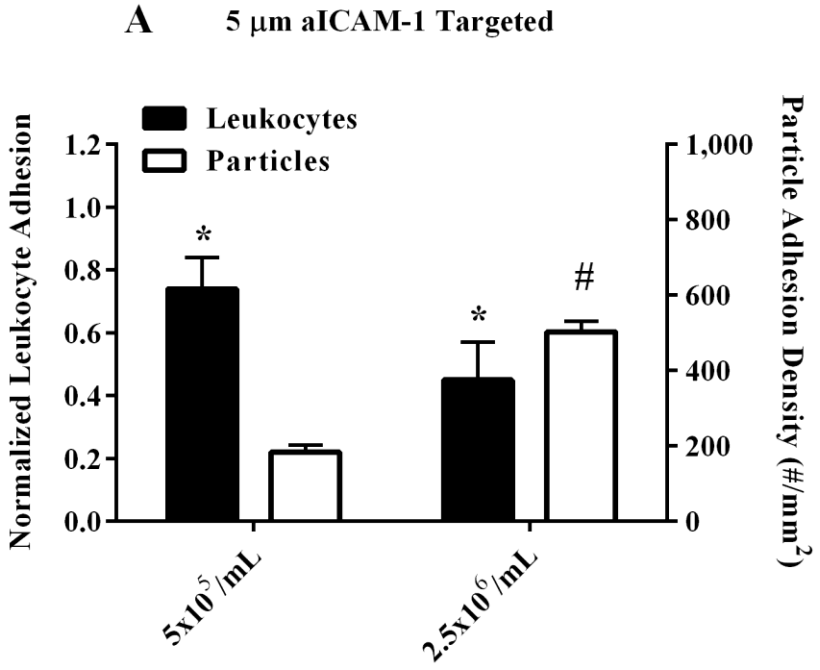

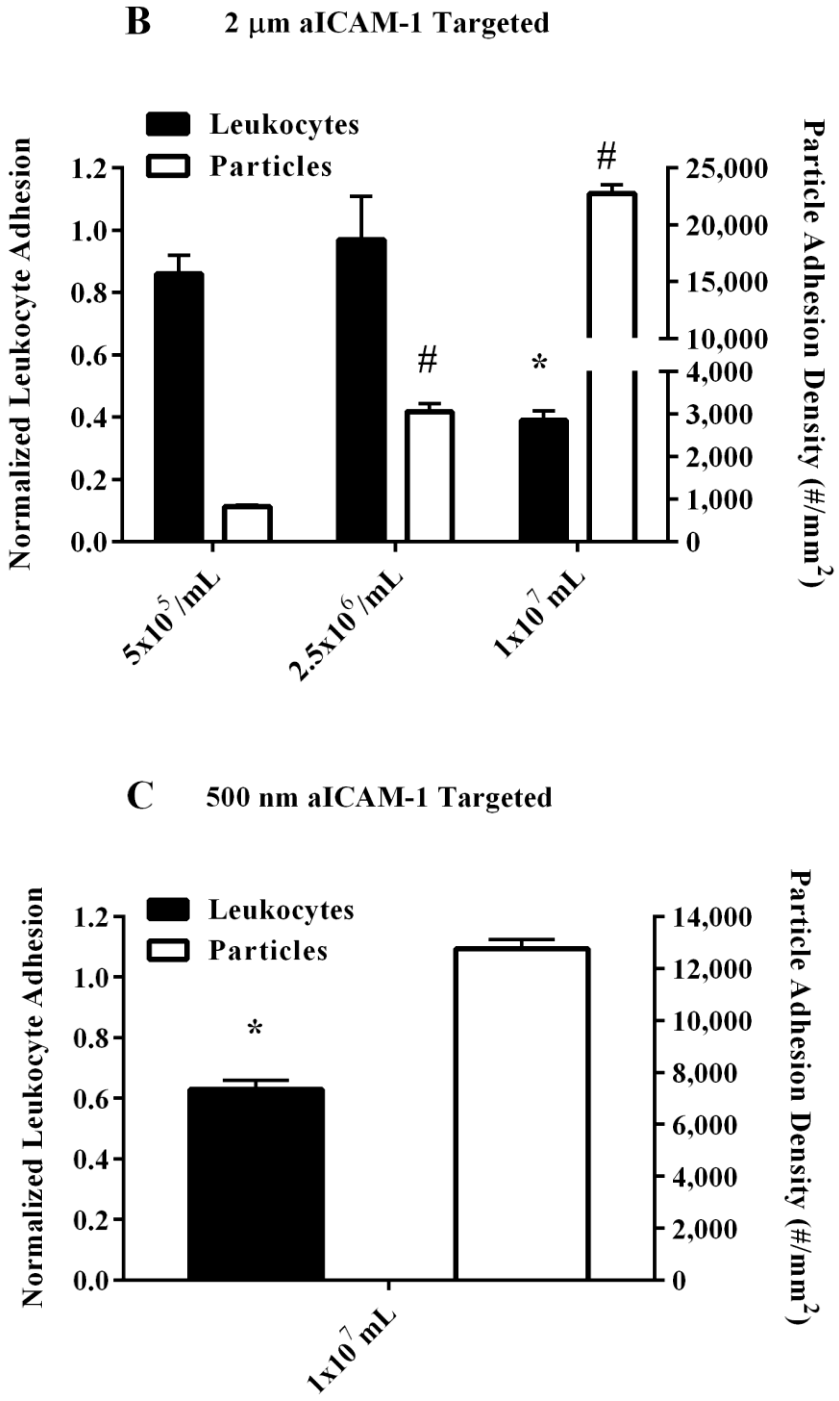

Figure 5.9. Normalized leukocyte adhesion (black bars, left axis) and particle adhesion (white bars, right axis) of (A) 5 μm, (B) 2 μm, and (C) 500 nm aICAM-1 targeted spheres (~6,000 sites/μm^2) under oscillating blood flow. * indicates significant difference in leukocyte adhesion relative to particle-free blood. # indicates significant difference in particle adhesion compared to the adhesion of the same particle size at 5x10^5 particles/mL ($p<0.01$).

5.2.5. Influence of VTCs on Leukocyte Adhesion in Laminar Flow

To investigate if the influence of VTCs on leukocyte adhesion would be limited to oscillating blood flow, the effect of 5 μm, 2 μm, and 500 nm sLe^a-targeted spheres on leukocyte adhesion was examined under laminar blood flow conditions with 200 and 1,000 s^{-1} WSR. There was no significant effect on leukocyte adhesion with 5 μm targeted spheres at 200 s^{-1} ($5x10^5$ particles/mL, Fig. 5.10.A). With 1,000 s^{-1} WSR, 5 μm targeted spheres significantly decreased leukocyte adhesion by 45% even though there was no significant difference in particle adhesion between 200 and 1,000 s^{-1} WSRs. The presence of 2 μm or 500 nm sLe^a-targeted spheres in blood with $1x10^7$ particles/mL did not significantly affect leukocyte adhesion with 200 s^{-1} WSR of laminar blood flow (Fig. 5.10.A, B). When increasing the WSR to 1,000 s^{-1}, 2 μm and 500 nm targeted spheres significantly reduced the leukocyte adhesion by 71% and 33%, respectfully. The particle adhesion for 2 μm and 500 nm targeted spheres under 1,000 s^{-1} laminar flow increased by 3-fold and 10-fold, respectfully, relative to the particle adhesion of the same spheres with 200 s^{-1} of laminar flow. There was no effect on leukocyte adhesion with 5 μm, 2 μm, or 500 nm non-targeted spheres at the WSRs explored for laminar blood flow (Fig. 5.11)

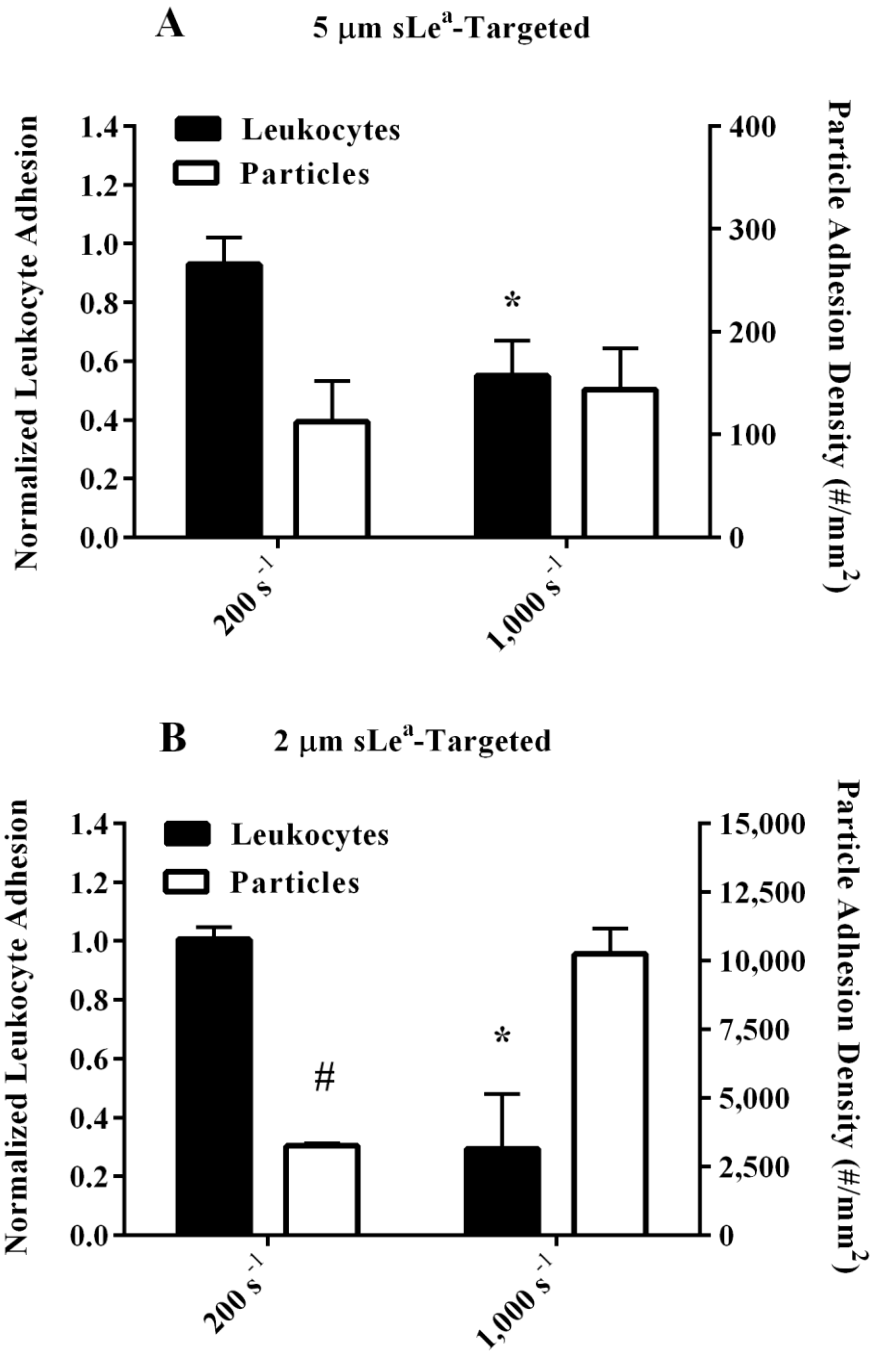
A
5 μm sLe^a-Targeted
Leukocytes
Particles
Normalized Leukocyte Adhesion
Particle Adhesion Density (#/mm^2)
1.4
1.2
1.0
0.8
0.6
0.4
0.2
0.0
400
300
200
100
0
*
200 s^-1
1,000 s^-1
B
2 μm sLe^a-Targeted
Leukocytes
Particles
Normalized Leukocyte Adhesion
Particle Adhesion Density (#/mm^2)
1.4
1.2
1.0
0.8
0.6
0.4
0.2
0.0
15,000
12,500
10,000
7,500
5,000
2,500
0
#
*
200 s^-1
1,000 s^-1

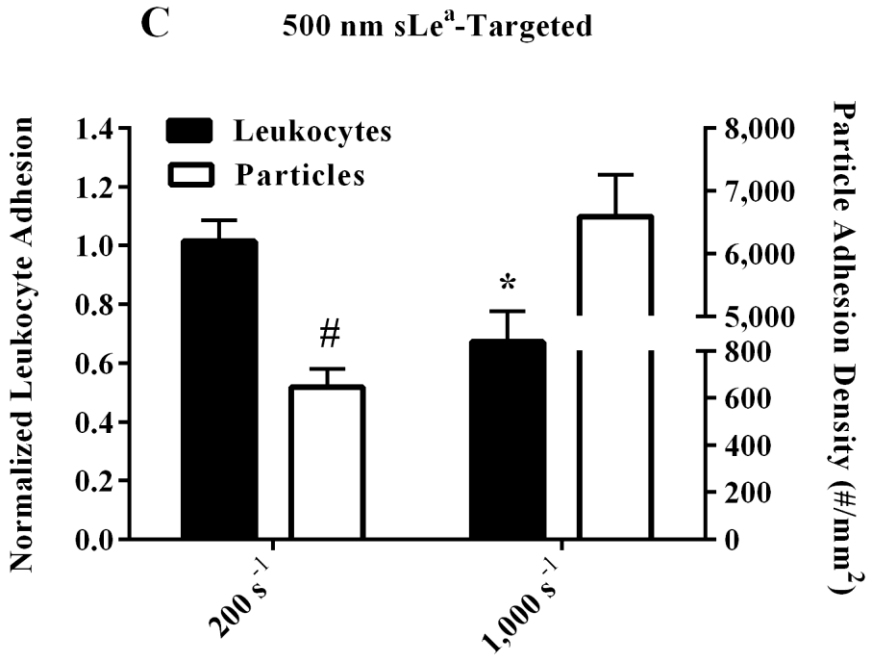

Figure 5.10. Normalized leukocyte adhesion in laminar blood flow with (A) 5 μm, (B) 2 μm, and (C) 500 nm sLe^a-targeted spheres with blood concentrations of $5x10^5$, $1x10^7$, and $1x10^7$ particles/mL, respectfully, as a function of WSR. * indicates significant difference in adhesion relative to particle-free blood at the same wall shear rate. # indicates significant difference compared to the particle adhesion of the same spheres at 1,000 s^{-1} WSR ($p<0.01$).

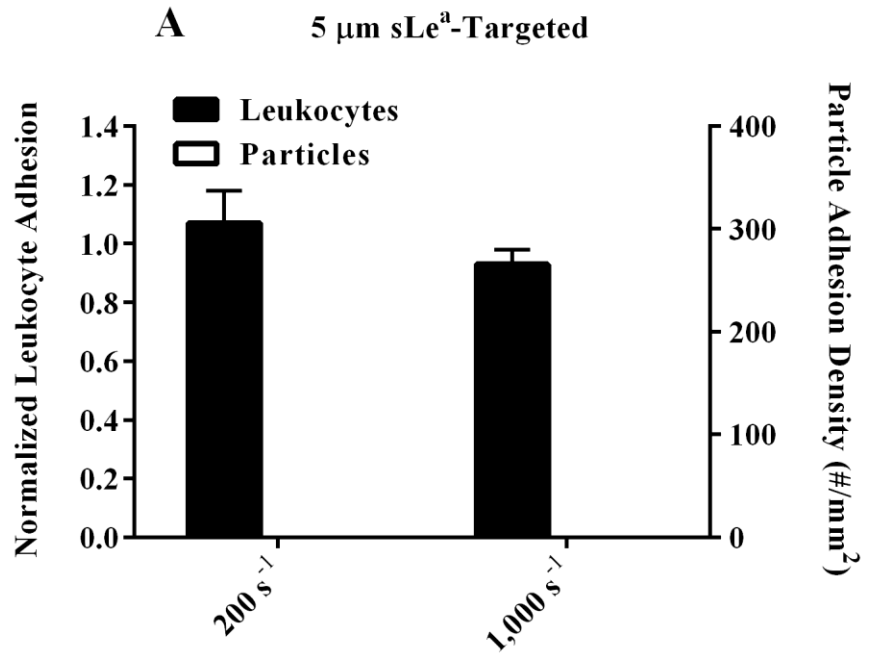
A
5 μm sLe^a-Targeted
Leukocytes
Particles
Normalized Leukocyte Adhesion
Particle Adhesion Density (#/mm^2)
1.4
1.2
1.0
0.8
0.6
0.4
0.2
0.0
400
300
200
100
0
200 s^-1
1,000 s^-1

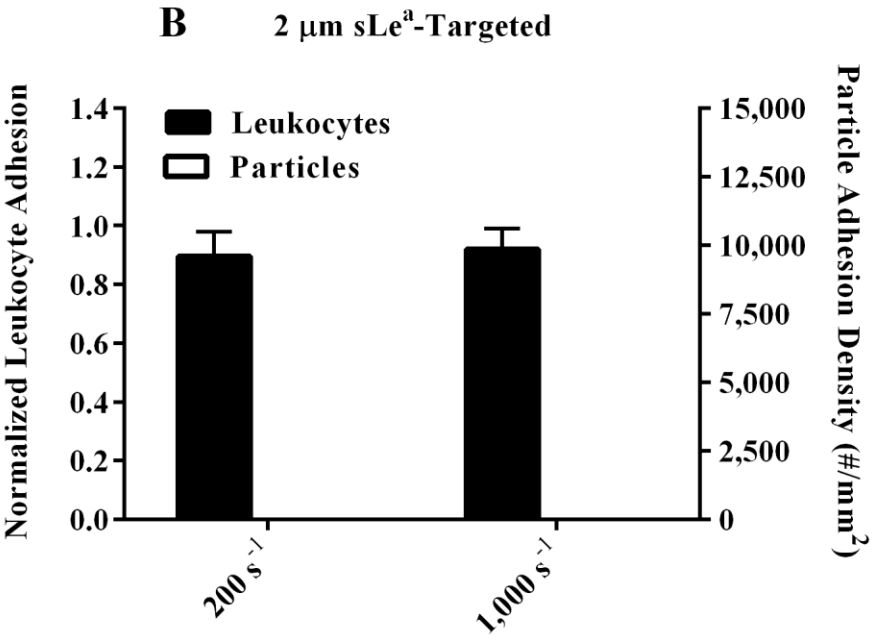
B
2 μm sLe^a-Targeted
Leukocytes
Particles
Normalized Leukocyte Adhesion
Particle Adhesion Density (#/mm^2)
1.4
1.2
1.0
0.8
0.6
0.4
0.2
0.0
15,000
12,500
10,000
7,500
5,000
2,500
0
200 s^-1
1,000 s^-1

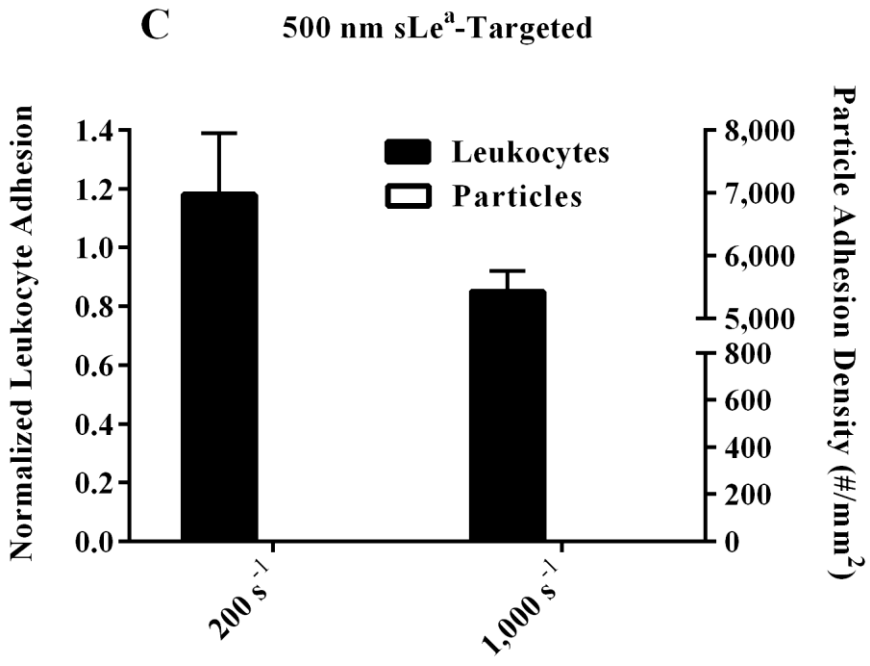

Figure 5.11. Normalized leukocyte in laminar blood flow adhesion with non-targeted (A) 5 µm, (B) 2 µm, and (C) 500 nm spheres at blood concentrations of $5x10^5$, $1x10^7$, and $1x10^7$ particles/mL, respectfully, as a function of WSR.

5.3. Discussion

Vascular targeting is a viable strategy for the therapeutic intervention of many inflammatory diseases, including atherosclerosis and other cardiovascular diseases, aimed towards tissue specific drug delivery that results in enhanced drug efficacy and minimized systemic side effects. The redistribution of leukocytes, platelets, and inflammation targeting drug carriers to the cell-free layer during blood flow may generate competition for the targeted receptors such as E-selectin and ICAM-1, which play pivotal roles in the LAC. While leukocytes were previously shown to decrease levels of particle adhesion, to date, little is known as to whether VTCs enhance, diminish, or have no effect on the inflammatory recruitment of leukocytes in blood flow to the same targeted tissue.[22] Understanding the capacity of VTCs to positively or negatively impact leukocyte adhesion to the vascular wall would be critical to their eventual clinical use for drug delivery in inflammation-associated diseases. For example in atherosclerosis and sepsis, where excessive leukocyte recruit is known to negatively impact pathology, a positive impact of VTCs on leukocyte recruitment would likely counteract the effect of the delivered therapy.[3, 4] Conversely, a negative VTC impact on leukocyte recruitment (separate from drug action) would likely enhance treatment. In the case of the latter, the VTCs themselves may then be developed as an anti-inflammatory therapy, separate from targeted delivery, for effective local treatment of inflammatory diseases.

Overall, the results of this work show that spherical VTCs targeted towards inflammatory molecules either have no impact or significantly reduce the recruitment and adhesion of leukocytes to an inflamed endothelium in human blood flow, depending on the particle size and concentration in blood. For most particle sizes explored, the impact of the VTCs on leukocyte recruitment requires the molecular targeting of specific EC-expressed inflammatory molecules.

No significant reductions in leukocyte adhesion were observed with 5 μm spheres at $5x10^5$ particles/mL or with smaller non-targeted particles at all the blood concentrations explored. Exceptions were found with non-targeted 5 μm spheres at higher blood concentrations of $1x10^6$, $2.5x10^6$, and $1x10^7$ particles/mL, where significant decreases in leukocyte adhesion occurred regardless of targeting (Fig. 5.3A). However, the addition of targeting ligand (sLe^a) provided up to a 2-fold increase in percent leukocyte reduction, relative to non-targeted 5 μm spheres at the same blood concentrations (Figs. 5.1.A, 5.3.A). The increase in percent leukocyte reduction with the addition of targeting ligand (sLe^a) was dependent on particle concentration in blood, as there was nearly a 2-fold increase in percent leukocyte reduction with $1x10^6$ particles/mL for 5 μm targeted spheres, relative to non-targeted spheres, but only a 1.1-fold increase with $1x10^7$ particles/mL. Particle-leukocyte collisions were previously shown to remove adherent 5 μm sLe^a-targeted spheres from an activated EC monolayer in blood flow under the same oscillating flow conditions explored in this work.[22] I anticipate similar dynamics between leukocytes present on the endothelium and 5 μm spheres such that the collision impact from these large microspheres weakens the interaction between leukocytes and the endothelium, which under high shear conditions, would result in leukocyte detachment from the endothelium. The observed impact with non-targeted 5 μm sphere, but not smaller spheres, suggests that there is a minimum impact force and collision frequency required to observe reductions in leukocyte adhesion with non-targeted spheres, which is linked to particle size and concentration in blood.

The maximum reduction in leukocyte adhesion with targeted spheres was observed when either 5 μm or 3 μm sLe^a-targeted spheres were present at the highest blood concentration ($1x10^7$ particles/mL), resulting in nearly 100% prevention of leukocyte binding to the EC monolayer (Fig. 5.4.B). Both particles sizes similarly impacted leukocyte adhesion despite significant

differences in their particle adhesion density. This is likely a result of 5 μm spheres impacting leukocyte adhesion through collisions, which was minimal for 3 μm spheres. As a result, VTCs < 5 μm require high particle adhesion densities (i.e. endothelial surface coverage) to achieve similar levels of leukocyte reduction relative to 5 μm spheres. Interestingly, the adhesion of 2 μm spheres at this same blood concentration ($1x10^7$ particles/mL) was not significantly different than 3 μm spheres; however, the presence of 2 μm targeted spheres resulted in only a 69% reduction in leukocyte adhesion (Fig. 5.4.B). Here, the fact that smaller 2 μm spheres occupy less endothelial surface area, relative to 3 μm spheres, and the absence of physical collisions having an impact, likely allows for more endothelial area and receptors available for leukocyte adhesion (given similar levels of particle adhesion, Fig. 5.4.B). Overall, I suspect that for smaller micron-sized spheres (2 μm and 3 μm), the endothelial surface coverage, which is dependent on the particle size and adhesion density, is the primary factor in reducing leukocyte adhesion. For spheres 5 μm or larger, physical collisions with leukocytes at wall are the leading factor in decreasing leukocyte adhesion in blood flow. [22]

Submicron, 500 nm and 200 nm, sLe^a-targeted spheres were also shown to significantly reduce leukocyte adhesion at high blood concentrations, even though the particle adhesion densities for nanospheres were significantly lower than that of microspheres at a fixed blood concentration (Fig. 5.4). For example at $2.5x10^6$ particles/mL blood concentration, the reduction in leukocyte adhesion with 500 nm was similar to that observed with 3 μm spheres at the same blood concentration, despite a 4-fold greater particle adhesion for the 3 μm spheres relative to the 500 nm spheres (Fig. 5.4.A). In fact, the maximum leukocyte reduction with 2 μm targeted spheres at the $1x10^7$ particles/mL blood concentration was also only 1.5-fold greater than the maximum reduction observed with nanospheres, compared to a 4- and 6-fold higher adhesion for

the 2 μm sLe^a-targeted spheres relative to the adhesion of 500 nm and 200 nm targeted spheres at $1x10^7$ and $1.8x10^8$ particles/mL, respectfully (Fig. 5.4.B). The results suggest that the mechanism behind nanospheres reducing leukocyte adhesion may be a result of a combined effect of particle adhesion at the vessel wall and nanospheres interacting with leukocytes away from the endothelium in blood flow. Recent literature supports this notion that nanoparticle interaction with leukocytes can occur in free stream. In one work, E-selectin-coated nano-sized liposomes (~118 nm) were shown to effectively target and adhere to neutrophils in low shear blood flow (188 s^{-1}).[24] I suspect that sLe^a-targeted nanospheres may interact with L-selectin expressed on leukocytes possibly through coating the leukocyte or aiding in the formation of leukocyte aggregates which would experience increased drag forces, relative to a single leukocyte, and reduce the adhesive ability of leukocytes under high shear. However, it is unclear if particle-leukocyte aggregates are stable under high shear conditions due to the fast on-/off-rates of L-selectin and sLe^a used in this work.[25, 26] Interestingly, increasing the sLe^a-density on 2 μm and 5 μm spheres (to improve the likelihood of VTC-leukocyte interactions in flow) had no significant effect on leukocyte adhesion (Fig. 5.8). This suggests that the potential for particle-leukocyte aggregates through sLe^a-L-selectin may be limited to nanospheres. Leukocyte aggregates with microspheres in blood flow may require a sLe^a density >2,000 sites/μm^2 or implementing leukocyte specific ligands with more favorable adhesive dynamics than that of sLe^a with L-selectin.

Ellipsoidal particles (rods) have been proposed for improving VTC adhesion in blood due to their enhanced adhesive dynamics in flow.[19, 27] The influence of AR4 and AR9 rods on leukocyte adhesion was examined and shown to have no significant impact on leukocyte adhesion, despite the fact that that the area of the endothelium occupied by AR4 rods was

approximately 1.8-fold greater than 2 μm spheres with an equivalent volume (due to AR4 rods having a greater surface area than equivalent volume spheres) given similar particle adhesion densities (Fig. 5.6.A). This may be a result of a minimum VTC endothelial surface coverage, which is dependent on VTC shape and adhesion density, required for influencing leukocyte adhesion. Previous work with AR9 rods in RBCs+Buffer systems under the similar oscillating flow conditions showed improve adhesion relative to equivalent volume spheres; however, hear I report that the adhesion of AR9 rods in whole blood was significantly lower than 2 μm equivalent volume spheres and AR4 rods.[19] The adhesion vs. time curve shows that the adhesion of AR9 ellipsoids plateaued after 5 minutes of oscillating blood flow (Fig. 5.7.B), a trend that was similar to that observed with 5 μm spheres (Fig. 5.5.C) where collision with leukocytes resulted in decreased particle and leukocyte adhesion with time. Unlike 5 μm spheres, AR9 rods did not significantly influence leukocyte adhesion relative to particle-free blood, indicating that a leukocyte collision effect similar to that observed with 5 μm targeted spheres at the same blood concentration ($5x10^5$ particles/mL) does not occur with AR9 rods in blood.

I also demonstrate that both E-selectin and ICAM-1 targeted particles affect leukocyte adhesion in blood flow. However, there appears to be a difference in the sensitivity of leukocyte adhesion to two the different VTC targeting systems, which is also dependent on the particle size and adhesion density (Fig. 5.9). For instance, similar levels of leukocyte reduction were observed with both sLe^a and aICAM-1 targeted 5 μm spheres, further highlighting physical collisions between these large microspheres and leukocytes as the dominant factor in reducing leukocyte adhesion. In contrast, the reduction in leukocyte adhesion induced by 2 μm targeted spheres showed sensitivity towards targeting ligand type in that at $2.5x10^6$ particles/mL, sLe^a-

targeted spheres resulted in a 27% decrease in leukocyte adhesion whereas no effect on leukocyte adhesion was observed with aICAM-1 targeted spheres at the same blood concentration. This may be due to sLe^a-targeted spheres reducing the amount of E-selectin available for initial leukocyte capture from blood flow, which is critical for leukocyte recruitment and subsequent adhesion under high shear conditions.[26] Even though 2 μm aICAM-1 targeted spheres would reduce the number of ICAM-1 sites available for leukocyte firm adhesion, the smaller particle size (relative to leukocytes which are ~7-12 μm in diameter) may allow leukocytes to navigate the endothelial surface through available E-selectin until firm adhesion can be established. However, above a critical particle adhesion density for this VTC size, sensitivity towards targeting ligand is lost due to targeted microspheres occupying a critical endothelial surface area which minimizes the potential for endothelial-leukocyte interactions through either inflammatory receptor (E-selectin or ICAM-1). The 500 nm aICAM-1 targeted spheres with blood concentration of $1x10^7$ particles/mL also significantly reduced leukocyte adhesion. Interestingly, both aICAM-1 and sLe^a-targeted spheres reduced leukocyte adhesion by approximately 40%, despite the adhesion density for aICAM-1 nanospheres being 2.5-fold higher than sLe^a-targeted spheres at the same blood concentration. To my knowledge, no leukocyte receptors exist for the aICAM-1 targeting ligand used in this work, suggesting that molecular interactions between aICAM-1 targeted nanospheres and leukocytes are minimal or non-existent. Thus, it is evident that the influence on leukocyte adhesion from the presence of nanospheres in blood is not solely dependent on molecular interactions with leukocytes, but a component exists in which nanospheres occupying CAMs on the endothelium contributes to reducing leukocyte adhesion. The results also suggest that targeted nanospheres with the potential to interact with leukocytes in flow are more effective in reducing leukocyte adhesion,

as sLe^a-targeted nanospheres achieved a similar level of leukocyte reduction as aICAM-1 targeted nanospheres with lower particle adhesion density at the same particle concentration in blood (Fig. 5.9.C, 5.4.B).

The results also indicate that a hemodynamic component exists with VTCs influencing leukocyte adhesion in blood flow. Significant reductions in leukocyte adhesion were observed for 5 μm, 2 μm, and 500 nm sLe^a-targeted spheres under laminar blood flow at WSR of 1,000 s^{-1}, but not at 200 s^{-1}. The adhesion of 2 μm spheres under 200 s^{-1} of laminar blood flow ($1x10^7$ particles/mL, Fig. 5.10.B) was also similar to that observed with 2 μm spheres under oscillating flow with $2.5x10^6$ particles/mL (~3,400 particles/mm^2, Fig. 5.4.A), which decreased leukocyte adhesion by ~ 20%. Under high shear conditions (i.e. 1,000 s^{-1} WSR), leukocytes must interact with a greater number of CAMs to combat higher drag forces and maintain adhesion with the endothelium. This is of particular importance for initial capture and rolling adhesion during the leukocyte recruitment process. VTCs are more effective in reducing leukocyte adhesion under high shear conditions due to adherent particles reducing the number of CAMs available for leukocyte capture and adhesion. Leukocytes also experience slower rolling velocities under low shear conditions, which allows them to maintain sufficient contact with the endothelium when navigating endothelial-bound VTCs.[28] Interestingly, 2 μm spheres were more effective in influencing leukocyte adhesion under high shear laminar flow compared to oscillating flow, as both flow profiles decreased leukocyte adhesion by ~70%. However, the particle adhesion under laminar flow was 2-fold lower than that observed under oscillating blood flow with the same blood concentration ($1x10^7$ particles/mL, Figs. 5.10.B, 5.4.B). This may be a function of the oscillating flow profile allowing greater contact time between leukocytes and the endothelium, due to a zero shear point occurring in the oscillating profile during flow reversal. As a result, a

higher particle adhesion density is required to combat the enhanced contact between leukocytes and the endothelium and achieve similar levels of leukocyte reduction relative to high shear laminar flow. The hemodynamic component to VTCs influencing leukocyte adhesion is of particular interest for optimizing VTCs as anti-adhesion therapy. The result suggests that VTCs would be effective at reducing leukocyte adhesion under high shear conditions, as is this case in medium to large arteries susceptible to cardiovascular disease, while maintaining homeostatic leukocyte recruitment in low shear vessels, such as post-capillary venules, where leukocyte recruitment and tissue extravasation occurs to combat local infections

Overall, leukocyte adhesion was shown to be affected by the presence of VTCs in blood. The mechanism of reduced leukocyte adhesion with VTCs appears to be dependent on VTC size and adhesion density. The effect on leukocyte adhesion with 5 μm spheres is dependent on particle adhesion density and collisions with endothelial-interacting leukocytes. For microspheres 2 -3 μm in diameter, leukocyte adhesion is sensitive to particle adhesion density, endothelial surface coverage, and targeting system. The impact on leukocyte adhesion from targeted nanospheres in blood may be due to a combined effect of occupying CAMs on the endothelium and interacting with leukocytes away from the vessel wall. The influence of VTCs on leukocyte adhesion is also sensitive to hemodynamics, such that reduced leukocyte adhesion levels were observed under high shear conditions and with oscillating flow. The results show that the presence of VTCs can influence blood cell response to an inflamed endothelium in blood flow, which may potentially provide therapeutic benefits for inflammatory diseases whose pathogenesis is enhanced by leukocyte recruitment.

References

[1] Schmidt, S., Moser, M., and Sperandio, M., *The Molecular Basis of Leukocyte Recruitment and its Deficiencies.* Molecular Immunology, 2013. **55**: p. 49-58.

[2] Ley, K., *Molecular Mechanisms of Leukocyte Recruitment in the Inflammatory Process.* Cardiovascular Research, 1996. **32**: p. 733-752.

[3] Woollard, K.J. and Geissmann, F., *Monocytes in Atherosclerosis: Subsets and Functions.* Nature Reviews Cardiology, 2010. **7.2**: p. 77.

[4] Weber, C. and Noels, H., *Atherosclerosis: Current Pathogenesis and Therapeutic Options.* Nature Medicine, 2011. **17**(11): p. 1410-1422.

[5] Damas, P., Canivet, J.-L., De Groote, D., et al., *Sepsis and Serum Cytokine Concentrations.* Critical Care Medicine, 1997. **25**(3): p. 405-412.

[6] Brown, K.A., Brain, S.D., Pearson, J.D., et al., *Neutrophils in the Development of Multiple Organ Failure in Sepsis.* The Lancet, 2006. **368**: p. 157-169.

[7] Tavares-Muarta, B.M., Machado, J.S., Ferreira, S.H., et al., *Nitric Oxide Mediated the Inhibition of Neutrophils Migration Induced by Systemic Administration of LPS.* Inflammation, 2001. **25**(4): p. 247-253.

[8] Russwurm, S., Vickers, J., Meier-Hellmann, A., et al., *Platelet and Leukocyte Activation Correlation with the Severity of Septic Organ Dysfunction.* Shock, 2002. **17**(4): p. 263-268.

[9] Jordan, J.E., Zhao, Z.-Q., and Vinten-Johansen, J., *The Role of Neutrophils in Myocardial Ischemia-Reperfusion Injury.* Cardiovascular Research, 1999. **43**: p. 860-878.

[10] Alves-Filho, J.C., Freitas, A.d., Spiller, F., et al., *The Role of Neutrophils in Severe Sepsis.* Shock, 2008. **30**(7): p. 1-7.

[11] Alves-Filho, J.C., Freitas, A., Russo, M., et al., *Toll-like Receptor 4 Signaling Leads to Neutrophil Migration Impairment in Polymicrobial Sepsis.* Critical Care Medicine, 2006. **34**(2): p. 461-470.

[12] Singbartl, K. and Ley, K., *Protection from Ischemia-Reperfusion Induced Severe Acute Renal Failure by Blocking E-Selectin.* Critical Care Medicine, 2000. **28**(7): p. 2507-2514.

[13] Ma, X.L., Lefer, D.J., Lefer, A.M., et al., *Coronary Endothelial and Cardiac Protective Effects of a Monoclonal Antibody to Intercellular Adhesion Molecule-1 in Myocardial Ischemia and Reperfusion.* Circulation, 1992. **86**: p. 937-946.

[14] Harlan, J. and Winn, R.K., *Leukocyte-Endothelial Interactions: Clinical Trials of Anti-Adhesion Therapy.* Critical Care Medicine, 2002. **30**(5): p. S214-S219.

[15] Yu, B., Tai, H.C., Xue, W., et al., *Receptor-Targeted Nanocarriers or Therapeutic Delivery to Cancer.* Molecular Membrane Biology, 2010. **27**(7): p. 286-298.

[16] Hajitou, A., Pasqualini, R., and Arap, W., *Vascular Targeting: Recent Advances and Therapeutic Perspectives.* Trends in Cardiovascular Medicine, 2006. **16**(3): p. 80-88.

[17] Melder, R.J., Yuan, J., Munn, L.L., et al., *Erythrocytes Enhance Lymphocyte Rolling and Arrest In Vivo.* Microvascular Research, 2000. **59**(316-322).

[18] Kumar, A. and Graham, M.D., *Margination and Segregation in Confined Flows of Blood and other Multicomponent Suspensions.* Soft Matter, 2012. **8**: p. 10536-10548.

[19] Thompson, A.J., Mastria, E.M., and Eniola-Adefeso, O., *The Margination Propensity of Ellipsoidal Micro/Nanoparticles to the Endothelium in Human Blood Flow.* Biomaterials, 2013. **34**(23): p. 5863-5871.

[20] Charoenphol, P., Huang, R.B., and Eniola-Adefeso, O., *Potential Role of Size and Hemodynamics in the Efficacy of Vascular-Targeted Spherical Drug Carriers.* Biomaterials, 2010. **31**: p. 1392-1402.

[21] Muro, S., Garnacho, C., Champion, J.A., et al., *Control of Endothelial Targeting and Intracellular Delivery of Therapeitic Enzymes by Modulating the Size and Shape of ICAM-1-Targeted Carriers.* Molecular Therapy, 2008. **16**(8): p. 1450-1458.

[22] Charoenphol, P., Onyskiw, P.J., Carrasco-Teja, M., et al., *Particle-Cell Dynamics in Human Blood Flow: Implications for Vascular-Targeted Drug Delivery.* Journal of Biomechanics, 2012. **45**(16): p. 2822-2828

[23] Charoenphol, P., Mocherla, S., Bouis, D., et al., *Targeting Therapeutics to the Vascular Wall in Atherosclerosis - Carrier Size Matters.* Atherosclerosis, 2011. **217**(2): p. 364-370.

[24] Mitchell, M.J., Wayne, E., Rana, K., et al., *TRAIL-Coated Leukocytes that Kill Cancer Cells in the Circulation.* PNAS, 2014. **111**(3): p. 930-935.

[25] Berg, E.L., Magnani, J., Warnock, R.A., et al., *Comparison of L-selectin and E-selectin Ligand Specificities: the L-selectin can bind the E-selectin Ligands Sialyl le^x and Sialyl le^a*. Biochemical and Biophysical Research Communications, 1992. **184**(2): p. 1048-1055.

[26] Lawrence, M.B. and Springer, T.A., *Leukocytes Roll on a Selectin at Physiological Flow Rates: Distinction from and Prerequisite for Adhesion through Integrins.* Cell, 1991. **65**: p. 859-873.

[27] Namdee, K., Thompson, A.J., Phapanin, C., et al., *Margination Propensity of Vascular-Targeted Spheres from Blood Flow in a Microfluidic Model of Human Microvessels.* Langmuir, 2013. **29**(8): p. 2530-2535.

[28] Lie, X., Lawrence, M.B., and Dong, D., *Influence of Cell Deformation on Leukocyte Rolling Adhesion in Shear Flow*. Journal of Biomedical Engineering, 1999. **121**: p. 636-643.

CHAPTER 6

INFLUENCE OF VTCs ON PLATELET ADHESION IN BLOOD FLOW

6.1. Introduction

Platelets in flow play a critical role in limiting blood loss after vascular injury through the adhesion and formation of a platelet plug at the injury site.[1-3] In healthy tissue, the blood vessel endothelium limits platelet interactions by releasing soluble factors, such as nitric oxide and prostacyclin, which keep circulating platelets in a quiescent state.[4] However, there are cases related to vessel inflammation in which the adhesion of activated platelets to the endothelium enhances or initiates disease pathogenesis. For example, in arterial and venous thrombosis, activated platelets initiate blood coagulation onto the vessel wall after which the thrombus (aggregated platelets cross-linked with a fibrin network) may rupture due to shear stress and initiate a cardiac event such as a stroke or myocardial infarction (heart attack). Thus, in order for VTCs to be biocompatible with blood and implemented for treating diseases such as venous thrombosis, they must not alter platelet function where necessary (i.e. vascular injury) or induce platelet activation and aggregation at inflammatory sites.

One factor in determining platelet compatibility is investigating the upregulation of P-selectin.[5, 6] P-selectin expressed on activated platelets, or released on platelet microparticles (PMPs), plays a significant role in forming platelet-platelet and platelet-leukocyte aggregates.[7] Dynamics with activated platelets are of particular interest regarding sLe^a-targeted VTCs due to

sLe^a also being a ligand for P-selectin.[8, 9] It is unclear if locally activated platelets interact with sLe^a-targeted spheres in circulation and what effect targeted spheres have on platelet adhesion to an inflamed endothelium, i.e. does the presence of sLe^a-targeted spheres induce and enhance platelet adhesion to the endothelium through P-selectin-sLe^a bridging.

Utilizing particle-platelet dynamics in flow has also been proposed as viable strategy for enhancing platelet adhesion and aggregation in traumatic injuries with rapid blood loss, specifically for patients with thrombocytopenia (< $1x10^8$ platelets/mL blood).[10] Synthetic platelets are VTCs designed to mimic platelet function; that is, (1) synthetic platelets target and adhere to exposed collagen and vWF during vessel injury under a range of shear stresses, and (2) co-localized with platelets and aide in forming a stable platelet plug.[11-13] Nano-liposomes have commonly been explored as synthetic platelet options due to their low toxicity in blood and ability to mimic platelet function when decorated with peptides which interact with platelet receptors such as collagen, vWF, and fibrinogen. However, previous work has demonstrated that nanospheres (200 nm – 500 nm) do not effectively marginate in human blood flow.[14, 15] Despite the fact that 2 – 3 μm spheres are approximately the same size of human platelets and efficiently marginate and adhere to the vessel wall in blood flow, this size range has not been extensively explored for mimicking and enhancing platelet function.

In this study I examine the effect of particle-platelet dynamics on platelet adhesion in blood containing physiological and low platelet concentrations ($1x10^8$ platelets/mL or $5x10^7$ platelets/mL, respectfully). First, the influence of 2 μm sLe^a-targeted spheres on platelet adhesion to an inflamed endothelium is assessed to determine if the presence of targeted microspheres activate platelets in reconstituted blood flow. Second, the adhesion of activated platelets was examined to determine if targeted spheres present in flow enhances the adhesion of

activated platelets to an inflamed endothelium. Finally, 2 μm spheres targeted with two dual-peptide systems, (1) collagen binding peptide (PEG-CBP)/PEG-cRGD or (2) and vWF binding peptide (PEG-VBP)/PEG-cRGD, were explored as possible platelet mimicking VTCs to enhance platelet adhesion to collagen or vWF under laminar blood flow.

6.2 Results

The experimental set up used in this chapter is described in detail in Chapter 2.

6.2.1. Unactivated Platelet Adhesion to an Activated Endothelial Monolayer in the Presence of sLe^a-Targeted Microspheres.

In order to investigate if inflammation targeting VTCs influence platelet adhesion in blood flow, reconstituted blood (plasma, RBCs, leukocytes) containing unactivated platelets ($1x10^8$ platelets/mL) and 2 μm sLe^a-targeted spheres ($5x10^5$ particles/mL) was perfused over an activated endothelium and the adhesion of platelets and targeted spheres was examined at 200 s^{-1}, 500 s^{-1}, and 1,000 s^{-1} WSR (Fig. 6.1). There was no significant effect on platelet adhesion between particle-free blood and blood containing targeted spheres at all WSRs examined. The particle adhesion density significantly increased with increasing WSR. Platelets adhesion, however, decreased by 2-fold and 4-fold, relative to the platelet adhesion with 200 s^{-1} WSR, when increasing the WSR from 500 s^{-1} to 1,000 s^{-1}, respectfully. PEGylated 2 μm spheres (2.3 kDa PEG, 32,270 PEG chains/μm^2, intermediate-brush conformation) were also examined to determine if the addition of a PEG corona would induce platelet adhesion through activation. PEGylated spheres were shown to have no significant effect on platelet adhesion at 500 s^{-1} WSR, and the platelet and particle adhesion levels were similar to that observed with non-PEGylated

spheres at the same WSR (Fig. 6.1, 6.2).

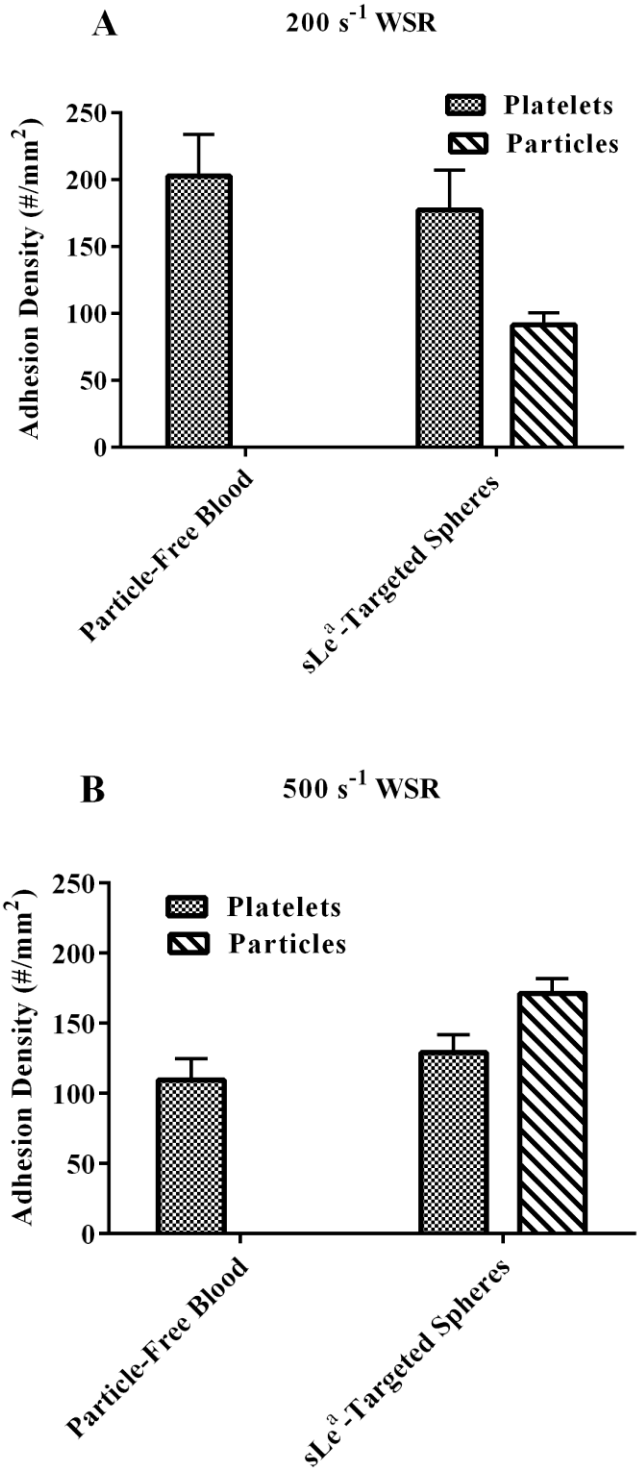

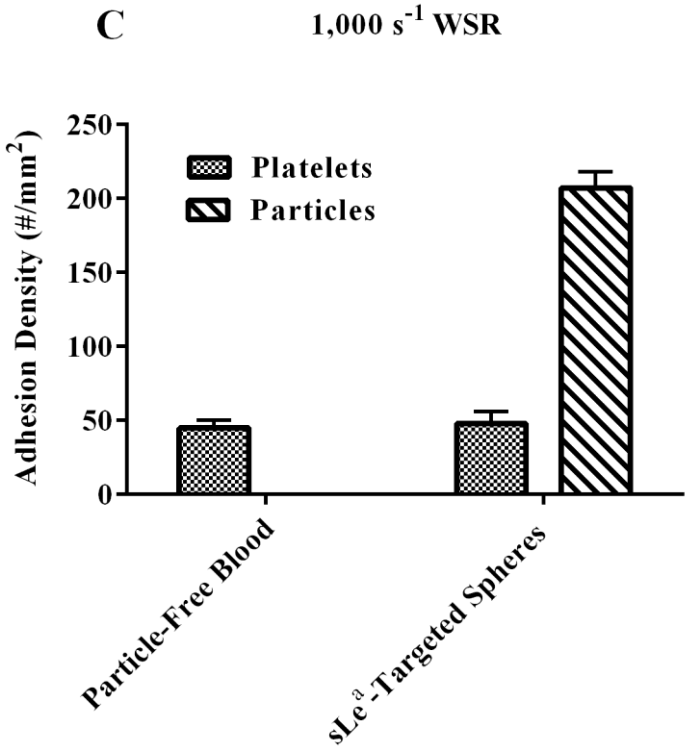

Figure 6.1. Adhesion of unactivated platelets ($1x10^8$/mL) and 2 µm sLe^a-targeted spheres (1,000 sLe^a sites/μm^2, $5x10^5$/mL) to an activated endothelium in reconstituted blood flow at (A) 200 s^{-1} WSR for 5 minutes, (B) 500 s^{-1} WSR for 3 minutes, and (C) 1,000 s^{-1} WSR for 3 minutes.

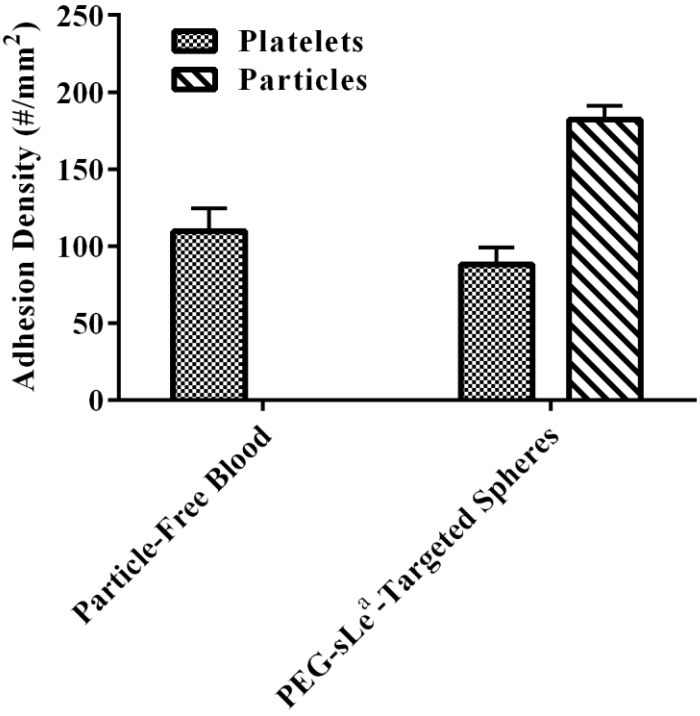

Figure 6.2. Adhesion of unactivated platelets ($1x10^8$ platelets/mL) and 2 μm PEGylated (2.3 kDa PEG, 32,270 PEG chains/μm^2) sLe^a-targeted spheres (1,000 sLe^a sites/μm^2) to an activated endothelium in reconstituted blood flow at 500 s^{-1} WSR for 3 minutes.

6.2.2. Activated Platelet Adhesion to an Activated Endothelial Monolayer in the Presence of sLe^a-Targeted Microspheres.

The adhesion of activated platelets to an activated endothelium in blood flow was examined with the presence of non-targeted and sLe^a-targeted 2 μm spheres in blood at a concentration of $5x10^5$ particles/mL. Similar to what was observed with non-activated platelets, 2 μm spheres did not significantly affect platelet adhesion to an activated endothelium (Fig. 6.3). The presence of targeted spheres on activated platelet adhesion in blood with a thrombocytopenic platelet concentration ($5x10^7$ platelets/mL) was also examined to determine if the lack of a significant effect on activated platelet adhesion was a result of the ~3-orders of magnitude difference in blood concentration between platelets and microspheres ($1x10^8$ platelets/mL and $5x10^5$ particles/mL, respectfully). With $5x10^5$ particles/mL blood concentration, 2 μm non-targeted spheres decreased platelet adhesion by 2-fold; however, the presence of sLe^a-targeted spheres at the same blood concentration had no significant effect on platelet adhesion to the endothelium (Fig. 6.4.A). There was also no significant effect on activated platelet adhesion with targeted spheres in $1x10^6$ particles/mL blood concentration (Fig. 6.4.B), even though the particle adhesion was ~2.3-fold higher than the adhesion of targeted spheres with $5x10^5$ particles/mL blood concentration (Fig. 6.4.A). Non-targeted spheres at $1x10^6$ particles/mL in blood did not significantly affect activated platelet adhesion at the WSR explored (1,000 s^{-1}). The effect sLe^a ligand density on activated platelet adhesion was examined using microspheres with 900 and 2,800 sLe^a sites/μm^2 to investigate if increased sLe^a density on target microspheres would promote sLe^a-mediated capture of platelets to the endothelium. There was no significant effect on platelet adhesion from the presence of targeted spheres with either ligand densities (Fig. 6.5).

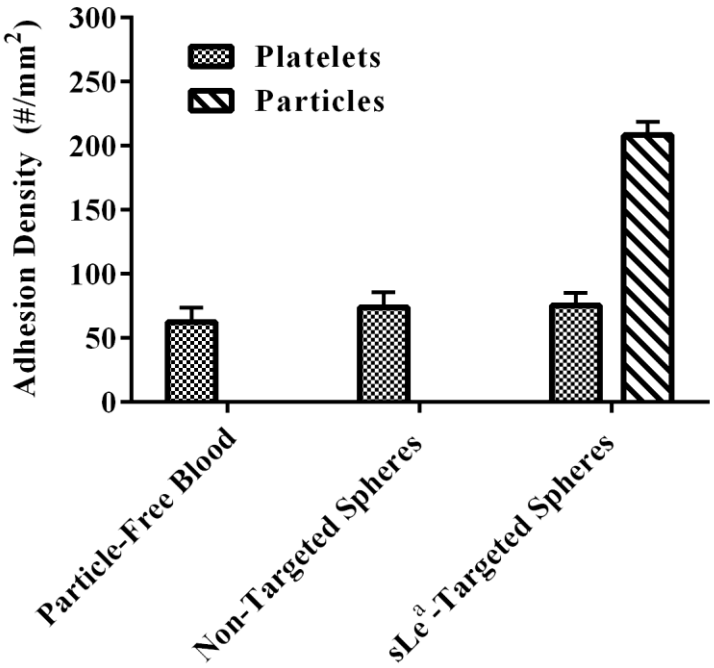

Figure 6.3. Adhesion of α-thrombin (1 nM) activated platelets ($1x10^8$/mL) with non-targeted or sLe^a-targeted 2 μm spheres ($5x10^5$/mL, 1,000 sLe^a sites/μm^2) at 1,000 s^{-1} WSR.

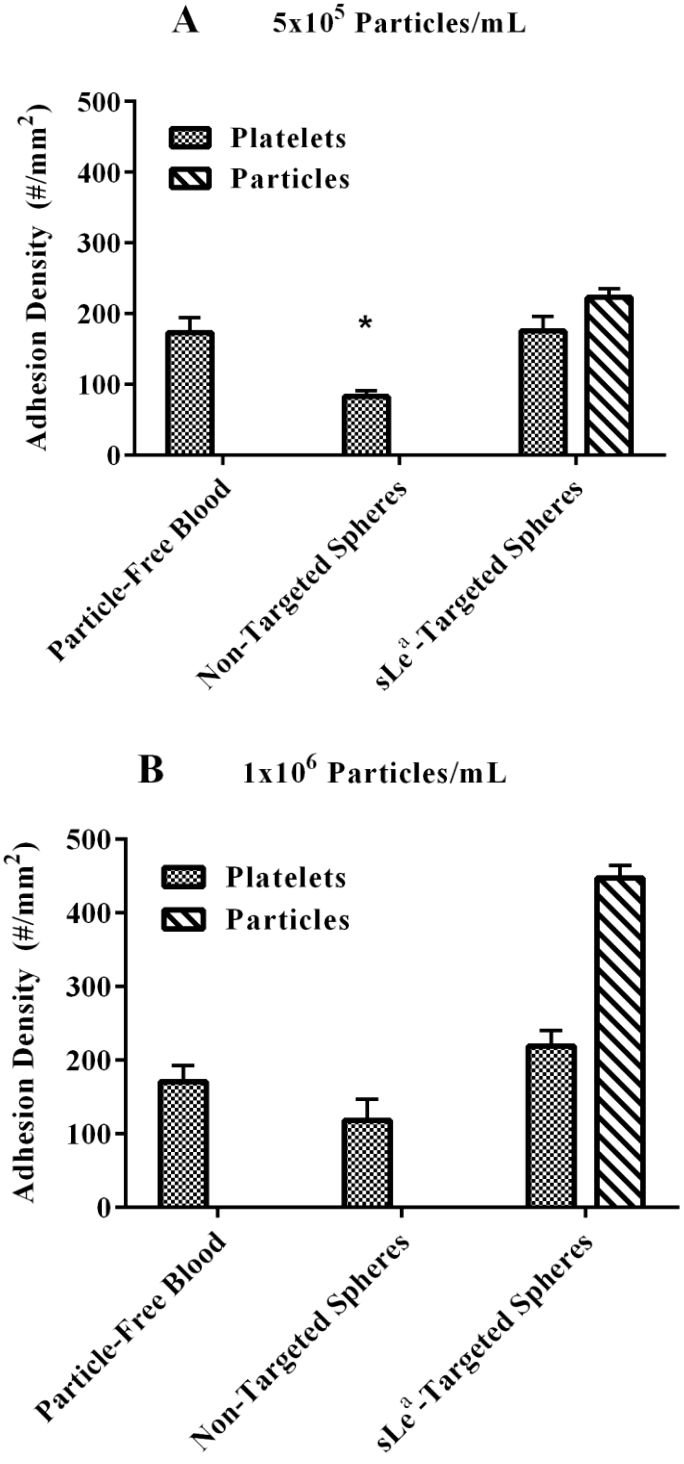

Figure 6.4. Adhesion of ADP (adenosine diphosphate, 1 μM) activated platelets ($5x10^7$/mL) with 2 μm sLe^a-targeted spheres with blood concentrations of (A) $5x10^5$ particles/mL and (B) $1x10^6$ particles/mL (1,000 sLe^a sites/μm^2) in reconstituted blood flow with 1,000 s^{-1} WSR. (A) * indicated significant difference compared to particle-free blood.

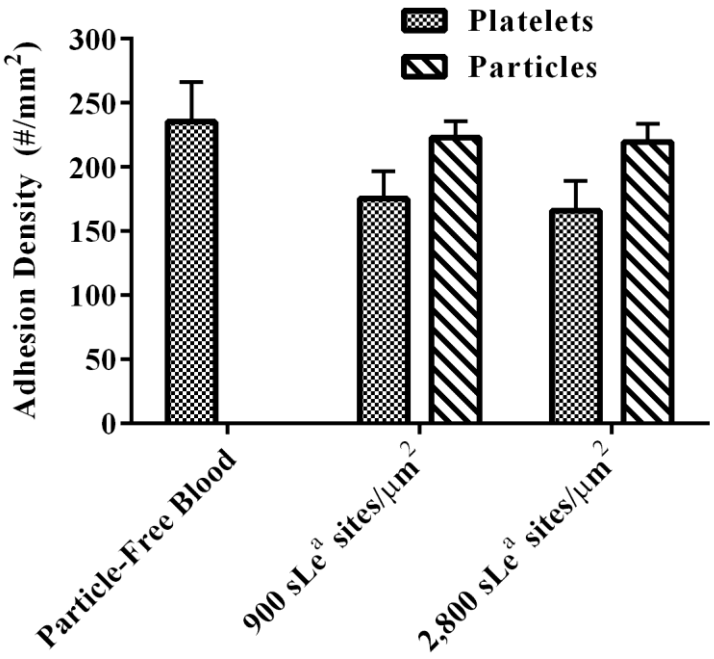

Figure 6.5. Influence of sLe^a density on ADP (1 μM) activated platelet adhesion ($5x10^7$/mL) at 1,000 s^{-1} WSR.

6.2.3. Tri-Peptide Targeted Microspheres for Enhancing Platelet Adhesion to an Injury Model

To investigate whether platelet-mimicking microspheres promote platelet adhesion and aggregation to collagen or vWF surfaces in blood containing low platelet concentration ($5x10^7$ platelets/mL), 2 μm avidin-coated polystyrene microspheres were incubated with biotin-$PEG_{3.4kDa}$-CBP or biotin-$PEG_{3.4kDa}$-VBP along with $PEG_{3.4kDa}$-cRGD in a 50-50 ratio (50% CBP or VBP and 50% cRGD, 5 μg/mL working concentration for each peptide). The particle and platelet adhesion was assessed at 200 s^{-1} or 1,000 s^{-1} to collagen or vWF coated glass coverslips, respectfully (peptides were procured by Christa Modery-Pawlowski and Dr. Anirban Sen Gupta at Case Western Reserve University). For all blood conditions, platelet adhesion was significantly greater to collagen and vWF surfaces compared to BSA surfaces, indicating that the platelet adhesion was mediate through collagen or vWF and not through non-specific interactions with BSA or exposed glass (Fig. 6.6). The addition of non-targeted microspheres slightly increased platelet adhesion to collagen under 200 s^{-1} of laminar blood flow relative to particle-free blood; however, this increase was not significantly different with a 99% confidence level ($p=0.0469$). The presence of CBP/cRGD-coated microspheres did not affect platelet adhesion to collagen under the same shear conditions, relative to particle-free blood (Fig. 6.6.A). The platelet adhesion level to collagen with the presence of peptide-targeted microspheres was not significantly different than the platelet level observed with non-targeted microspheres at the same particle concentration in blood ($p = 0.1255$, Fig. 6.6.A). Both non-targeted and VBP/cRGD-coated microspheres did not influence platelet adhesion to vWF under 1,000 s^{-1} of laminar blood flow (Fig. 6.6.B). No particle adhesion was observed with either CBP/cRGD or VBP/cRGD targeted 2 μm spheres. In order to elucidate if the lack of particle adhesion, and

thus influence on platelet adhesion, was due to low peptide densities on the microspheres, biotin-PEG-CBP-FITC was incubated with avidin-coated microspheres at a same peptide concentration used to prepare the targeted particles used in Fig. 6.6.A (5 μg/mL). Flow cytometry was used to obtain a fluorescent histogram to indicate if the fluorescent peptide was grafted to the microsphere's surface. There was a minimal shift in fluorescent histogram, compared to non-fluorescent peptide-targeted spheres, indicating that there was a minimal peptide density grafted onto the microspheres (Fig. 6.7).

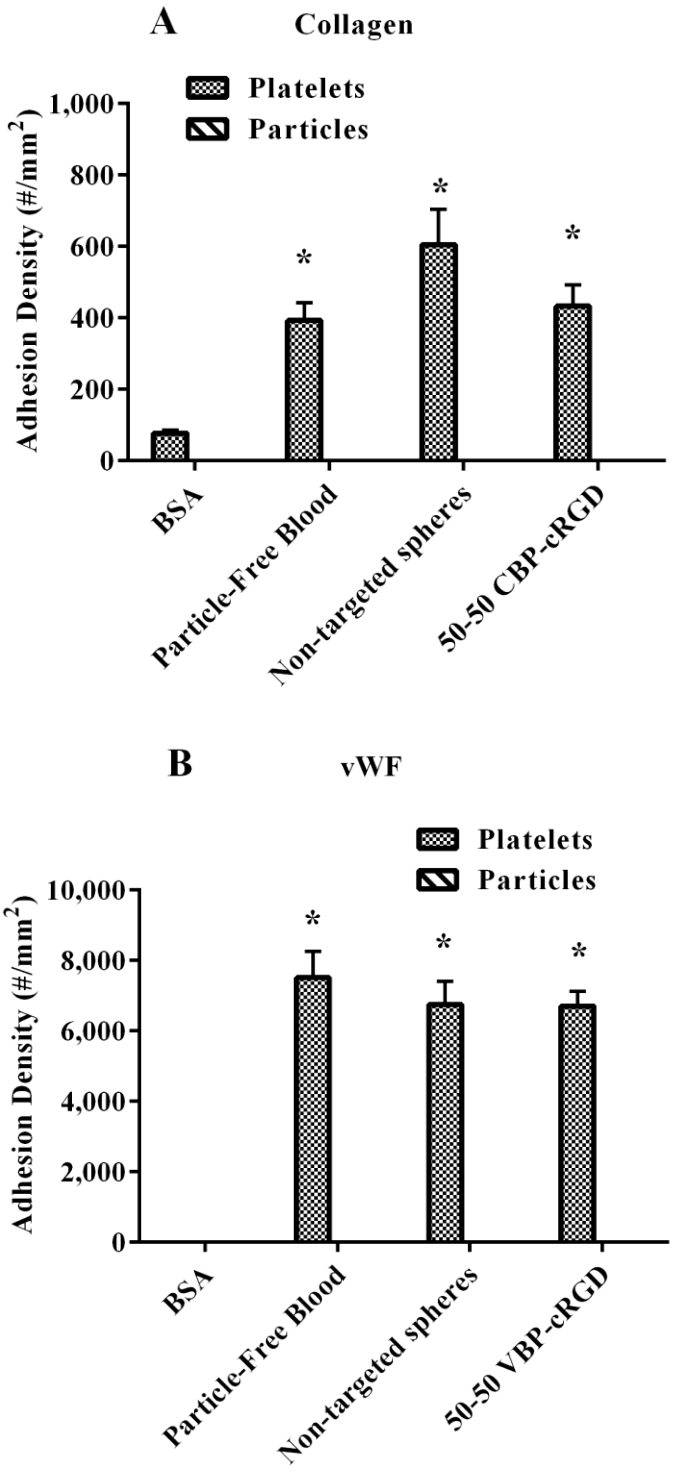

Figure 6.6. Adhesion of platelets ($5x10^7$/mL, 1 μM ADP activated) to (A) collagen (200 s^{-1} WSR) and (B) von Willebrand binding (1,000 s^{-1}) with peptide-targeted microspheres. * indicates significant difference in platelet adhesion compared to BSA coated glass coverslips ($p<0.01$).

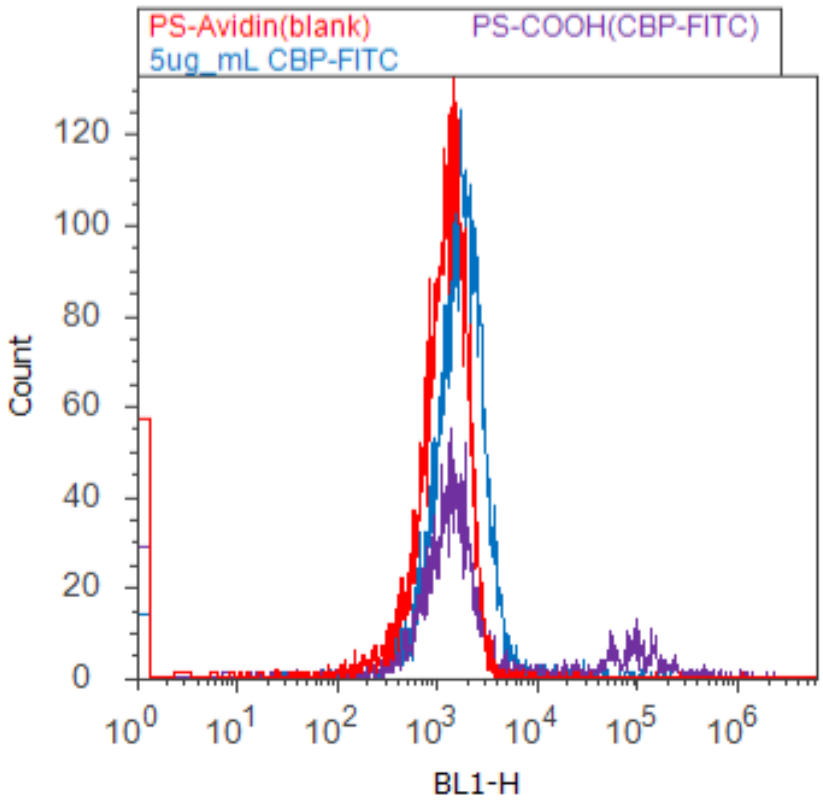

Figure 6.7. Fluorescent histogram of 2 µm avidin-coated microspheres incubated with 5 µg/mL biotin-PEG-CBP-FITC (blue); control histograms of avidin coated microspheres without incubation (red) and carboxylated polystyrene microspheres incubated with 100 µg/mL biotin-PEG-CBP-FITC (purple).

6.3. Discussion

Platelet activation, aggregation, and adhesion at injury sites are critical processes in minimizing blood loss at sites of vessel injury. However, platelet adhesion and aggregation at inflammatory sites may result in thrombus formation leading to cardiovascular events such as a stroke or complete vessel occlusion. Thus, it is crucial that VTCs designed to therapeutically treat inflammation do not induce platelet activation, adhesion, or thrombus formation at the targeted vessel wall. This study shows that 2 μm sLe^a-targeted polystyrene spheres have no significant effect on the adhesion of activated or unactivated platelets to an inflamed endothelium. Unactivated platelets, via the surface protein GP1bα within the GPIb-IX-V complex, interact through rolling adhesion with ultra-large vWF (ULVWF) secreted by cytokine-stimulated endothelium.[2, 16] However under shear stress, protease ADAMTS-13 in plasma rapidly cleaves ULVWF into smaller chains in order to minimize platelet-endothelial interactions during inflammation.[17] Activation induced platelet aggregation, through platelet activating factors such as ADP or α-thrombin or exposure to shear rates >10,000 s^{-1} can strengthen platelet-vWF interactions and lead to platelet firm adhesion to the endothelium.[18] The lack of a significant difference in platelet adhesion with the presence of targeted microspheres, relative to particle-free blood, suggests that inflammation targeting microspheres: (1) do not interfere with the enzymatic mechanism in place to minimize platelet-endothelial interactions in blood flow, (2) do not promote firm adhesion to the endothelium through platelet activation and subsequent aggregation. Interestingly, non-targeted carboxylated and amidine polystyrene spheres (< 100 nm) have been shown to activated platelets and upregulate P-selectin expression of platelets in plasma.[19] While only 2 μm spheres were explored in this work, it is possible that polystyrene targeted spheres < 100 nm may significantly activate platelets in blood flow; however, it is not

anticipated that this would correlate to an increase in platelet adhesion to the endothelium in blood flow due to the lack of evidence suggesting that targeted particles interfere with the enzymatic cleavage of endothelial released vWF.

Platelet activation induced by exposure to activating agents such as ADP or α-thrombin, results in an increase in platelet P-selectin expression which may induce platelet-particle aggregates through P-selectin and sLe^a on targeted VTCs.[20, 21] Thus, I examined if sLe^a-targeted spheres affect activated platelet adhesion to an endothelium through P-selectin-sLe^a interactions (i.e. increase in platelet adhesion mediated by sLe^a-targeted spheres present on the endothelium). SLe^a-targeted microspheres did not affect activated platelet adhesion to the endothelium, relative to particle-free blood (Fig. 6.3). Increasing the particle blood concentration (resulting in a higher particle adhesion density) or sLe^a ligand density in blood containing ADP activated platelets also had no significant impact on platelet adhesion in blood flow (Fig. 6.4.B and Fig. 6.5). Previously, sLe^a-targeted microbubbles were shown to adhere to immobilized activated platelets under flow; however, the capture efficiency significantly decreased from 16% to 3.4% when increasing shear stress from 5 dyn/cm^2 to 40 dyn/cm^2 (~125 s^{-1} and 1,000 s^{-1} blood WSR, respectfully).[22] It is likely that the lack of an increase in platelet adhesion through sLe^a capturing from endothelial bound microspheres may be a result of the high WSR explored (1,000 s^{-1}), which is similar to the WSRs present in large arteries susceptible to cardiovascular disease.[23] Overall, the results suggest that sLe^a-targeted model VTCs do not influence platelet adhesion to an activated endothelium in blood flow; however, further investigation is required to elucidate if platelet capture via sLe^a-targeted microspheres would occur with greater particle blood concentrations or under venous shear conditions (< 200 s^{-1}) relevant to vessels which develop venous thrombosis.[23]

The potential for particle-platelet dynamics influencing platelet adhesion in blood flow was also explored using two dual-peptide systems proposed for mimicking platelet adhesion to ECM proteins, collagen or vWF, and promote platelet aggregation at sites of vessel injury. In this work, 2 μm peptide-targeted spheres were shown to have no significant effect on platelet adhesion to collagen or vWF surfaces (Fig. 6.6). Interestingly, no particle adhesion to collagen or vWF surfaces was observed under 200 s^{-1} or 1,000 s^{-1} WSR, respectfully. Nano-liposomes decorated with similar CBP and VBP peptides were shown to firmly adhere to collagen and vWF surfaces under shear stresses ranging from 5–55 dyn/cm^2 (~125–1,364 s^{-1} blood WSR).[12, 13] The lack of an effect on platelet adhesion with 2 μm peptide-targeted spheres may be a result of the particles not establishing firm adhesion to collagen or vWF, thus preventing any particle-platelet aggregation through cRGD on the microspheres from localizing to the protein coated surfaces and increasing overall platelet adhesion density. Fluorescent histograms of avidin-coated microspheres with biotin-PEG-CBP-FITC show minimal attachment of the CBP-FITC peptide to the particle surface (Fig. 6.7). Thus, it is likely that the steric hindrance from the PEGylated peptides used in this work reduced the coupling to avidin-coated microspheres, resulting in insufficient ligand densities for establishing firm adhesion under the shear conditions explored in this work. This may also be the case for not observing particle adhesion through platelet linkage to collagen or vWF, i.e. the lack of cRGD on microspheres did not induce microsphere aggregation with platelets bound to ECM surfaces. Overall, sLe^a-targeted microspheres did not induce platelet adhesion to an activated endothelium in blood and ECM peptide-targeted spheres did not promote or interfere with platelet adhesion to collagen and vWF.

References

[1] Broos, K., Feys, H.B., Meyer, S.F.d., et al., *Platelets at Work in Primary Hemostasis.* Blood Reviews, 2011. **25**(4): p. 115-167.

[2] Ruggeri, Z.M., *Platelet Adhesion Under Flow.* Microcirculation, 2009. **16**: p. 58-83.

[3] Gay, L.J., Felding-Habermann, B., *Contribution of Platelets to Tumor Metastasis.* Nature Reviews Cancer, 2011. **11**(123-134). doi:10.1038/nrc3004.

[4] Klinger, M.H.F. and Jelkmann, W., *Role of Blood Platelets in Infection and Inflammation.* Journal of Interferon & Cytokine Research, 2002. **22**: p. 913-922.

[5] Ramtoola, Z., Lyons, P., Keohane, K., et al., *Investigation of the Interaction of Biodegradable Micro- and Nanoparticulate Drug Delivery Systems with Platelets.* Journal of Pharmacy and Pharmacology, 2010. **63**(1): p. 26-32.

[6] Ruf, A. and Patscheke, H., *Flow Cytometric Detection of Activated Platelets: Comparison of Determining Shape Change, Fibrinogen Binding, and P-selectin Expression.* Seminars in Thrombosis and Hemostasis, 1995. **21**(2): p. 146-151.

[7] Forlow, S.B., McEver, R.P., and Nollert, M.U., *Leukocyte-Leukocyte Interactions Mediated by Platelet Microparticles Under Flow.* Blood, 2000. **95**(4): p. 1317-1323.

[8] Nelson, R.M., Dolich, S., Aruffo, A., et al., *Higher-affinity Oligosaccharide Ligands for E-selectin.* Journal of Clinical Investigation, 1993. **91**(3): p. 1157-1166.

[9] Rodgers, S.D., Camphausen, R.T., and Hammer, D.A., *Sialyl Lewis^x-Mediated, PSGL-1-Independent Rolling Adhesion on P-selectin.* Biophysical Journal, 2000. **79**(2): p. 694-706.

[10] Lee, G.M., Arepally, G. M., *Diagnosis and Management of Heparin-Induced Thrombocytopenia.* Hematol. Oncol. Clin. North Am., 2013. **27**(3): p. 541-563.

[11] Ravikumar, M., Modery, C.L., Wong, T.L., et al., *Peptide-Decorated Liposomes Promote Arrest and Aggregation of Activated Platelets under Flow on Vascular Injury Relevant Protein Surfaces in Vitro.* Biomacromolecules, 2012. **13**: p. 1495-1502.

[12] Anselmo, A.C., Modery-Pawlowski, C.L., Menegatti, S., et al., *Platelet-like Nanoparticles: Mimicking Shape, Flexibility, and Surface Biology of Platelets to Target Vascular Injuries.* ACS Nano, 2014.

[13] Ravikumar, M., Modery, C.L., Wong, T.L., et al., *Mimicking Adhesive Functionalities of Blood Platelets using Ligand-Decorated Liposomes.* Bioconjugate Chemistry, 2012. **23**: p. 1266-1275.

[14] Namdee, K., Thompson, A.J., Phapanin, C., et al., *Margination Propensity of Vascular-Targeted Spheres from Blood Flow in a Microfluidic Model of Human Microvessels.* Langmuir, 2013. **29**(8): p. 2530-2535.

[15] Charoenphol, P., Mocherla, S., Bouis, D., et al., *Targeting Therapeutics to the Vascular Wall in Atherosclerosis - Carrier Size Matters.* Atherosclerosis, 2011. **217**(2): p. 364-370.

[16] Bernardo, A., Ball, C., Nolasco, B.L., et al., *Platelets Adhere to Endothelial Cell-Bound Ultra-Large von Willebrand Factor Strings Support Leukocyte Tethering and Rolling Under High Shear Stress.* Journal of Thrombosis and Haemostasis, 2005. **3**: p. 562-570.

[17] Dong, J.F., Moake, J.L., Nolasco, L., et al., *ADAMTS-13 Rapidly Cleaves Newly Secreted Ultralarge von Willebrand Factor Multimers on the Endothelial Surface Under Flowing Conditions.* Hemostasis, Thrombosis, and Vascular Biology, 2002. **100**(12): p. 4033-4039.

[18] Ruggeri, Z.M., Orje, J.N., Habermann, R., et al., *Activation-Independent Platelet Adhesion and Aggregation Under Elevated Shear Stress.* Blood, 2006. **108**(6): p. 1903-1910.

[19] Mayer, A., Vadon, M., Rinner, B., et al., *The Role of Nanoparticle Size in Hemocompatibility.* Toxicology, 2009. **258**(2-3): p. 139-147.

[20] Merten, M. and Thiagarajan, P., *P-selectin Expression on Platelets Determines Size and Stability of Platelet Aggregates.* Circulation, 2000. **102**: p. 1931-1936.

[21] Sugama, Y., Tiruppathi, C., Janakidevi, K., et al., *Thrombin-Induced Expression of Endothelial P-selectin and Intercellular Adhesion Molecule-1: A Mechanism for Stabilizing Neutrophil Adhesion.* Journal of Cellular Biology, 1992. **119**(4): p. 935-944.

[22] Guenther, F., Muhlen, C.v.z., Ferrante, E.A., et al., *An Ultrasound Contrast Agent Targeted to P-selectin Detects Activated Platelets at Supra-arterial Shear Flow Conditions.* Investigative Radiology, 2010. **45**(10): p. 586-591.

[23] Kroll, M.H., Hellums, J.D., McIntire, L.V., et al., *Platelets and Shear Stress.* Blood, 1996. **88**: p. 1525-1541.

CHAPTER 7

CONCLUSIONS AND FUTURE WORK

7.1. Conclusions and Significant Contributions

Tissue-specific drug delivery is a strategy for improving therapeutic intervention in many serious diseases through minimizing therapeutic exposure to healthy tissue and reducing systemic side effects. Inflammation of the vessel wall is a strong candidate for tissue-specific therapy due to the prevalence of the vasculature throughout the body, minimally invasive access through injections, and the contribution of inflammation to the pathogenesis of several serious diseases including atherosclerosis, sepsis, and various cancers. The complex nature of blood and unique roles that each component (RBCs, leukocytes, platelets, and plasma) has on VTC margination and adhesion provide challenges when optimizing VTC performance. While simplified blood models, such as RBCs-only in buffer or plasma, offer insight into the biophysical dynamics of particle margination and adhesion to the vessel wall, it is important to remember that whole blood is the end-all working fluid for particle transport throughout the vasculature. In this work, I show that VTC dynamics with plasma and blood cells (leukocytes and platelets) have significant implications on not only VTC design, but also blood cell homeostasis during inflammation. Specifically, the application of PEGylation to combat plasma protein adsorption, VTC design characteristics (size, shape, targeting system, concentration in

blood), and endothelial surface coverage significantly impact particle adhesion and leukocyte recruitment to the vascular wall in blood flow.

7.1.1. PEGylation and VTC Design and Applications

I demonstrated that the implementation of a PEG corona, with the intent of minimizing plasma adsorption, significantly impacts VTC adhesion in physiological blood flow conditions. The adhesion characteristics of the targeting system providing tissue specificity ultimately determine how PEG affects targeting and which PEG corona parameters, molecular weight and/or conformation, are important for VTC performance and application. For a less efficient targeting system, such as the aICAM-1/ICAM-1 system used in this work, both conformation and PEG molecular weight affect VTC design. For applications in high shear, such as the conditions in medium to large arteries susceptible to cardiovascular diseases, large PEG spacers (5.5 kDa and 10 kDa) oriented in the extended conformation are best suited for effective adhesion to the vessel wall. However, PEG's ability to maintain the adhesion efficiency of a less favorable targeting system has significant implications on tissue specificity, as high levels of VTC adhesion with low ligand densities may result in VTCs targeting diseased and healthy tissue if the targeted receptor is expressed in both states (as in the case of ICAM-1). Conversely, the enhanced adhesiveness may provide VTCs access to additional targeting systems such as monovalent ligands, peptides, and other receptor-ligand systems with adhesive kinetics similar to aICAM-1/ICAM-1. Ultimately, PEGylated VTCs may work best in conjunction with a less efficient and highly disease-specific targeting system, or an efficient targeting system.

For efficient targeting systems like sLe^a/E-selectin, where the ligand kinetics allow for adhesion at WSRs >500 s^{-1} in blood, PEG conformation (i.e. grafted PEG density) is the

important factor for maintaining adhesion in blood flow (as the mushroom conformation reduced adhesion under WSRs >500 s^{-1}). Moreover, the steric hindrance provided by a unimodal PEG corona (single PEG length) in the extended brush orientation, which is the conformation suggested to reduce plasma protein adsorption and minimizing particle clearance from blood, does not reduce the adhesiveness of targeted micro- and nano-spheres under physiological blood flow conditions. However, an extended brush conformation or high molecular PEG spacer may provide a limitation to cellular internalization. As a result, VTCs for intracellular drug delivery may be limited to highly efficient (and disease-specific) targeting systems with low molecular weight PEG spacers (≤ 2.3 kDa) in the extended brush conformation. On the other hand, imaging or diagnostic applications would benefit more from high levels of endothelial surface coverage (i.e. particle adhesion density) and the limitation on internalization from larger PEG spacers would be less important. Thus for cardiovascular diagnostics or imaging, a 10 kDa PEG spacer may provide the best surface coverage through ensuring adhesion under high shear conditions, particularly if one were to image highly late-stage develop atherosclerosis where shear rates can be >1,000 s^{-1}.

Regardless of the application, the VTC itself must be composed of a biocompatible material. PLGA is the most common biomaterial for drug delivery. The negative human plasma effect on the adhesion of PLGA micro- and nano-spheres provides a significant challenge for the application of PLGA VTCs. While it is commonly thought that PEGylation may neutralize this effect through minimizing plasma protein adsorption, the influence of PEG on the adhesion of PLGA spheres in human blood has not been thoroughly examined. I show that the addition of a 5.5 kDa or 10 kDa PEG spacer corresponding to in an intermediate-brush conformation (~16,000 and 3,200 PEG chains/μm^2, respectfully) was unable to restore the adhesion of sLe^a-targeted

PLGA spheres in human blood, relative to plasma-free systems. However, increasing the PEG density of a 5.5 kDa spacer to ~35,000 PEG chains/μm^2 did restore the adhesiveness of polystyrene spheres in pig plasma in which a similar plasma effect as PLGA spheres in human blood has been identified. Based on this result, I hypothesize that a PEG density of at least 35,000 PEG chains/μm^2 is required to restore the adhesiveness of PLGA spheres in human blood. While this high of a PEG density (and dense brush conformation) will allow researchers to optimize VTC targeting or tissue specificity in a pig *in vivo* system (which is a good *in vivo* system for cardiovascular disease), it may significantly hinder cellular internalization for drug delivery applications. Similarly, increasing the PEG density onto PLGA VTCs still remains a challenge due to the limited functional groups available for PEGylation. The inability to achieve a dense brush conformation or restore the adhesion of PLGA VTCs with low PEG densities may restrict PLGA VTCs to therapeutic formulations where a low therapeutic dose is highly effective, such as gene delivery. Overall, PEGylation is more than a strategy for minimizing plasma adsorption. The significant influence of the PEG corona parameters (PEG density and molecular weight), targeting system, hemodynamics, and plasma adsorption all contribute to the eventual applicability of PEGylated VTCs. Figure 7.1 shows my general recommendations for designing PEGylated VTCs to target inflammation associated with cardiovascular disease based on the results of this work.

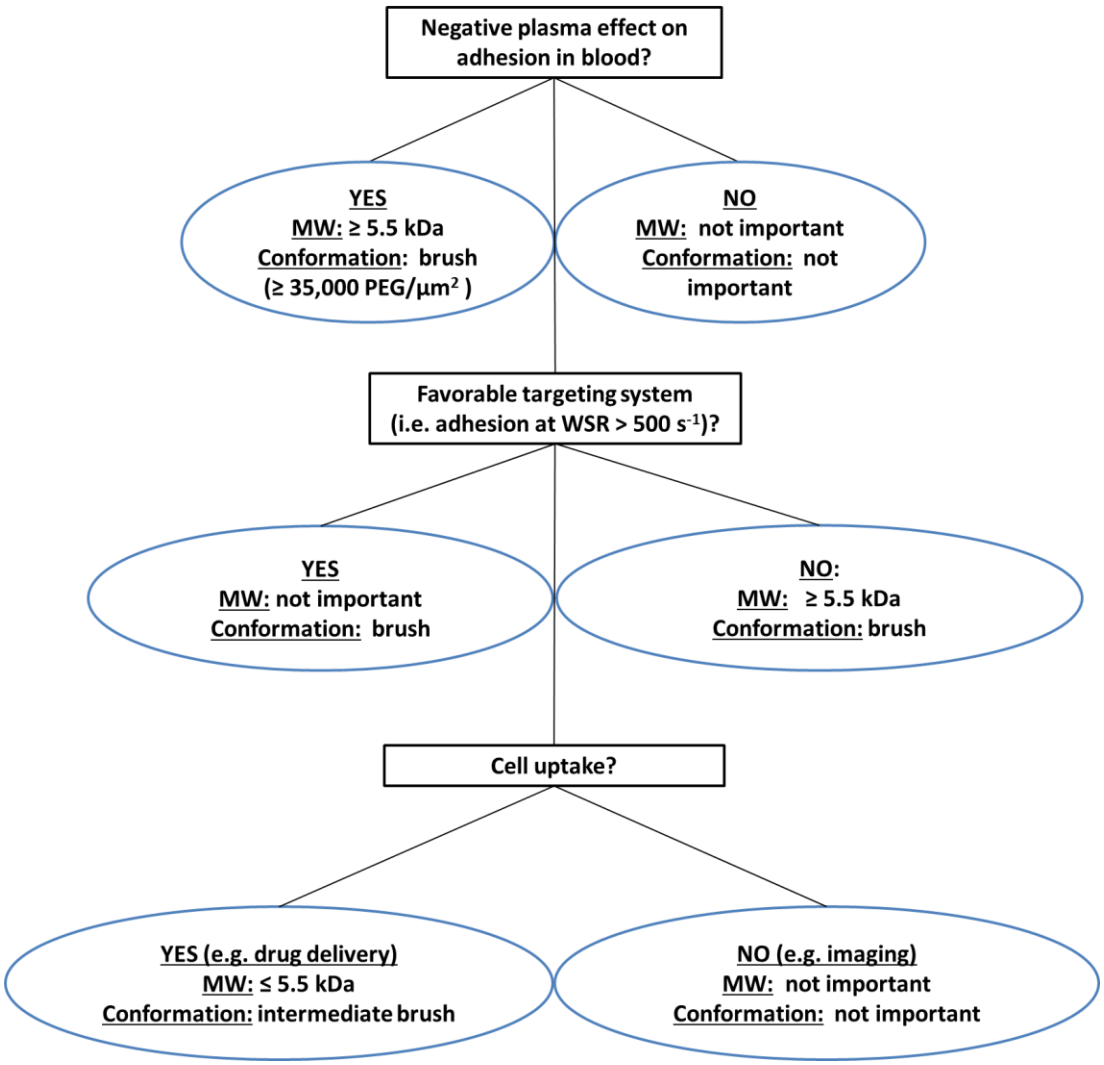

Figure 7.1. Schematic of recommendations for designing and applying PEGylated VTCs for targeting inflammation associated with cardiovascular disease in blood.

7.1.2. VTCs and Blood Cell Recruitment to Targeted Tissue

While drug delivery formulations are often designed to specifically target or affect one particular tissue/cell type, it is important to remember that diseased tissue is a multicellular environment which may induce a natural and healthy response from blood cells. The disruption of healthy functioning cells at the diseased site may have significant repercussions on the effectiveness and applicability of targeted drug delivery systems. For example, VTCs increasing platelet interaction with the vessel wall and initiating a thrombus at the target site would inherently be counterproductive. In this work, I show that the presence of VTCs do not initiate platelet aggregation at the target site. More importantly, the presence of VTCs in blood or at the vessel wall does not disrupt the homeostatic cleavage of endothelial released vWF by plasma enzymes, which is a mechanism used to minimize platelet interaction with inflammatory tissue. This alleviates potential concerns of VTCs inducing blood coagulation at the vascular wall.

On the other hand, reducing the accumulation of blood cells at the target site that accelerate disease pathogenesis could provide a therapeutic benefit. In Chapters 5, I show that particles targeted with either sLe^a or aICAM-1 significantly reduce leukocyte recruitment to the same targeted endothelium. The reduction in leukocyte adhesion was determined to be dependent on carrier size, particle adhesion density, and hemodynamics. In fact, 5 μm and 3 μm present at the highest concentration explored ($1x10^7$ particles/mL in blood) reduced leukocyte adhesion by nearly 100%. Most interestingly, nanospheres (500 nm) were also shown to significantly reduce leukocyte recruitment by nearly 40%. A potential benefit of this phenomenon may be in the application of VTCs as a passive anti-inflammatory therapy. Current anti-inflammation (anti-leukocyte adhesion) therapies include functional blocking antibodies directed towards key CAMs (i.e. ICAM-1 or E-selectin) and therapeutics geared towards

reducing CAMs expression. However, to date, these strategies have not shown long-term benefits due to short half-lives of the antibodies/therapeutics. A major concern with these systemic molecular-based anti-adhesion therapies is balancing the therapeutic blocking of leukocyte recruitment to chronically inflamed tissue, associated with diseases, without affecting recruitment to inflammatory sites where needed (i.e. local infection). Tissue-specific drug delivery may potentially alleviate this effect by delivering anti-inflammatory therapeutics directly to diseased tissue. Additionally, VTCs reducing leukocyte accumulation at inflammatory tissue, via physical/competitive interactions with leukocytes at the vessel wall, may significantly enhance the therapeutic treatment of inflammatory diseases associated with leukocyte recruitment such as atherosclerosis, sepsis, or reperfusion injury. In this case, VTCs themselves may be developed as therapy, or work in conjunction with an anti-inflammatory therapeutic, for effective and local treatment of inflammatory diseases. Examining the effect of targeted drug carriers in a multicellular environment not only examines the effect of drug carriers on healthy cell function, but may provide new information or identify new avenues for enhancing disease treatment.

7.2. Future Work

The contributions of this work have provided valuable information demonstrating how the dynamics between blood and VTCs in circulation affect VTC performance and potential applications. However, there are still specific areas in which VTC-blood dynamics can be developed for optimizing VTC function. For example, studying tissue-site retention of PEGylated spheres, relative to non-PEGylated spheres, will add an additional specification to PEGylated VTC design. While there has been significant work investigating how PEGylation

influences the biodistribution (organ accumulation) of model VTCs, there has been little work examining target site retention. This could have significant applications in real-time imaging and tracking treatment progress. Additionally, highly developed atherosclerotic tissue can reach wall shear rates of up to 10,000 s^{-1}. Examining the influence of PEGylation on VTC adhesion at shear rates greater than the 1,000 s^{-1} used in this work, would determine whether the sizes of the PEG spacer used in this work (2.3 kDa, 5.5 kDa, and 10 kDa) are sufficient for targeting late-stage atherosclerosis or would be limited tissue with low levels of plaque.

The high PEG density recommended for improving PLGA adhesion in human blood (~35,000 PEG chains/μm^2) provides a serious challenge for PLGA drug delivery systems. Due to the limited functional groups available with PLGA, I recommend developing a one-step fabrication procedure for simultaneous particle fabrication and PEGylation using PLGA-PEG-copolymers or PLGA/PLGA-PEG-copolymer blends and an emulsion-solvent-evaporation technique. This would eliminate the need for a post-fabrication PEGylation step, such as the carboxyl-amine chemistry used in this work, of which the amount of PEG grafted to the particles is is limited by the density of functional groups present on the surface of PLGA particles. It will also be important to determine the uptake efficiency of the PEGylated spheres by the targeted tissue, i.e. an activated endothelium in the case for inflammation, as this would determine whether restoring PLGA adhesion in human blood using a high PEG density would also limit the potential implementation of PEGylated PLGA spheres for intracellular delivery.

PEGylation should also be investigated as a VTC modification for improving the effectiveness of nanospheres in reducing leukocyte recruitment to inflammatory tissue. I hypothesize that nanospheres reduce leukocyte recruitment to inflammatory tissue through a combined effect of occupying adhesion molecules at the target site and interacting with

leukocytes away from the vessel wall. Specifically, sLe^a-targeted nanospheres are more efficient than aICAM-1 targeted nanospheres due to the sLe^a spheres potentially interacting with L-selectin on leukocytes. The stability of these potential nanosphere-leukocyte aggregates is unknown, as the interaction of sLe^a with L-selectin has much faster adhesive kinetics (on-/off-rate), relative to the kinetics of sLe^a and E-selectin. The improved adhesiveness with PEGylation may stabilize leukocyte-nanosphere aggregates or promote the formation of more aggregates, thus improving the effectiveness of nanospheres in reducing leukocyte accumulation. This would have a significant implication on the applicability of VTCs as an anti-inflammatory therapy as the maximum reduction in leukocyte recruitment was observed with 5 μm and 3 μm spheres, which are susceptible to capillary entrapment due to their size.

Another possible way to improve the effectiveness of small VTCs (2 μm or 500 nm) would be to examine the effect of material density on leukocyte reduction. VTCs < 5 μm primarily influence leukocyte recruitment through endothelial surface coverage (particle adhesion density) and not through physical collisions with endothelial interacting leukocytes. Increasing the density of the particle provide a collision component, in addition to the effect from endothelial surface coverage, and increase the effectiveness of small VTCs. As an example, based on a simple estimation of momentum (particle volume x material density x velocity), if the particle velocity is assumed to be similar to that recorded in Fig. 2.5 (~40 mm/s), a 2 μm sphere would require a particle density of approximately 15 g/cm^3 (which is similar to that of gold, ~19 g/cm^3), to achieve a similar momentum as 5 μm polystyrene spheres and possibly provide a collision effect for 2 μm spheres in reducing leukocyte adhesion.

Overall, it is important to examine whether VTCs provide an enhanced therapeutic benefit, relative to current antibodies used for anti-adhesion therapies, before devoting

significant resources to improving nanoparticle effectiveness on reducing leukocyte adhesion. This could potentially be examined by implementing endothelial permeability studies in combination with the flow assays used in this work, as an increase in endothelial permeability is one symptom of non-regulated leukocyte accumulation associated with diseases like ischemia-reperfusion injury. However, investigating the therapeutic effect of VTCs reducing platelets aggregation to inflammatory tissue in diseases such as deep vein thrombosis is more challenging. *In vivo* animal models are commonly implemented for studying deep vein thrombosis; however, developing *in vitro* assays using human platelets may provide better analysis before eventual pre-clinical trials due to differences in animal blood functionality relative to humans. My recommendation for developing an *in vitro* thrombosis assay is to implement a cone-and-plate viscometer in a similar fashion used to culture bacterial biofilms *in vitro*. This would allow for determining if the presence of VTCs influences the development of thrombus formation or if VTCs destabilize thrombi, which could potentially put patients at high risk for a cardiac event.

In summary, while simplified blood models are often used to gain a better understanding as to the biophysics of VTC adhesion, VTC performance in blood with all its components present will determine VTC design and applicability. A simple modification such as PEGylation for minimizing plasma adsorption has a significant effect on VTC adhesion in blood. The high PEG density required to restore adhesion of a plasma-sensitive drug delivery system in blood may in turn reduce its uptake efficiency and limit its potential for intracellular drug delivery. Conversely, the ability of 500 nm spheres to reduce leukocyte accumulation at inflammatory tissue in blood may be a new therapeutic avenue for vascular targeting. Overall, targeted drug delivery systems must be examined in multicomponent systems similar to that of the targeted

environment, as the success of tissue-specific drug delivery will ultimately be determined by its ability to effectively treat diseases without affecting healthy tissue function.